ESCUELA TÉCNICA SUPERIOR DE INGENIERÍA

DEPARTAMENTO DE INEGNIERÍA DE SISTEMAS Y AUTOMÁTICA

DOCTORAL THESIS

Stochastic Model Predictive Control for Robust Operation of Distribution Systems

Pablo Velarde Rueda

Supervisors:
Dr. José M. Maestre
Dr. Carlos Bordons

Seville, 2017

Acknowledgments

First, I would like to thank my family. In particular, my mom who has been there with me in spite of the distance. This dream is possible, and I am sure that my father is glad for this moment.

I would like to express my special appreciation and thanks to Dr. José M. Maestre for his unconditional help, friendship, and dedication along these years. I also want to thank Dr. Carlos Bordons for his time spent reviewing my works. Your advice was an important part of my studies.

I would especially like to thank Dr. Carlos Ocampo-Martinez for his comments, suggestions, and his patience. Besides, my admiration and acknowledgment to everybody who collaborated and taught me how is a realistic academic life.

Moreover, I can not forget of my friends from Spain and Ecuador; I want to say them thank you for their real friendship. Thanks, in particular, to Jesús and Mario.

At last, but not least. I want to acknowledge to “Secretaria Nacional de Educacin Superior, Ciencia y Tecnología” (Senescyt) from Ecuador for its economic support of my doctoral studies.

Abstract

There are many systems in which uncertainties are present in their model, either in the same system description or as disturbances. Among many random variables we can mention the electrical demand of a generation network, the amount of rainfall in an irrigation system, the number of people occupying a room in a system of heating. Among others, they are examples of stochastic systems, in which the idea of scenarios can be considered for their solution. Specifically, the stochastic model predictive control seeks to generate a solution for several scenarios that can be established under a probabilistic condition. In this work is carried out an analysis and comparison regarding performance among the three well-known stochastic MPC approaches, namely, multi-scenario, tree-based, and chance-constrained model predictive control. The possibility of application in several distribution sectors is also analyzed. Moreover, some improvements are proposed in terms of robustness. To this end, the stochastic MPC controllers are designed and implemented in a real renewable-hydrogen-based microgrid as well as to the drinking water network of Barcelona via simulation. Finally, an application of CC-MPC to inventory management in a hospital pharmacy, is also presented.

Stochastic MPC controllers are applied in a hierarchical and distributed fashion. In this sense, a scenario-based hierarchical and distributed MPC is applied for water resources management by considering dynamical uncertainty. In addition, a multicriteria optimal operation of a microgrid considering risk analysis and MPC is shown. For all applications, their design has considered the important role that uncertainty plays in these kind of systems.

Finally, in order to analyze different types of the so-called insider attacks in a DMPC scheme is presented. In particular, the situation where one of the local controllers sends false information to others is considered to manipulate costs for its own advantage. Then, some mechanisms based on stochastic MPC techniques are proposed to protect or, at least, relieve the consequences of the attack in a typical DMPC negotiation procedure is addressed along this work.

Contents

Chapter 1

Introduction

Model Predictive Control (MPC) is a control strategy widely used in the industry compared with other control techniques. MPC provides a control framework capable of dealing with delays, nonlinearities, constraints on the states as well as on the input variables, moreover, it can be easily extended to multi-variable systems, to name a few advantages of this technique [1, 2]. The main idea of MPC is to obtain a control signal by solving, at each time step, a finite-horizon optimization problem (FHOP) that takes into account a model of the system to predict its evolution and to steer it in accordance to given objectives. The first component of the obtained control sequence is applied to the system at the current time step and the problem is solved again at the next time step, following a receding horizon strategy [3].

However, the classical formulation of MPC does not allow considering systems with uncertainties, although some MPC schemes have been proposed to ensure stability and compliance with constraints in the presence of disturbances [4]. As summarized in [5], alternative approaches of MPC for stochastic systems are based on *min-max* MPC, *tube-based* MPC, and *stochastic* MPC (SMPC). The first two approaches are oriented to ensure worst-case robustness and consequently are conservative, while the third approach relies on stochastic programming (SP) techniques to offer a probabilistic constraint fulfillment [6]. Since some violations are allowed with some stochastic approaches, the solutions obtained are less conservative and hence the performance is better in terms of cost from the objective function. In this way, disturbances are modeled as random variables, and the control problem is stated by using the expected value of the system variables, i.e., states and control inputs. A less conservative approach is the stochastic one, which is based on the design of predictive controllers for dynamical systems subject to disturbances and/or uncertainty in terms of the *probability* that a

certain solution is feasible [7], mainly because it is not strictly possible to speak about guaranteed feasibility in this context.

Nevertheless, there exist other MPC schemes reported in the literature that aim to ensure robust stability and compliance with constraints in the presence of stochastic disturbances, see e.g., [4, 5].

The stochastic approach is a mature theory in the field of optimization [8], but renewed attention has been given to it due to its great potential in control applications, see e.g., [9] and references therein. From the wide range of SMPC methods, this work is focused on three specific techniques, namely: *multiple-scenario MPC* (MS-MPC), also called Multiple MPC in [10], *tree-based MPC* (TB-MPC), and *chance-constrained MPC* (CC-MPC).

MS-MPC consists in calculating a single control sequence that takes into account different possible evolutions of the process disturbances. Hence, the control sequence calculated has a certain degree of robustness against the potential realizations of the uncertainties. This approach is used for example in [10] for water systems and in [11, 12] within the context of the control of smart grids. One of its advantages is that it is possible to calculate bounds on the probability of constraint violation as a function of the number of scenarios considered [13].

An alternative to model the uncertainty that is faced by this type of systems is to use rooted trees. The rationale behind this approach is that uncertainty spreads with time, i.e., it is possible to predict –more accurately– both the energy demand and energy production by a renewable source in a short horizon than in a large one. For this reason, the possible evolutions of the disturbances can be confined to a tree. In the tree, there is a bifurcation point whenever the disturbances branch into two possible trajectories. Consequently, the outcome, the so-called TB-MPC, is a rooted tree of control actions. This approach is used for example in [14] for a semi-batch reactor example, in [15] for the energy management of a renewable hydrogen-based microgrid, and in [16] in the context of water systems.

CC-MPC uses an explicit probabilistic modeling of the system disturbances to calculate explicit bounds on the system constraint satisfaction. For instance, [17] presents a chance-constrained two-stage stochastic program for unit commitment with uncertain wind power output and [18] shows an autoregressive-moving-average (ARMA) type prediction model for the underlying uncertainties (load/generation) into chance-constrained finite-horizon optimal control. An application of this technique in the context of the drinking water network of the city of Barcelona is reported in [19]. In addition, [20] shows a comparison between TB-MPC and CC-MPC approaches applied to drinking water systems. Further, this subject has drawn significant interest; a stochastic optimization model implemented in the context of the control of microgrids can be seen in [21–24] and references therein.

An important aspect here is the way the control can be implemented from a decentralized viewpoint. Some systems – e.g., power dispatch system, water and navigation system, logistic systems, among others– often spread over large-scale areas. The whole system may be divided into smaller ones that can be governed by different local entities. If the local controllers do not communicate at all, the control architecture is said to be decentralized. By other side, when all the controllers are equally important and share information to find the most appropriate control actions from a global perspective, it is using a distributed control scheme, see e.g., [25, 26]. Moreover, a possibility is to use a hierarchical structure where an upper control layer provides instructions to the lower control layers, the latter are in charge of the regulation of smaller regions controlled by local agents. In this way, coordination is attained [27–29].

Since the uncertainties and disturbances can be presented on different geographically disperse subsystems, their structures are different and need to be reviewed in the hierarchy for sending reliable information to multi-subsystem. At this point, this work shows a scenario based Hierarchical and Distributed MPC (HD-MPC) in one of its chapters. The overall control architecture is composed of two layers. On the one hand, the top layer collects global forecast information and sends to the local agents a set of different scenarios one per each subsystem to deal with the uncertainty. On the other hand, the bottom layer solves the optimal control problem in a distributed fashion by using a distributed scheme, where the role played by the uncertainties is carried out by multi-subsystem scenario based MPC.

Moreover, many approaches for DMPC schemes have been developed in recent years, as described in [30]. A topic that deserves attention is the regular exchange of information during the negotiation process among the controllers. In this sense, DMPC schemes have been carried out by considering a coordinated negotiation process where all controllers work in a reliable way. However, a malicious controller could exploit the vulnerabilities of the network by sharing false information with other controllers, producing an undesirable behavior in the optimization process. At this point, it is possible to speak about cyber-security in the context of DMPC. At this point, cyber-security issues have not been considered in the DMPC literature. Hence, in this work it is analyzed one of the most popular schemes, Lagrange based DMPC. In particular, it is shown how a malicious controller in the network can take advantage of the vulnerabilities of the scheme to increase its own benefit at the cost of other controllers. Also, these issues are addressed by considering some stochastic based MPC techniques to ensure robustness within the DMPC network.

1.1 Objectives of the thesis

The main objective of this thesis is to carry out an analysis and comparison regarding performance among the three stochastic MPC approaches, namely, multi-scenario, tree-based, and chance-constrained model predictive control. The possibility of application in several distribution sectors has been also analyzed. Finally, some improvements have been proposed in terms of robustness. To this end, the stochastic MPC controllers have been designed and implemented in first place in a real renewable-hydrogen-based microgrid. Moreover, on the comparison of these stochastic techniques is applied to the drinking water network of Barcelona. Finally, an application of CC-MPC to inventory management in hospitalary pharmacy, is also presented.

As a second objective in this work is to apply stochastic MPC controllers in a hierarchical and distributed fashion. In this sense, a scenario-based hierarchical and distributed MPC is applied for water resources management by considering dynamical uncertainty. In addition, a multicriteria optimal operation of a microgrid considering risk analysis and MPC is shown. For all applications, their design has considered the important role that uncertainty plays in these kind of systems.

To analyze different types of the so-called insider attacks in a DMPC scheme is presented as the last objective of this thesis. In particular, the situation where one of the local controllers sends false information to others is considered to manipulate costs for its own advantage. Then, some mechanisms based on stochastic MPC technique are proposed to protect or, at least, relieve the consequences of the attack in a typical DMPC negotiation procedure is addressed along this work.

1.2 Thesis outline

The remainder of this thesis is organized as follows. To cope with uncertainty present in the most kind of distribution systems, the use of three stochastic MPC approaches is proposed: multiple-scenario MPC, tree-based MPC, and chance-constrained MPC. A comparative assessment of these approaches is performed when they are applied to real case studies, specifically, a hydrogen based microgrid situated at the University of Seville, a sector and an aggregate version of the Barcelona drinking water network, and the stock management in a hospital pharmacy using chance-constrained model predictive control, are shown in the Chapter 2.

Chapter 3 is focused on the hierarchical stochastic MPC. On the one hand, the optimal power dispatch taking into account risk management and renewable resources in the real laboratory-scale plant is addressed. To this end, identification of potential risks has been performed and two MPCs are designed: one for risk mitigation and another

for the optimal control of the microgrid. The proposed algorithm considers an external loop where information about risk evaluation is updated. The risk mitigation policy may change setting points and constraints as well as execute actions. Results show improvements in terms of costs and demand satisfaction. On the other hand, a tree based hierarchical and distributed Model Predictive Control (HD-MPC) is applied to deal with operational water management problems under dynamical uncertainty. A two layer-hierarchical structure is proposed, the higher layer collects and coordinates forecast information for sending different scenarios that take into account the uncertainties to the local agents. The lower layer, comprised of local agents, solves an optimization problem in a distributed fashion. The HD-MPC method is tested on a real-world case, the North Sea Canal system. At this point, results show the benefits of the proposed method regarding control performance of large-scale systems.

Chapter 4 provides an analysis of the vulnerability of a distributed model predictive control scheme in the context of cyber-security. A distributed system can be easily attacked by a malicious agent that modifies the reliable information exchange. We consider different types of so-called insider attacks. In particular, it is analyzed a controller that is part of the control architecture that sends false information to others to manipulate costs for its own advantage. In addition, mechanisms to protect or, at least, relieve the consequences of attack in a typical DMPC negotiation procedure is proposed. More specifically, a consensus approach that dismisses the extreme control actions is presented as a way to protect the distributed system from potential threats. In this sense, secure dual decomposition techniques based on stochastic MPC is developed to mitigate the impact that an attacker can cause to the other controllers. A distributed local electricity grid of households is considered as case study to illustrate both the consequences of the attacks and the defense mechanisms.

Finally, conclusions are drawn in Chapter 5.

Chapter 2

Centralized Stochastic Model Predictive Control

In this chapter, three popular stochastic MPC techniques (MS-MPC, TB-MPC, and CC-MPC) are briefly introduced. Moreover, these stochastic approaches have been applied on the framework of centralized distribution applications. In first place, stochastic MPC controllers have been designed to power dispatch in a real hydrogen-based microgrid. Moreover, a comparison among these controllers is carried out on a second case study, the Barcelona drinking water network. Finally, CC-MPC is applied to stock management in a hospital pharmacy. These three applications have been presented previously in [31–33], respectively.

2.1 Model Predictive Control (MPC)

MPC is a strategy based on the explicit use of a dynamical model of the plant to predict the state/output evolution of the process in future time instants along a prediction horizon N_{p} [2]. The set of future control signals is calculated by the optimization of a criterion or objective function. Only the control signal calculated for the time instant k is applied to the process, whereas the others are withdrawn. One of the advantages of MPC over other control methods includes the easy extension to the multivariable case.

The optimization problem to be solved at each time instant k is formulated as

$$\min_{\{u(k),\ldots,u(k+N_\mathrm{p}-1)\}} \sum_{i=0}^{N_\mathrm{p}-1} J(x(k+i), u(k+i)), \tag{2.1}$$

subject to

$$x(i+1) = Ax(i) + Bu(i) + D\omega(i), \tag{2.2a}$$
$$x(0) = x(k), \tag{2.2b}$$
$$x(i+1) \in \mathcal{X}, \tag{2.2c}$$
$$u(i) \in \mathcal{U}, \quad \forall i \in \mathbb{Z}_0^{N_\mathrm{p}-1}, \tag{2.2d}$$

where $x \in \mathbb{R}^{n_x}$, $u \in \mathbb{R}^{n_u}$, and $\omega \in \mathbb{R}^{n_d}$ represent the state vector of the system, the manipulated variables, and the system disturbances, respectively. Moreover, $A \in \mathbb{R}^{n_x \times n_x}$, $B \in \mathbb{R}^{n_x \times n_u}$, and $D \in \mathbb{R}^{n_x \times n_d}$ are the matrices that defines the linear dynamic system. The sequence of inputs that must be applied to the system along the horizon is denoted by $\{u(k), ..., u(k+N_\mathrm{p}-1)\}$. Note that only $u(k)$ is actually applied.

A common approach used to cope with perturbed systems is to rely on the so-called certainty equivalence property [34], which in the MPC framework leads to a perturbed nominal deterministic MPC strategy, also named *certainty-equivalent* MPC (CE-MPC) in [35]. This strategy addresses perturbed systems by considering nominal models that do not include the uncertainty. Hence, the expected value of system inputs will lead to an average performing system. In the case of linear systems with uniformly distributed scenarios, the certainty equivalence property holds [36] and this strategy is optimal. Nevertheless, this may not be the case due to factors such as the presence of nonlinearities. Hence, the CE-MPC is usually complemented with a (de)tuning of the controller. Although, in one hand, a frequent violation of soft constraints can occur, on the other hand, infeasible solutions would result if the constraints were hard due to the ignored effects of future uncertainty.

Next, the description of the stochastic MPC techniques designed and implemented is presented.

2.1.1 Multiple-scenarios MPC approach (MS-MPC)

The optimization based on scenarios provides an intuitive way to approximate the solution to the stochastic optimization problem. In order to design the MS-MPC, it is required to know several scenarios with possible evolutions of the energy demand and

generation. The scenario forecasts can be obtained either from historical data or by introducing a random scenario generation. The idea behind this approach is that a general control sequence that optimizes all the considered scenarios is calculated, obtaining in this way a certain robustness against the different possible evolutions of the disturbances. The scenario-based approach is computationally efficient since its solution is based on a deterministic convex optimization, even when the original problem is not [37]. One advantage of this approach is that it does not assume a prior knowledge of the statistical properties that characterize the uncertainty (e.g., a certain probability function) as generally required in stochastic optimization.

The main idea for optimization with a finite number of scenarios is to consider the same system for each one of the known disturbance realizations. The problem consists in solving

$$\min_{\{u(k),\ldots,u(k+N_{\mathrm{p}}-1)\}} \sum_{j=1}^{N_s} \left(\sum_{i=0}^{N_{\mathrm{p}}-1} J(x_j(k+i), u(k+i)) \right), \tag{2.3}$$

subject to

$$x_j(i+1) = Ax_j(i) + Bu(i) + D\omega_j(i), \tag{2.4a}$$
$$x_j(0) = x(k), \tag{2.4b}$$
$$\omega_j(i) = \widehat{\omega}_j(i), \tag{2.4c}$$
$$x_j(i+1) \in \mathcal{X}, \tag{2.4d}$$
$$u(i) \in \mathcal{U} \quad \forall i \in \mathbb{Z}_0^{N_{\mathrm{p}}-1}, \quad \forall j \in \mathbb{Z}_1^{N_s}, \tag{2.4e}$$

where $N_s \in \mathbb{Z}_+$ is the finite number of scenarios considered and $\widehat{\omega}_j(k)$ is the disturbance forecast for scenario$j \in \mathbb{Z}_1^{N_s}$.

Due to the stochastic nature of the disturbances, the number of scenarios considered N_s deserves special attention to ensure compliance with the state constraints with a certain confidence degree, i.e.,

$$\mathbb{P}\left[x_j(i+1) \in \mathcal{X}\right] > 1 - \delta_x,$$

where $\mathbb{P}[\cdot]$ denotes the probability operator and $\delta_x \in (0,1)$ is the *risk acceptability level* of constraint violation for the states. The number of scenarios needed to achieve this goal can be calculated as a function of δ_x, the number of variables in the optimization problem (z), and a quite small confidence level $(\beta \leq 10^{-6})$, as indicated

in [38]

$$N_s \geq \frac{z + 1 + \ln(\frac{1}{\beta}) + \sqrt{2(z+1)\ln(\frac{1}{\beta})}}{\delta_x}. \tag{2.5}$$

Furthermore, the sample scenarios must meet the following assumptions, as pointed out in [37]:

1. The uncertainties $\widehat{\omega}_j$; $\forall j \in \mathbb{Z}_1^{N_s}$ are independent and identically distributed (IID) random variables on a probability space.

2. A "sufficient number" of IID samples of $\widehat{\omega}_j$ can be obtained, either empirically or by a random-number generator.

In this manner, a control sequence is optimized for the system given by (2.4a), which includes different possible evolutions of the original one. The calculation of the controller will result in a unique robust control action that satisfies all the potential realizations of the disturbances with a certain probability.

2.1.2 Tree-based MPC (TB-MPC)

This technique consists of transforming the different possible evolutions of the disturbances into a rooted tree that, through its evolution, diverges and generates a reduced number of scenarios. The points of divergence are called *bifurcations* and they represent moments in time in which the potential evolution of the disturbances is uncertain enough to consider more than one trajectory, as shown in Figure 2.1. The formulation of the control problem involves making tree-based optimization scenarios, where only the most relevant disturbance patterns are modeled, starting with a common root that corresponds to the current disturbance at each time instant. It must be noted that TB-MPC formulates the optimization problem by means of Multistage Stochastic Programming [39, 40]. The number of scenarios used to build the tree should be coherent with the computational capability of the controller and the risk probability, δ_x.

Being a scenario-based approach, it is possible to determine δ_x by taking into account the number of discarded scenarios R from the initial N_s scenarios for any violation level $\upsilon \in [0, 1]$, as seen in [37]. The probability of satisfying the state constraints is given by

$$\mathbb{P}[x_{i+1} \in \mathcal{X}] \geq 1 - \delta_x,$$

where

$$\delta_x = \int_0^1 U(\upsilon) d\upsilon, \tag{2.6a}$$

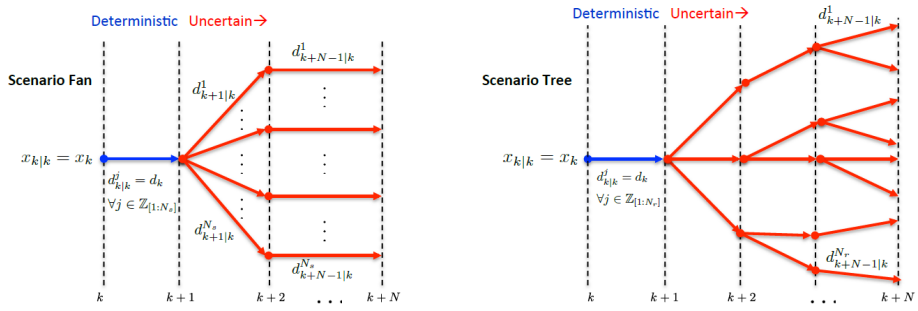

Figure 2.1: Scenario fan and scenario tree over the prediction horizon.

and

$$U(\upsilon) = \min\left\{1, \binom{R+z-1}{R} \sum_{j=0}^{R+z-1} \binom{N_s}{j} \upsilon^j (1-\upsilon)^{N_s-j}\right\}. \tag{2.6b}$$

In this way, the amount of N_r used in the optimization problem is calculated as $N_r = N_s - R$.

Unlike the MS-MPC approach, each scenario into the tree has its own control signal, which means that more optimization variables are needed. However, given that the control signal cannot anticipate events beyond the next bifurcation point, control sequences for different scenarios must be equal as long as the scenarios do not branch out. As a consequence, the solution of this control problem is a rooted-tree of control inputs. Notice that only the first component of this tree, which is equal for all the scenarios, is actually applied. For the design of this controller, the bifurcation points of the tree are checked: if they are equal, then the control actions are the same so that both the number of variables and the computational time can be reduced significantly.

The TB-MPC problem formulation to be solved at each time instant is represented by

$$\min_{\{u_j(k),\ldots,u_j(k+N_\mathrm{p}-1)\}} \sum_{j=1}^{N_r} \left(\sum_{i=0}^{N_\mathrm{p}-1} J(x_j(k+i), u_j(k+i)) \right), \tag{2.7}$$

subject to

$$x_j(i+1) = Ax_j(i) + Bu_j(i) + D\omega_j(i), \tag{2.8a}$$
$$x_j(0) = x(k), \tag{2.8b}$$
$$\omega_j(i) = \widehat{\omega}_j(i), \tag{2.8c}$$
$$x_j(i+1) \in \mathcal{X}, \quad \forall i \in \mathbb{Z}_0^{N_\mathrm{p}-1}, \tag{2.8d}$$
$$u_j(i) \in \mathcal{U}, \quad \forall j \in \mathbb{Z}_1^{N_r}. \tag{2.8e}$$

In addition, it is necessary to introduce non-anticipative constraints to force the controller to compute the control inputs only considering the observed uncertainty before the bifurcation points [40]. These constraints are given by

$$u_i(k) = u_j(k) \quad \text{if} \quad \widehat{\omega}_i(k) = \widehat{\omega}_j(k);\ \forall\, i \neq j. \tag{2.8f}$$

One way to satisfy (2.8f) is to introduce equality constraints into the optimization problem and solving it with a number of optimization variables defined as $z = N_\mathrm{p} \times N_r \times n_u$. Nevertheless, constraints in (4.19e) can be used to reduce the number of optimization variables by removing the redundancy to lower the computational burden.

As said before, a control sequence is optimized for the extended system with a disturbance tree, and only the first component of the input tree is applied to the system. The problem is repeated at each time instant $k \in \mathbb{Z}_+$.

2.1.3 Chance-Constrained MPC (CC-MPC)

Given that disturbances are stochastic, another way of addressing this problem is using CC-MPC. The stochastic behavior from the disturbances can be addressed by formulating hard constraints into probabilistic constraints related to a risk of constraint violation that determines the degree of the conservatism when computing the control inputs. Also, the cost function is expressed as its expected value in the formulation of the optimization problem. A major advantage of this approach is that the computational burden is not increased as in the scenario-based techniques.

Given that the disturbances in the dynamic model (2.45) are stochastic, the state constraints (2.19) must be formulated in a probabilistic manner, i.e.,

$$\mathbb{P}[x(i+1) \in \mathcal{X} \mid Gx \leq g] > 1 - \delta_x. \tag{2.9}$$

Here, $G \in \mathbb{R}^{n_r \times n_x}$ and $g \in \mathbb{R}^{n_r}$. The probabilistic constraints (2.9), also called *chance constraints*, can be written in two different manners [19]:

- *Individual chance constraints* that express a probabilistic equivalent for each constraint. They are formulated as

$$\mathbb{P}[G_{(m)}x < g_{(m)}] > 1 - \delta_{x,m}, \quad \forall m \in \mathbb{Z}_1^{n_x}, \tag{2.10}$$

  where $G_{(m)}$ and $g_{(m)}$ are the m^{th} row of G and g, respectively. Each m^{th} row satisfies its respective $\delta_{x,m}$.

- *Joint chance constraints*, which take into account an unique risk of constraint violation for all stochastic constraints. They are written as

$$\mathbb{P}[G_{(m)}x < g_{(m)}, \quad \forall m \in \mathbb{Z}_1^{n_x}] > 1 - \delta_x. \tag{2.11}$$

  All rows jointly satisfy the unique δ_x.

The application of (2.11) along N_p is necessary to implement the controller. To this end, it is assumed that the disturbances behave as Gaussian random variables, with a known cumulative distribution function. The deterministic equivalent of these chance constraints can be formulated as follows:

$$\begin{aligned}\mathbb{P}[G_{(m)}x(k+1) < g_{(m)}] &> 1 - \delta_x \\ &\Leftrightarrow F_{G_{(m)}D\omega(k)}(g_{(m)} - G_{(m)}(Ax(k) + Bu(k))) > 1 - \delta_x \\ &\Leftrightarrow G_{(m)}(Ax(k) + Bu(k)) < g_{(m)} - F^{-1}_{G_{(m)}D\omega(k)}(1 - \delta_x). \end{aligned} \tag{2.12}$$

Here, $F_{G_{(m)}D\omega(k)}(\cdot)$ represents the cumulative distribution function of the random variable $G_{(m)}D\omega(k)$, and $F^{-1}_{G_{(m)}D\omega(k)}(\cdot)$ is its inverse cumulative distribution function.

Note that the expression (2.12) is the deterministic equivalent of the chance constraints and is built based on historical data.

The optimization problem formulation related to the design of the CC-MPC controller is stated as

$$\min_{\{u(k),\ldots,u(k+N_\mathrm{p}-1)\}} \sum_{i=0}^{N_\mathrm{p}-1} \mathbb{E}[J(x(k+i), u(k+i))], \tag{2.13}$$

subject to

$$x(i+1) = Ax(i) + Bu(i) + D\omega(i), \tag{2.14a}$$
$$x(0) = x(k), \tag{2.14b}$$
$$\omega(i) = \widehat{\omega}(i), \tag{2.14c}$$
$$G_{(m)}(Ax(k) + Bu(k)) < g_{(m)} - F^{-1}_{G_{(m)}D\omega(k)}(1 - \delta_x), \tag{2.14d}$$
$$u(i) \in \mathcal{U}, \quad \forall i \in \mathbb{Z}_1^{N_\mathrm{p}-1}, \tag{2.14e}$$

where $\mathbb{E}[\cdot]$ denotes the expected value of the cost function.

2.2 Case Study: A Hydrogen-based Microgrid

A microgrid is a network of electric generators that may take advantage of several renewable energy sources: solar panels, wind mini-generators, micro-turbines, fuel cells, among others, to meet the consumer demand by working together with the centralized grid or autonomously [41]. In a microgrid, the energy is generated only at certain times, being necessary to provide continuous service to meet the demand at any time of the day. Challenges arise from the natural intermittency of renewable energy sources and the requirements to satisfy the user energy demand [42]. Thereby, storage devices become very important in the operation of this type of systems. Among well-established energy storage technologies, there are batteries, super-capacitors, conventional capacitors, etc. In this case study, the use of hydrogen as an energy vector for energy storage is focussed. Hydrogen, combined with other renewable energy sources, is a safe and viable option to mitigate the problems associated with hydrocarbon combustion because the entire system can be developed as an efficient, clean, and sustainable energy source, as mentioned in [43]. The hydrogen is converted into electrical energy by using fuel cells; the reverse process, i.e., the transformation of electric energy into hydrogen, is conducted by electrolysis [44], or ethanol reforming [45], among other techniques.

The control problem in a microgrid is to satisfy the electricity demand under economical and optimal conditions despite the uncertainties and disturbances that might appear in the processes. Taking into account that there are mathematical models available that represent the main dynamics and the load of these systems [46], and that the control problem here requires the simultaneous handling of constraints, delays, and disturbances, model predictive control (MPC) emerges as a solution to this problem. In this, sense, uncertainty in the load and generation profiles has been mainly addressed indirectly in the dispatch problem by using the MPC approach [47].

2.2.1 Hydrogen-based Microgrid Description

The microgrid under study is the lab-scale microgrid called *HyLab* [48]. The microgrid test bench used in this study is an experimental platform specifically designed for testing control strategies. HyLab is composed of a modular system equipped with various components that allow experimentation and simulation of several types of renewable energy sources. In the Figure 2.2, a picture of the experimental Hylab platform is shown.

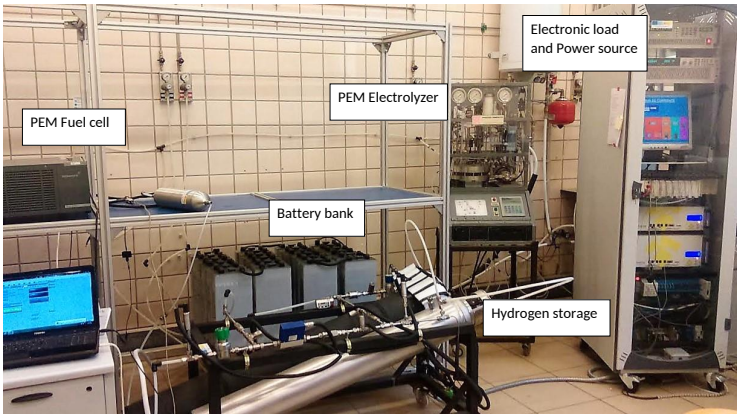

Figure 2.2: Experimental HyLab Plant.

The system consists of a solar field, emulated by an electronic power source, which produces electricity to supply the electronic load. Any excess of power can be either stored in a battery bank or derived to the electrolyzer. If the power obtained from renewable energy is not enough, both the fuel cell and the battery bank can support the load, which is emulated electronically. This type of hybrid storage operation allows implementing strategies in separated times scales: the battery can either absorb or contribute to balance small amounts of energy in fast transient periods while the hydrogen path complements larger variations [49]. The microgrid can work either connected to the utility network or as an isolated system. The Hydrogen Path is composed of three subsystems: the electrolyzer, which is proton exchange membrane (PEM) type [50], for producing hydrogen; a metal-hydride hydrogen storage tank; and finally a PEM fuel cell [51, 52] that provides power to the loads/batteries. It is important to notice that both subsystems –electrolyzer and fuel cell– cannot work simultaneously. DC/DC power converters are used as power interfaces that allow energy transfer between different distributed generation units. The equipment is connected to $48\ V_{\mathrm{DC}}$ bus that is held by the battery bank. Table 2.1 presents the nominal values of the HyLab equipment.

Microgrid linear model and constraints

As it can be inferred, behind the experimental setup there is a set of complex nonlinear subsystems. The detailed description of sub-models and the physical equations are out

Table 2.1: HyLab equipment.

Equipment	**Nominal Value**
Electronic power source	$6\,\mathrm{kW}$
Electronic load source	$2.5\,\mathrm{kW}$
PEM fuel cell	$1.2\,\mathrm{kW}$
PEM electrolyzer	$0.23\,\mathrm{Nm^3h^{-1}}$ @5barg
	$1\,\mathrm{kW}$
Metal hydrides tank	$7\,\mathrm{Nm^3}$
	$5\,\mathrm{bar}$
Battery bank	$C_{120} = 367\,\mathrm{Ah}$
DC/DC converters	$1.5\,\mathrm{kW}$, $1\,\mathrm{kW}$

of the scope of this work. The complete non-linear model of the plant, its simulation, and validation are presented in [53].

Remark 1 *To apply linear MPC techniques is required to find a linear model of the system around a working point (x^*, u^*). The identification process for obtaining the linear model of the plant is developed in [54]. The continuous linear system was discretized using Tustin's method with a sampling time of 30 s. Also, the working point is given by $u^* = [0\,\mathrm{kW}, 1.75\,\mathrm{kW}]^T$ and $x^* = [50\,\%, 50\,\%]^T$.*

The linear discrete-time model of the plant consists of two input variables, $P_{\mathrm{H_2}}(k)$ and $P_{\mathrm{grid}}(k)$, which are measured in kilowatts (kW). Here, $P_{\mathrm{H_2}}(k)$ represents the power of the electrolyzer and the power of the fuel cell: when it is greater than zero, the PEM fuel cell is working ($P_{\mathrm{fc}}(k)$), and when $P_{\mathrm{H_2}}(k)$ is negative, it indicates that the electrolyzer is operating ($P_{\mathrm{ez}}(k)$). Both the electronic load and the electronic power source can either deliver or absorb power from the utility power grid (UPG). The connection with the electric network is "virtual", since it is emulated by the source and electronic load. Moreover, $P_{\mathrm{grid}}(k)$ represents the power of UPG, which is positive when the power is imported by the microgrid from the UPG, and it is negative when exporting power to the UPG. The system is subject to uncertainties from the power produced by a renewable energy source; in this case, it is the power from the solar field, ($P_{\mathrm{res}}(k)$) and the power demanded by the consumers ($P_{\mathrm{dem}}(k)$); the difference between them can be considered as disturbances ($P_{\mathrm{net}}(k)$) to the system. Moreover, the plant counts with an additional variable, the power of the batteries (P_{batt}), which is

controlled indirectly, resulting of the power balance. The states are given by the state of charge of the batteries ($SOC(k)$), and the metal hydrides level ($MHL(k)$) of the storage tank, both measured in percentage ($\%$). A scheme of the power variables is shown in Figure 2.3. The discrete-time linear model of the plant, for each time instant $k \in \mathbb{Z}_+$, around a working point (u^*, x^*), can be written as

$$x(k+1) = Ax(k) + Bu(k) + D\omega(k), \tag{2.15a}$$

that is,

$$x(k+1) = x(k) + \begin{bmatrix} 8.1360 & 5.958 \\ -15.2886 & 0 \end{bmatrix} u(k) + \begin{bmatrix} 5.958 \\ 0 \end{bmatrix} \omega(k). \tag{2.15b}$$

In this model, $u(k) = [P_{\mathrm{H2}}(k), P_{\mathrm{grid}}(k)]^T$ represents the vector of manipulated variables, $x(k) = [SOC(k), MHL(k)]^T$ is the state vector of the system and $\omega(k) = P_{\mathrm{net}}(k) \in \mathbb{R}^{n_d}$ represents the system disturbance, where $n_d = 1$.

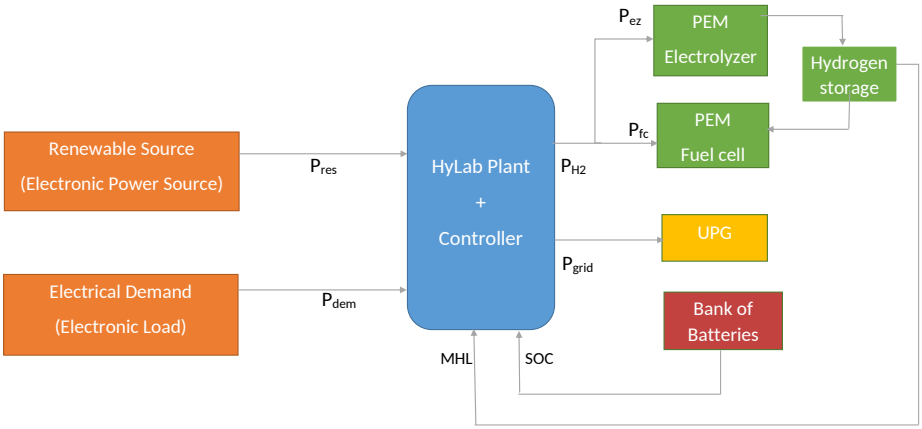

Figure 2.3: HyLab variables scheme.

The system is subject to constraints that avoid equipment damage and guarantee its safe operation. In particular, the Hydrogen Path –both the electrolyzer and the fuel cell– has constraints for limiting the values of $P_{\mathrm{H}_2}(k)$ since its power capacity is limited to 0.9 kW; this value reflects some conservatism and it ensures that the hydrogen path does not work at its nominal value to protect the equipment. In this way, a longer lifespan is expected. Also, the Hydrogen Path has a dead zone between -0.1 kW

and 0.1 kW that ensures a minimum production of power from both the electrolyzer and the fuel cell. The constraints for $P_{\mathrm{grid}}(k)$ correspond to physical limitations of the electronic units. Furthermore, it is necessary to include constraints on their incremental signals $\Delta P_{\mathrm{H_2}}(k)$ and $\Delta P_{\mathrm{grid}}(k)$, to guarantee the physical safety of the equipment. These constraints are mathematically expressed as follows:

$$-0.9\,\mathrm{kW} \leq P_{\mathrm{H_2}}(k) \leq 0.9\,\mathrm{kW}, \tag{2.16a}$$
$$-2.5\,\mathrm{kW} \leq P_{\mathrm{grid}}(k) \leq 2\,\mathrm{kW}, \tag{2.16b}$$
$$-20\,\mathrm{Ws}^{-1} \leq \Delta P_{\mathrm{H_2}}(k) \leq 20\,\mathrm{Ws}^{-1}, \tag{2.16c}$$
$$-2.5\,\mathrm{kWs}^{-1} \leq \Delta P_{\mathrm{grid}}(k) \leq 2\,\mathrm{kWs}^{-1}. \tag{2.16d}$$

Overall constraints have to be considered as *hard constraints*, since the equipment lifespan could be drastically reduced. Both the battery bank and the metal hydrides storage tank have limited capacity to prevent any plant damage by overcharge or undercharge. Constraints on $SOC(k)$ guarantee suitable voltage levels in the 48 V_{DC} bus. Also, they protect the battery bank of strong load voltage variations. These state constraints are written as

$$40\,\% \leq SOC(k) \leq 90\,\%, \tag{2.17a}$$
$$10\,\% \leq MHL(k) \leq 90\,\%. \tag{2.17b}$$

The input constraints given by (2.16) can be properly rewritten as

$$u(k) \in \mathcal{U} \subseteq \mathbb{R}^{n_u}, \tag{2.18}$$

with $n_u = 2$, while the state constraints defined by (2.17) are expressed as

$$x(k) \in \mathcal{X} \subseteq \mathbb{R}^{n_x}, \tag{2.19}$$

with $n_x = 2$. Furthermore, the total power delivered to the load, in order to satisfy the consumer demand, must satisfy the energy balance

$$P_{\mathrm{dem}}(k) = P_{\mathrm{H2}}(k) - P_{\mathrm{batt}}(k) + P_{\mathrm{grid}}(k) + P_{\mathrm{res}}(k). \tag{2.20}$$

The multi-objective cost function to be minimized is given by

$$\begin{aligned} J(x(k), u(k)) &= a_1(SOC(k) - SOC_{\mathrm{ref}})^2 \\ &+ a_2(MHL(k) - MHL_{\mathrm{ref}})^2 \\ &+ b_1 P_{\mathrm{H_2}}^2(k) + b_2 P_{\mathrm{grid}}^2(k). \end{aligned} \tag{2.21}$$

Here, $SOC_{\text{ref}} = 65\%$ and $MHL_{\text{ref}} = 40\%$ are the references given for the state of charge of the batteries and the metal hydride level, respectively. The tuning of the cost function weights seeks for a soft tracking of the output variables towards the given references and an efficient use of the energy. More specifically, the controller is designed such that the batteries are the first way of energy storage. If there exists a big difference between the demanded energy and the produced energy by the renewable sources, it proceeds to the production of hydrogen. These prioritization weights a_i, b_i have been adjusted by trial and error approach carried out on simulation tests reported in previous works with this plant, see, e.g. [44, 54, 55]. In this sense, they have been established as $a_1 = a_2 = 10$, $b_1 = 5000$, and $b_2 = 8000$. As can be seen, the weight associated with the hydrogen production is lower than the weight related to the power of the grid in order to minimize the power interchange with the UPG. The weights associated with the outputs take low values compared with the others to give flexibility to the smart grid. However, these values can be modified in the multi-objective function (4.4) for tracking the reference. In this work, the energy management is the main objective, therefore the weights associated with the hydrogen path and the grid are higher than those associated with the outputs of the system.

2.2.2 Results and Discussion

The experiments were conducted in the microgrid described in Section 2.2.1 during a trial period of eight hours for each experiment. The controller receives the measured variables $SOC(k)$ and $MHL(k)$, which are used to compute the optimal control signals $P_{\text{H2}}(k)$ and $P_{\text{grid}}(k)$) by means of Simulink Real-Time workshop toolbox. The control signals are sent to the SCADA via the OPC Matlab Library and finally the PLC carries out these control actions.

The prediction horizon was $N_{\text{p}} = 5$ and the sampling time was 30 s. The selected weather and load profiles for verifying the performance of the three proposed controllers were the scaled difference between the real solar generation and the demand registered by the Spanish National Electricity Network (SNEN)[1] on May 23, 2014. These values were sampled each 3 s and scaled for the microgrid allowable power values, which are shown in Figure 2.4(a). The initial conditions for all experiments were $SOC(0) = 70\%$ and $MHL(0) = 50\%$.

An issue that deserves particular attention is the amount of scenarios to be considered into the optimization problem. This number should be selected by taking into account a trade-off between robustness and computational burden. In this sense, it is possible to establish the number of scenarios that guarantees a particular risk level,

[1] SNEN demand data can be obtained at: https://demanda.ree.es/movil/peninsula/demanda/total

according to (2.5), as shown Table 2.2.

Table 2.2: Number of scenarios (N_s) that fulfills an specific risk level (δ_x).

δ_x	0.20	0.15	0.10	0.05	0.01
N_s	152	203	316	611	3005

MS-MPC was performed by using the electricity demand and the solar generation registered during $N_s = 316$ different days of one year from historical data, obtained from the SNEN. For these scenarios, it is expected a risk of violation of constraints less than $\delta_x \leq 10\%$. This number of scenarios offers an acceptable risk and ensures a reasonable computational burden when solving the optimization problem. Furthermore, this set of scenarios considers days with enough solar energy generation as well as cloudy days, which makes the controllers more robust and somehow relieves the need for increasing the number of scenarios used. TB-MPC was performed by using an original number of $N_s = 316$ scenarios, which were reduced to $N_r = 250$ scenarios forming a tree using GAMS [56]. This reduction tried to replicate the main dynamics of all original disturbances considered in a small disturbance tree. This reduction introduces a boundary that guarantees $\delta_x \leq 10\%$, according to (2.6). Finally, CC-MPC approach was performed considering the failure probability $\delta_x = 10\%$. The disturbances were considered as a random function with a cumulative distribution function (cdf), which were obtained from the historical daily data registered in 2014.

The scheme of the microgrid operation, from a general point of view, follows similar patterns for the three proposed controllers. At this point, given that the energy from the renewable source is not sufficient to meet the energy demand, the fuel cell turns on, the battery SOC and the MHL decrease gradually without going below their forbidden levels. Also, energy is imported from the grid to meet the load beyond demand. When the energy from the renewable source greatly exceeds demand, the electrolyzer is switched on, the batteries are fully charged, and the excess of energy is stored in the hydrogen tank, and the remaining power that cannot be stored in the form of hydrogen is exported to the grid. However, each stochastic MPC approach shows particular differences, as reported below, which are highlighted to offer a suitable comparison among them.

In order to compare all the considered strategies, Figure 2.4(b) shows the battery power for the three aforementioned stochastic predictive controllers. As can be noticed, CC-MPC controller performs a deep cycle using the batteries. It strives for using the full capacity, reaching the upper and lower levels. In contrast, TB-MPC controller,

although partly discharges and recharges the batteries, it does in a softer way. This implies that the excess of energy must be balanced through either the electrolyzer or the grid. It is observed that MS-MPC technique behaves between the two other approaches. Therefore, MS-MPC controller achieves a trade-off between using the full capacity of the batteries and the energy derived either to the electrolyzer or the grid.

Figure 2.4(c) presents the fuel cell and electrolyzer power along the test duration. The fuel cell performance signals obtained are similar for all the three controllers, except for CC-MPC controller, which shows a peak between the first and second hour, to satisfy an increase in the energy demand at that time. When there is an excess of energy from the renewable source, the electrolyzer starts its operation. Results show a clear difference in the electrolyzer operation. On the one hand, with CC-MPC technique, the electrolyzer presents a larger use of the power, as expected. On the contrary, the electrolyzer utilization is restricted quite more with TB-MPC approach, reaching only a peak of 200 W, while CC-MPC controller sets the electrolyzer power to nearly 600 W. Regarding TB-MPC approach, it also shows a small ripple; this is explained because the controller seeks to primary satisfy the demand and compensate any power unbalance in the system. As it has been shown through experimental tests, there are clear differences in the way each controller manages the power signals of the electrolyzer and the fuel cell.

Figure 2.4(d) shows the grid power signal generated by applying the stochastic MPC controllers. From the point of view of the network operators (DSO[2]/TSO[3]), the use of the UPG is minimized with the CC-MPC approach. In this manner, the impact in the electrical system generated by the renewable sources present in the microgrid is reduced. On the other hand, for the consumer point of view, it might be convenient not to force the equipment to a deep duty cycle and take advantage of the grid to smooth the power profiles.

Figure 2.4(e) shows the evolution of the SOC and MHL for each proposed controllers along the test period. In general, for all the implemented controllers, the batteries are discharged until the fuel cell turns off at the first time, and then they raise their charge level lower than 85% for MS-MPC and CC-MPC controllers. Regarding TB-MPC controller, it holds a charge level around 75% for a longer period compared with the other ones. Then, the SOC starts to decrease again for all controllers under study. The MHL presents a minor variation, and it reduces its level below 40% until the renewable source can contribute with power to the load. After this, the MHL seeks to track its reference.

[2]DSO: Distributed System Operator
[3]TSO: Transmission System Operator

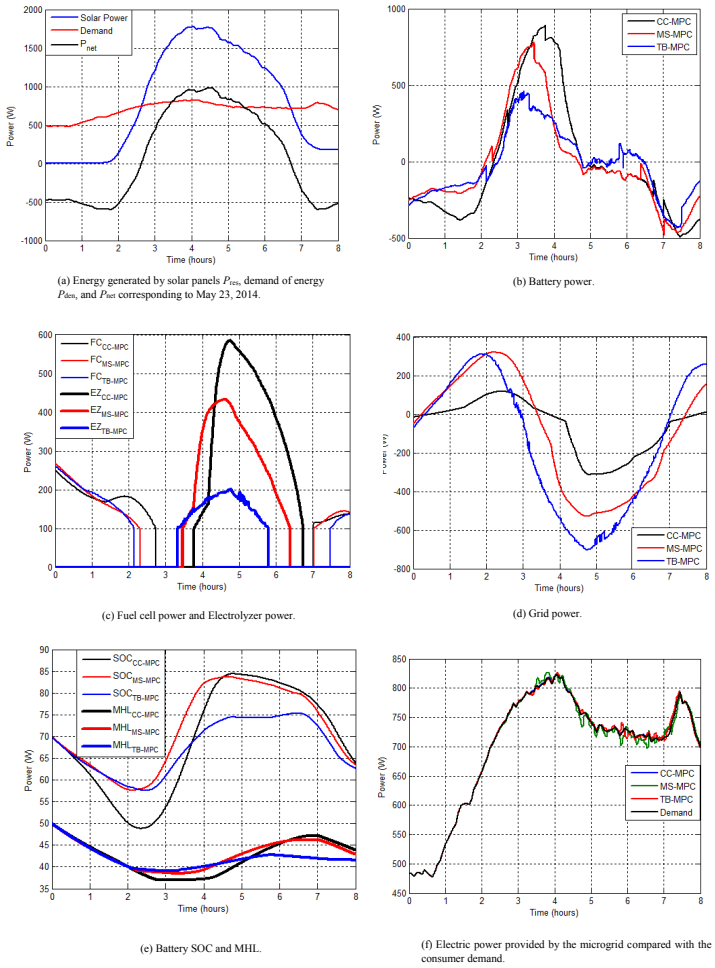

(a) Energy generated by solar panels P_{res}, demand of energy P_{den}, and P_{net} corresponding to May 23, 2014.

(b) Battery power.

(c) Fuel cell power and Electrolyzer power.

(d) Grid power.

(e) Battery SOC and MHL.

(f) Electric power provided by the microgrid compared with the consumer demand.

Figure 2.4: Experimental results applying the proposed stochastic MPC approaches.

Figure 2.4(f) shows the comparison among the different powers delivered to the load by applying the controllers. As seen, the demand is satisfied by the power from the microgrid for all the controllers as imposed in their design. Notice that, in some situations, using the "elasticity" of the consumer; it might be possible to momentarily

unbalance the power demand to satisfy other microgrid objectives [57]. Nevertheless, demand response is out of the scope of this work.

In order to quantitatively assess the performances of these three stochastic approaches that have been implemented in the HyLab microgrid laboratory, several KPIs have been defined as follows:

- KPI_1 defines the final cumulative cost given by (4.4) (in cost units).
- KPI_2 is the computational time to solve the optimization problem (in s).
- KPI_3 counts the average unmet demand with respect to the overall power demand (in %).
- KPI_4 is the time that the fuel cell is operating (in hours).
- KPI_5 is the time that the electrolyzer is operating (in hours).
- KPI_6 indicates the final value of SOC (in %).
- KPI_7 indicates the final value of MHL (in %).

Table 3 summarizes the numerical results of the KPIs. As it can be seen the highest value for KPI_1 is obtained when using MS-MPC. The rationale behind this value is that the controller optimizes a sequence of control actions valid for the most favorable scenarios as well as the least favorable ones. In this sense, an over-conservative control action is carried out. This issue can be relaxed by calculating a tree of control actions that is subject to non-anticipatory equality constraints. In this way, the control actions are calculated in a closed-loop fashion, i.e., the controller can adapt the future control actions to the evolution of the disturbances. As can be seen, TB-MPC reduces its cumulative cost by increasing the number of control variables involved into the optimization problem. Hence, its computational time is the biggest within this comparative study. Regarding CC-MPC, it has the lowest cumulative cost without increasing the number of control variables. For reference purposes, the final cumulative cost for an MPC with a perfect forecast (PF-MPC), obtained via simulation, is 2.05×10^{12}. The computational time comparison is provided by KPI_2.

The three tested controllers are able to meet the overall demand in a satisfactory way, as indicated by the performance comparison given by KPI_3. At this point, we must remark that the three tested controllers solve their optimization problems faster than the sampling time. Therefore, it is possible to select the approach that has the best performance in terms of the demand satisfaction and the use of the hydrogen path.

Table 2.3: Comparison of the MS-MPC, TB-MPC, and CC-MPC controllers applied to HyLab microgrid by means of $\text{KPI}_i, \quad i = 1, ..., 7$.

Controller	**KPI**$_1$ (cost units)	**KPI**$_2$ (s)	**KPI**$_3$ (%)	**KPI**$_4$ (hours)	**KPI**$_5$ (hours)	**KPI**$_6$ (%)	**KPI**$_7$ (%)
MS-MPC	3.89×10^{12}	7.76	0.12	3.26	2.90	63.53	42.91
TB-MPC	2.75×10^{12}	18.15	0.11	2.63	2.45	62.51	41.58
CC-MPC	2.44×10^{12}	1.04	0	3.70	2.97	63.71	43.85

The comparisons between the proposed controllers regarding the time when both the fuel cell and the electrolyzer are operating are given by KPI_4 and KPI_5, respectively. In this sense, TB-MPC shows the lowest time for the fuel cell and the electrolyzer. It offers a larger conservatism when working with the hydrogen path, which is obtained at the expense of a higher computational time since TB-MPC meets the current demand and reformulates its disturbance tree at each time step. Notice that the main difference is at the time that the hydrogen path is working.

The final values of SOC and MHL, which present similar values for the three controllers, are around 63% and 42%, respectively. These values are provided by KPI_6 and KPI_7.

Table 2.4 presents a comparison among the total energy produced by the fuel cell (E_{fc}), the electrolyzer (E_{ez}), the batteries (E_{batt}), and the grid (E_{grid}) during the test period. The negative sign in E_{grid} indicates that the amount of energy sold to UPG is greater than the energy purchased. The total energy of the batteries indicates the difference between the stored energy and the delivered energy to the load: the negative value means that the stored energy predominates over the delivered energy.

Table 2.4: Energy produced by the fuel cell, electrolyzer, batteries, and grid during the test period by applying the proposed stochastic MPC controllers.

Controller	E_{fc} (Wh)	E_{ez} (Wh)	E_{batt} (Wh)	E_{grid} (Wh)
MS-MPC	302	481	-62.2	-418
TB-MPC	261	217	-110.23	-661
CC-MPC	348	642	-43.09	-268

Notice that the absolute value of the energy amounts are taken to achieve a reliable comparison in terms of energy consumption for each component of the system. In this sense, CC-MPC has better performance regarding energy efficiency. CC-MPC achieves less exchange with UPG, and the batteries provide enough power to supply the load. Also, both the fuel cell and electrolyzer use energy in a wider range when compared to the MS-MPC and TB-MPC approaches. Note also that TB-MPC and MS-MPC handled more cautiously hydrogen energy from the path while performing more exchanges with the UPG, specially TB-MPC.

Another KPI to compare the performance of the controllers for energy management in a smartgrid is the number of start-ups for both equipment, the fuel cell and the electrolyzer. From the results obtained from the experimental setup, the number of start-ups is the same for all the controllers. However, it is a major factor that could reduce the lifespan of the hydrogen path.

Finally, Table 2.5 shows the range of values of each variable obtained during the experiments by applying the proposed approaches. As seen, the control actions satisfy the constraints given by (2.16) and (2.17).

Table 2.5: Range of values for the states and control inputs obtained during the test period by applying the proposed stochastic MPC controllers.

Variable	**MS-MPC**	**TB-MPC**	**CC-MPC**
$SOC\ (\%)$	$[57.61, 83.73]$	$[57.59, 75.30]$	$[48.82, 84.42]$
$MHL\ (\%)$	$[38.51, 50]$	$[39.07, 50]$	$[37.06, 50]$
$P_{\mathrm{fc}}(\mathrm{W})$	$[100, 268.13]$	$[100, 259.69]$	$[100, 250.44]$
$P_{\mathrm{ez}}(\mathrm{W})$	$[100, 432.9]$	$[100, 202.13]$	$[100, 584.94]$
$P_{\mathrm{grid}}(\mathrm{W})$	$[-529.4, 320.3]$	$[-705.02, 314.0]$	$[-312.8, 117.5]$

In order to extend the comparative analysis to general results and taking into account that the experimental setup of the plant is limited, the non-linear simulation model developed in [53] is used to compare the controllers in other situations and the same circumstances. This simulation model replicates the main dynamics of the real plant with enough accuracy. An additional case study for testing the three stochastic MPC controllers and a PF-MPC controller is introduced to enhance the results and obtain conclusions.

Figure 2.5 shows the evolution of the signals by applying the three stochastic MPC controllers and a PF-MPC controller for a cloudy day in the simulation model of the

HyLab microgrid. All controllers present the same evolution to satisfy the demand. The fuel cells are turned on when the power from the renewable sources is not enough to meet the electric demand. Hence, SOC and MHL decrease gradually to supply power to the load. For this particular day, the microgrid imports energy power from the UPG. Given that the excess of renewable energy production over the demand is not enough, the batteries are charged, and the electrolyzer stays off.

To compare the behavior of these MPC controllers, Table 2.6 shows the results from aforementioned KPIs. The results obtained from the comparison are similar to the previous experimental case study. As expected, the lowest value of KPI_1 is presented by standard MPC controller with perfect information; this value gives a target for the comparison. In this sense, CC-MPC controller results in a lower cumulative cost as well as the computational time compared with MS-MPC and TB-MPC controllers. The electrical demand is satisfied by all controllers. Regarding KPI_3, MS-MPC controller uses the hydrogen path longer than the other two approaches. Finally, KPI_6 shows very similar values for all controllers, the battery SOC is reduced until its lower constrained level. The lowest value of KPI_7 is presented by CC-MPC controller because this controller delivers a bigger amount of energy from the fuel cell. Finally, the electrolyzer stays off over the simulation period; therefore KPI_5 is zero for all controllers.

Table 2.6: Comparison of the MS-MPC, TB-MPC, CC-MPC, and PF-MPC controllers applied to the simulation model of HyLab microgrid for a cloudy day by means of $\text{KPI}_i, \quad i = 1, ..., 7$.

Controller	**KPI**$_1$ (cost units)	**KPI**$_2$ (s)	**KPI**$_3$ (%)	**KPI**$_4$ (hours)	**KPI**$_6$ (%)	**KPI**$_7$ (%)
MS-MPC	6.24×10^{12}	7.76	0.10	6.00	40.56	20.43
TB-MPC	5.33×10^{12}	18.20	0.11	5.67	40.64	23.46
CC-MPC	4.22×10^{12}	1.04	0.10	5.68	40.46	14.08
PF-MPC	4.05×10^{12}	0.98	0	5.90	40.01	19.77

Table 2.7 compares the stochastic MPC controllers regarding energy for a cloudy day via simulation. The CC-MPC controller results in higher energy consumption from the fuel cell. The energy from the renewable sources is not enough at the time to turn on the electrolyzer for storing energy as hydrogen. The batteries are used to provide energy to the load; both, MS-MPC and TB-MPC controllers, show a similar use of the energy of the batteries. A remarkable difference is shown in the energy exchanged with

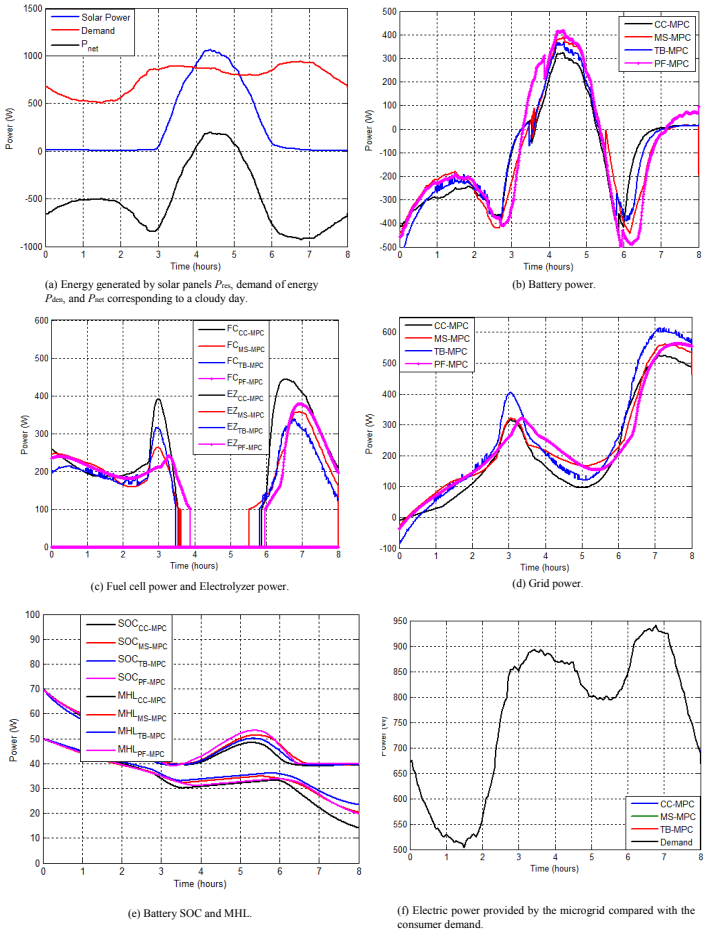

(a) Energy generated by solar panels P_{res}, demand of energy P_{den}, and P_{net} corresponding to a cloudy day.

(b) Battery power.

(c) Fuel cell power and Electrolyzer power.

(d) Grid power.

(e) Battery SOC and MHL.

(f) Electric power provided by the microgrid compared with the consumer demand.

Figure 2.5: Simulation results for a cloudy day applying the proposed stochastic MPC approaches and a standard PF-MPC.

the grid, in this case, the TB-MPC controller presents the highest value.

All in all, Table 2.8 shows priority factors for each one of the proposed stochastic

Table 2.7: Energy produced by the fuel cell, electrolyzer, batteries, and grid during the test period for the simulation model by applying the proposed stochastic MPC controllers.

Controller	E_{fc} (Wh)	E_{ez} (Wh)	E_{batt} (Wh)	E_{grid} (Wh)
MS-MPC	472	0	-285	688
TB-MPC	437	0	-287	721
CC-MPC	547	0	-295	604

Table 2.8: Priority factors for selecting one of the proposed stochastic MPC controllers.

Priority	**MS-MPC**	**TB-MPC**	**CC-MPC**
Maximization of hydrogen path lifespan		✓	
Minimization of energy exchanged with the UPG			✓
Cumulative cost			✓
Computational burden			✓
Demand satisfaction	✓	✓	✓
Availability of historical data	✓	✓	

MPC controllers based on the overall analysis at the time of selecting one of them.

Other factors that are important to take into account are the initial conditions for SOC and MHL. These values will determine the evolution of the variables. Besides, the final value of these variables will take an additional meaning of comparison after a longer time of use of the plant. However, they have been employed in a smaller period to show how they finish after the experiments.

These results have been published in [31].

2.3 Case study: Drinking Water Network

Drinking water networks (DWNs) transport water from sources to consumers ensuring the quality of service [58]. Nevertheless, limited water sources, conservation and sustainability policies, as well as the infrastructure complexity for meeting consumer demands with appropriate flow pressure and quality levels make water management a challenging problem [1]. Water demand forecasting based on historical data is com-

monly used for the operational control of water supply along a given prediction horizon. However, the optimality of such scheduling is affected by the one associated to water demand forecasts. Therefore, the scheduling of control inputs must be continuously adjusted. This leads to consider the DWNs as dynamical systems and their operation as optimal control problems, with the objective of satisfying water demands in an optimal manner despite the presence of disturbances and uncertainties, and considering additionally issues such as constraints on the manipulated and output variables and multiple conflicting control goals.

The MPC approaches presented in this work are assessed with two representative case studies based on the Barcelona DWN.

A DWN must satisfy water demands and guarantee service reliability by making optimal use of water sources and network components in order to minimize economic costs. The water network operates as a full-interconnected system driven by endogenous and exogenous flow demands. In the Barcelona DWN, water is taken from both superficial and underground sources. Flows coming from sources are regulated by pumps or valves. After being extracted from sources, water is purified up to levels suitable for human consumption in four water treatment plants (WTP). The water flow from any of the sources is limited and has costs associated to the extraction and the treatment required. The DWN is divided in two management layers: the *transport network*, which links the water treatment plants with the reservoirs located all over the city, and the *distribution network*, which is sectored in sub-networks, linking reservoirs directly to consumers. In this work, each sector of the distribution network is considered as a pooled demand to be satisfied by the transport network.

The two systems under study have been extracted from the Barcelona transport network. The first case study consists in a sector model and the second one is an aggregate model of the whole network. They differ mainly in the size of the network flow problems and the number of constitutive elements:

- The sector network considers only a small-scale subsystem related to a portion of the overall DWN (see Fig. 2.6). This case study considers 2 water sources, 3 tanks, 6 flows controlled by valves and pumps, 4 demand nodes and 2 intersection nodes.

- The aggregate network represents a simplification from the original DWN, where sets of elements are aggregated in a single element in order to reduce the size of the original model (see Fig. 2.7). It consists of 9 water sources, 17 tanks, 61 flows controlled by valves and pumps, 25 demand nodes and 11 intersection nodes.

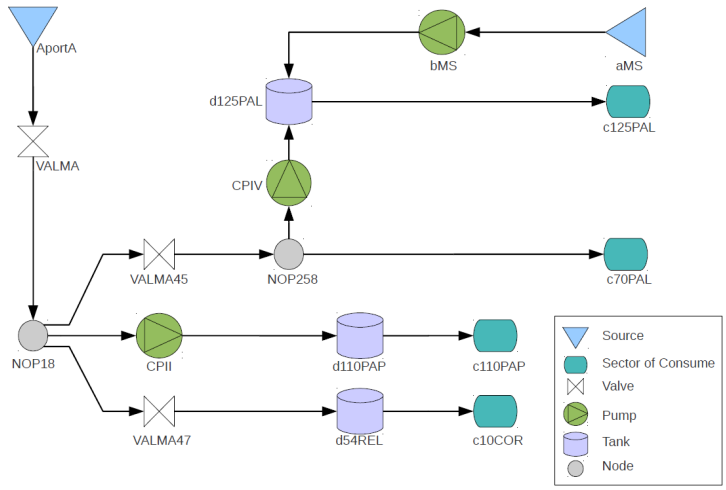

Figure 2.6: Sector diagram of the Barcelona DWN

Demand Modelling and Scenario Generation

In DWNs, the uncertainty is generally introduced by the stochastic behavior of water consumers. Therefore, a proper demand modeling is required to achieve an acceptable water supply service level. For the case studies of this work, time series forecasting based on auto-regressive integrated moving average (ARIMA) models are used due to its ability to capture complex linear dynamics from historical data [59]. In this way, it is possible to generate artificial scenarios with similar statistical properties to those obtained from historical data.

A correct sampling of scenarios is essential for developing the proposed SMPC approaches. For the CC-MPC approach, ARIMA models are used to generate a large number of possible demand scenarios by Monte Carlo sampling for a given time horizon $N_{\mathrm{p}} \in \mathbb{Z}_+$; the mean demand is then used for the controller design. For the MS-MPC approach, a set of $N_s \in \mathbb{Z}_+$ water demand scenarios is generated and used. Increasing the number of scenarios allows the controller to gain robustness but at the expense of additional computational effort and economic performance losses. MS-MPC is generally over-conservative, because it does not consider the controller capacity to adapt to the new observations of the uncertainty and reformulate its controller structure at each time instant. To cope with this drawback, a representative subset of scenarios might be chosen using scenario reduction algorithms [39, 60]. Moreover, the

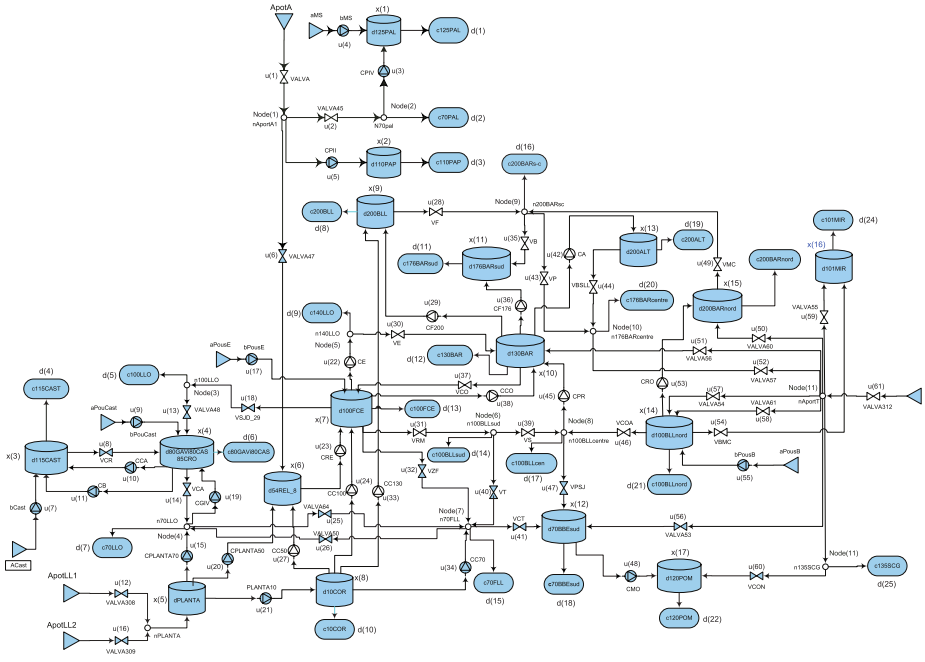

Figure 2.7: Aggregate model of the Barcelona DWN

reduced set of scenarios can be transformed into a rooted tree of possible evolutions of the demand [61], so that, it can be used with the TB-MPC approach, see, e.g., [14, 62]. More specifically, a reduction of the initial number of scenarios into a rooted tree of N_r scenarios, obtained by generating an ensemble forecast tree, only reduces the number of scenarios that have similar features with their adjacent scenarios. The disturbances tree remains the dominant scenarios. The rationale behind this approach is that uncertainty spreads with time, i.e., it is possible to predict more accurately the demand evolution in a short time horizon than in a large one. Besides, TB-MPC takes into account, within the optimization problem, the MPC capacity to adapt, i.e., a control input sequence is calculated for each branch of the tree at each time step, by implementing the so-called Multistage Stochastic Programming, as pointed in [40].

2.3.1 DWN Control Problem Statement

This section introduces the CE-MPC formulation, including the system defined by time-invariant state-space linear model in discrete time, its goals and constraints.

Control-oriented Model

The system model may be described considering the volume of water in tanks as the state variables $x \in \mathbb{R}^n$, the flow through the actuators as the manipulated inputs $u \in \mathbb{R}^m$, and the demanded flows as additive measured disturbances $d \in \mathbb{R}^p$. The control-oriented model of the network is described by the following equations for all time instant $k \in \mathbb{Z}_+$:

$$x_{k+1} = Ax_k + Bu_k + B_p d_k, \tag{2.22a}$$

$$0 = E_u u_k + E_d d_k, \tag{2.22b}$$

where (2.22a) and (2.22b) describe the mass balance equations for storage tanks and intersection nodes, respectively. Moreover, $A \in \mathbb{R}^{n_x \times n_x}$, $B \in \mathbb{R}^{n_x \times n_u}$, $B_p \in \mathbb{R}^{n_x \times n_d}$, $E_u \in \mathbb{R}^{n_q \times n_u}$ and $E_d \in \mathbb{R}^{n_q \times n_d}$, are time-invariant matrices dictated by the network topology.

Assumption 1 *The states in x and the demands in d are measured at any time instant $k \in \mathbb{Z}_+$.*

Assumption 2 *The pair (A, B) is controllable and* (2.22b) *is reachable*[4]*, provided that $n_q \leq n_u$ with $\text{rank}(E_u) = n_q$.*

Assumption 3 *The realization of disturbances at the current time instant k may be decomposed as*

$$d_k = \bar{d}_k + e_k, \tag{2.23}$$

where $\bar{d}_k \in \mathbb{R}^{n_e}$ is the vector of expected disturbances, and $e_k \in \mathbb{R}^{n_e}$ is the vector of forecasting errors with non-stationary uncertainty and a known (or approximated) quasi-concave probability distribution $\mathcal{D}$. Therefore, the stochastic nature of each j^{th} row of d_k is described by $d_{(j),k} \sim \mathcal{D}_i(\bar{d}_{(j),k}, \Sigma(e_{(j),k}))$, where $\bar{d}_{(j),k}$ denotes its mean, and $\Sigma(e_{(j),k})$ its variance.

Assumption 4 *The demands are bounded, i.e., $d_k \in \mathbb{D}$, for all $k \in \mathbb{Z}_+$, and input-disturbance dominance constraints hold, i.e., $B_d\mathbb{D} \subseteq -B\mathbb{U}$ and $E_d\mathbb{D} \subseteq -E_u\mathbb{U}$.*

[4]If $n_q < n_u$, then multiple solutions exist, so u_k should be selected by means of an optimization problem. Equation (2.22b) implies the possible existence of uncontrollable flows d_k at the junction nodes. Therefore, a subset of the control inputs will be restricted by the domain of some flow demands.

The system is subject to storage and flow capacity hard constraints considered here in the form of convex polyhedra defined as

$$x_k \in \mathbb{X} \triangleq \{x \in \mathbb{R}^{n_x} \mid Gx \leq g\}, \tag{2.24a}$$

$$u_k \in \mathbb{U} \triangleq \{u \in \mathbb{R}^{n_u} \mid Hu \leq h\}, \tag{2.24b}$$

for all k, where $G \in \mathbb{R}^{r_x \times n_x}$, $g \in \mathbb{R}^{r_x}$, $H \in \mathbb{R}^{r_u \times n_u}$, $h \in \mathbb{R}^{r_u}$, being $r_x \in \mathbb{Z}_+$ and $r_u \in \mathbb{Z}_+$ the number of state and input constraints, respectively.

Note that in (2.22b) a subset of controlled flows are directly related with a subset of uncontrolled flows. Hence, u does not take values in $\mathbb{R}^{n_u}$ but in a linear variety. This latter observation, in addition to Assumption 2, can be exploited to develop an affine parametrization of control variables in terms of a minimum set of disturbances as shown in [19, Appendix A], mapping control problems to a space with a smaller decision vector and with less computational burden due to the elimination of the equality constraints. Thus, the system (2.32) can be rewritten as

$$x_{k+1} = Ax_k + \tilde{B}\tilde{u}_k + \tilde{B}_d d_k, \tag{2.25}$$

and the input constraint (2.24b) replaced with a time-varying restricted set defined as

$$\tilde{\mathbb{U}}_k \triangleq \{\tilde{u} \in \mathbb{R}^{n_u - n_q} \mid H\tilde{P}_1\tilde{u} \leq h - H\tilde{P}_2 d_k\} \quad \forall k \in \mathbb{Z}_+, \tag{2.26}$$

where $\tilde{B} \in \mathbb{R}^{n_x \times (n_u - n_q)}$, $\tilde{B}_d \in \mathbb{R}^{n_x \times n_d}$, $\tilde{P}_1 \in \mathbb{R}^{n_u \times (n_u - n_q)}$ and $\tilde{P}_2 \in \mathbb{R}^{n_u \times n_d}$, are selection and permutation matrices (see [19, Appendix A] for details). The sets $\tilde{\mathbb{U}}_k$ are non-empty for all k due to Assumption 4.

Control Problem Statement

The goal is to design a control law that minimises a (possibly multi-objective) convex stage cost $\ell(k, x, \tilde{u}) : \mathbb{Z}_+ \times \mathbb{X} \times \tilde{\mathbb{U}}_k \to \mathbb{R}_+$, which bears a functional relationship to the economics of the system operation. Let $x_k \in \mathbb{X}$ be the current state and let $\mathbf{d}_k = \{d_{k+i|k}\}_{i \in \mathbb{Z}_{[0, N\mathrm{p}-1]}}$ be the sequence of disturbances over a given prediction horizon $N\mathrm{p} \in \mathbb{Z}_{\geq 1}$. The first element of this sequence is measured, i.e., $d_{k|k} = d_k$, while the rest of the elements are estimates of future disturbances computed by an exogenous system and are available at each time step $k \in \mathbb{Z}_+$. Hence, the MPC controller design is based on the solution of the following finite-horizon optimization problem:

$$\min_{\tilde{\mathbf{u}}_k} \sum_{i=0}^{N\mathrm{p}-1} \ell(k+i, x_{k+i|k}, \tilde{u}_{k+i|k}), \tag{2.27a}$$

subject to:

$$x_{k+i+1|k} = Ax_{k+i|k} + \tilde{B}\tilde{u}_{k+i|k} + \tilde{B}_d d_{k+i|k}, \quad \forall i \in \mathbb{Z}_{[0,N_\mathrm{p}-1]} \tag{2.27b}$$
$$x_{k+i|k} \in \mathbb{X}, \quad \forall i \in \mathbb{Z}_{[1,N_\mathrm{p}]} \tag{2.27c}$$
$$\tilde{u}_{k+i|k} \in \tilde{\mathbb{U}}_{k+i}, \quad \forall i \in \mathbb{Z}_{[0,N_\mathrm{p}-1]} \tag{2.27d}$$
$$x_{k|k} = x_k. \tag{2.27e}$$

Assuming that (2.27) is feasible, i.e., there exists a non-empty control input sequence $\tilde{\mathbf{u}}_k = \{\tilde{u}_{k+i|k}\}_{i\in\mathbb{Z}_{[0,N_\mathrm{p}-1]}}$, then the receding horizon philosophy and the model back-transformation commands to apply the control input

$$u_k = \kappa_N(k, x_k, \mathbf{d}_k) = \tilde{P}_1\tilde{u}^*_{k|k} + \tilde{P}_2 d_k. \tag{2.28}$$

This procedure is repeated at each time instant k, using the current measurements of states and disturbances and the most recent forecast of these latter over the next future horizon.

2.3.2 Results

The formulation of the SMPC problems for the case studies considered in this work addresses the design of a control law that (i) minimizes the economic operational cost, (ii) guarantees the availability of enough water to satisfy the demand and (iii) operates the network with smooth variations of the flow through actuators. These objectives can be expressed quantitatively by the following performance indicators[5] for all time steps $k \in \mathbb{Z}_+$:

$$\ell_E(x_k, \tilde{u}_k; c_{u,k}) \triangleq c_{u,k}^\top W_e\, \tilde{u}_k \Delta t, \tag{2.29a}$$
$$\ell_S(x_k; s_k) \triangleq \begin{cases} (x_k - s_k)^\top W_s (x_k - s_k) & \text{if } x_k \le s_k \\ 0 & \text{otherwise,} \end{cases} \tag{2.29b}$$
$$\ell_\Delta(\Delta\tilde{u}_k) \triangleq \Delta\tilde{u}_k^\top W_{\Delta\tilde{u}}\, \Delta\tilde{u}_k. \tag{2.29c}$$

The first objective, $\ell_E(x_k, \tilde{u}_k; c_{u,k}) \in \mathbb{R}_{\ge 0}$, represents the economic cost of network operation at time step k, which depends on a time-of-use pricing scheme driven by a time-varying price of the flow through the actuators $c_{u,k} \triangleq (c_1 + c_{2,k}) \in \mathbb{R}_+^{n_u - n_q}$, which in this application takes into account a fixed water production cost $c_1 \in \mathbb{R}_+^{n_u}$

[5]The performance indicators considered in this work may vary or be generalized with the corresponding manipulation to include other control objectives.

and a water pumping cost $c_{2,k} \in \mathbb{R}_+^{n_u}$ that changes according to the electricity tariff (assumed periodically time-varying). All prices are given in economic units per cubic meter (e.u./m^3). The second objective, $\ell_S(x_k; s_k) \in \mathbb{R}_{\geq 0}$ for all k, is a performance index that penalizes the amount of water volume going below a given safety threshold $s_k \in \mathbb{R}^{n_x}$ in m^3, which is desired to be stored in tanks and satisfies the condition $x_{\min} \leq s_k \leq x_{\max}$. Note that this safety objective is a piecewise continuous function, but it can be redefined as $\ell_S(\xi_k; x_k, s_k) \triangleq \xi_k^\top W_s \, \xi_k$, accompanied with two additional convex constraints, i.e., $x_k \geq s_k - \xi_k$ and $\xi_k \in \mathbb{R}_+^{n_x}$, for all k, being ξ_k a slack variable. The minimal volume of water required in a tank is given by its net demand, hence, $s_k = -B_p d_k$ for all k. The last objective, $\ell_\Delta(\Delta\tilde{u}_k) \in \mathbb{R}_{\geq 0}$, represents the penalization of control signal variations $\Delta\tilde{u}_k \triangleq \tilde{u}_k - \tilde{u}_{k-1} \in \mathbb{R}^{n_u - n_q}$. The inclusion of this latter objective aims to extend actuator's life and assure a smooth operation of the dynamic network flows. Furthermore, $W_e \in \mathbb{S}_{++}^{n_u - n_q}$, $W_s \in \mathbb{S}_{++}^{n_x}$ and $W_{\Delta\tilde{u}} \in \mathbb{S}_{++}^{n_u - n_q}$ are matrices that weight each decision variable in their corresponding cost function.

To achieve the control task, the above predefined objectives are aggregated in a multi-objective stage cost function, which depends explicitly on time due to the time-varying parameters of the involved individual objectives. The overall stage cost is defined for all $k \in \mathbb{Z}_+$ as

$$\ell(k, x_k, \tilde{u}_k, \xi_k) \triangleq \lambda_1 \ell_E(x_k, \tilde{u}_k; c_{u,k}) + \lambda_2 \ell_\Delta(\Delta\tilde{u}_k) + \lambda_3 \ell_S(\xi_k; x_k, s_k), \quad (2.30)$$

where $\lambda_1, \lambda_2, \lambda_3 \in \mathbb{R}_+$ are scalar weights that allow to prioritize the impact of each objective involved in the overall performance of the network. These weights are assumed to be fixed by the managers of the DWN.

Numerical results of applying the three different SMPC approaches (CC-MPC, TB-MPC and MS-MPC) to the Barcelona DWN case studies are summarized in Tables 2.9, 2.10 and 2.11.

Simulations have been carried out over a time horizon of eight days, i.e., $n_s = 192$ hours, with a sampling time of one hour. The patterns of the water demand in this work were synthesized from real values measured in the considered demand of the Barcelona DWN between July 23^{th} and July 27^{th}, 2007. Initial conditions, i.e., source capacities, initial volume of water at tanks and starting demands, are set a priori according to real data. The weights of the cost function (2.30) are $\lambda_1 = 100$, $\lambda_2 = 10$, and $\lambda_3 = 1$; these values allow to prioritize the impact of each objective involved in the overall performance of the network. The prediction horizon is selected as $N\mathrm{p} = 24$ hours, due to the periodicity of disturbances. The formulation of the optimization problems and the closed-loop simulations have been carried out using MATLAB R2012a (64 bits) and CPLEX solver, running in a PC Core i7 at 3.2 GHz with 16 GB of RAM.

The key performance indicators used to assess the aforementioned controllers are defined as follows:

$$\Phi_1 \triangleq \frac{24}{n_s} \sum_{k=1}^{n_s} \ell_k, \tag{2.31a}$$

$$\Phi_2 \triangleq |\left\{k \in \mathbb{Z}_{[1,n_s]} \mid x_k < -B_p d_k\right\}|, \tag{2.31b}$$

$$\Phi_3 \triangleq \sum_{k=1}^{n_s} \sum_{i=1}^{n_x} \max\{0, -B_{p(i)} d_k - x_{k(i)}\}, \tag{2.31c}$$

$$\Phi_4 \triangleq \frac{1}{n_s} \sum_{k=1}^{n_s} t_k, \tag{2.31d}$$

where Φ_1 is the average daily multi-objective cost with ℓ_k given by (2.30), Φ_2 is the number of time instants where water demands are not satisfied, Φ_3 is the accumulated volume of water demand that was not satisfied over the simulation horizon n_s, and Φ_4 is the average time in seconds required to solve the MPC problem at each time instant $k \in \mathbb{Z}_{[1,n_s]}$.

The effect of considering different levels of joint risk acceptability was analyzed for the CC-MPC approach using $\delta = \{0.3, 0.2, 0.1\}$. In the same way, the size of the set of scenarios selected for the MS-MPC is established by using (2.6) to guarantee the same risk levels of the CC-MPC approach. In this way, the total number of scenarios that represents the evolution of the water demand in the considered simulation time for the MS-MPC was $N_s = 192$. Likewise, the TB-MPC approach was applied considering different sizes for the set of reduced scenarios, i.e., $N_r = \{5, 10, 19, 38, 75, 107, 129, 149\}$. The last three N_r scenarios allow to compare the behavior between MS-MPC and TB-MPC, while the remaining scenarios were used to analyze the performance with respect to a small number of scenarios.

Table 2.9 summarizes the results of applying the SMPC approaches to the sector model of the Barcelona DWN presented in Fig. 2.6. The different values of δ in the CC-MPC approach highlight that both reliability and control performance are conflicting objectives, i.e., the inclusion of safety mechanisms in the controller increases the reliability of the DWN in terms of demand satisfaction, but also the cost of its operation. The main advantage of the CC-MPC is its formal methodology, which leads to obtain optimal safety constraints that tackle uncertainties and allow to achieve a specified global service level in the DWN. Moreover, the CC-MPC robustness is achieved with a low computational burden given that the only extra load is the computation of the stochastic characteristics of disturbances propagated along the prediction horizon

Table 2.9: Comparison of the CC-MPC, TB-MPC and MS-MPC applied to the sector model of the DWN.

CC-MPC					TB-MPC					MS-MPC					
δ	Φ_1	Φ_2	Φ_3	Φ_4	Φ_1	Φ_2	Φ_3	Φ_4	N_r	Φ_1	Φ_2	Φ_3	Φ_4	N_s	δ
					58397.14	0	0	1.2548	5						
0.3	58535.80	0	0	0.0919	58515.40	1	0.4813	1.9701	10	60831.33	0	0	16.1547	107	0.3
					58589.15	1	4.155	3.0145	14						
					58515.37	0	0	3.2218	19						
0.2	58541.19	0	0	0.707	58678.12	2	0.7443	7.5362	38	69342.48	0	0	17.2401	129	0.2
					58647.27	4	4.0329	27.0914	75						
					58705.28	1	0.2136	35.6572	107						
0.1	58558.29	0	0	0.716	58713.15	0	0	42.7024	129	66011.29	0	0	21.7521	149	0.1
					58761.98	0	0	54.4587	149						

Np. In this way, the CC-MPC approach is suitable for real-time control of large-scale DWNs.

Regarding the TB-MPC and MS-MPC approaches, numerical results show that considering a large number of scenarios, increments (in average) the stage cost while reducing the volume of unsatisfied water demand. This might be influenced by the quality of the information that remains after the reduction algorithms, consequently, it affects the robustness of the approach being subject of further research.

Results show that all the proposed methods take less than 1 minute to solve the optimization problem in each case, being much shorter than the sampling time of 1 hour. Hence, it is possible to select an approach that may show the best performance in terms of demand satisfaction (in practice).

The main drawback of the TB-MPC approach is the solution average time and the computational burden. The implementation for all cases taking scenarios greater than $N_r = 149$ was not possible due to memory issues. Hence, some simplification assumptions as those used in [63] or parallel computing techniques might be useful. Another way to address the problem generated by the computer effort is to use a MS-MPC based on the three-scenarios approach. At this point, the best, the worst and the average disturbance scenarios were obtained by generating 100 different possible evolutions of the disturbance, then they were lumped and averaged the 10 lowest, 10 highest, and 80 middle, respectively. It means that the occurrence probabilities were established as 0.1, 0.1, and 0.8 for the best, the worst, and the average disturbance scenario, respectively, as proposed in [10].

Additionally, Table 2.10 summarizes the simulation results of applying the studied SMPC approaches again to the sector model DWN. The configuration of the controllers in this case is as follows: the CC-MPC with a probability of risk of 5%, the TB-MPC reducing to $N_r = 3$ branched disturbances, the MS-MPC based on the three

scenarios approach (i.e., best, worst and average), and the CE-MPC with an average disturbance. On the one hand, the CE-MPC approach presents the lower cost but on the other hand it has problems with the demand satisfaction. The TB-MPC approach presents a lower accumulated volume of unsatisfied water demand compared with respect to the CE-MPC approach. The MS-MPC and CC-MPC approaches are able to satisfy the water demand required by the consumers. The CC-MPC approach presents a better performance regarding cost and computational time compared to the MS-MPC approach.

Table 2.10: Comparison of the MS-MPC, TB-MPC, CC-MPC and CE-MPC applied to the sector model DWN.

$Controller$	Φ_1	Φ_2	Φ_3	Φ_4
CC-MPC	585401.16	0	0	0.1069
TB-MPC	58425.59	1	1.2229	1.4235
MS-MPC	60567.62	1	0.6965	0.5314
CE-MPC	58327.55	1	0.7411	0.1041

As for the second case study, Table 2.11 presents the results obtained after the application of the SMPC approaches to the aggregate model DWN, as a way to show the strengths and weaknesses of each of the aforementioned approaches applied to a larger system. For this reason, TB-MPC and MS-MPC with a large number of scenarios, could not be applied due to memory issues. TB-MPC was implemented with a reduction to $N_r = 3$ branched scenarios. MS-MPC has been designed considering the three scenarios (minimum, average and maximum) as explained in the previous case study. CC-MPC is applied to this system with a risk probability of 5%. As it can be seen from the results, the TB-MPC approach does not offer benefits in terms of satisfaction of water demand and computational time with this limited amount of scenarios for the DWN aggregate model. MS-MPC presents encouraging results regarding demand satisfaction and computational time well below that TB-MPC. MS-MPC approach presents a higher average daily multi-objective cost and a computational time required to solve the FHOP around three times more regarding CC-MPC. Furthermore, MS-MPC and CC-MPC, have a good performance with respect to water demand satisfaction. Based on the obtained results, the CC-MPC approach offers better performance in terms of demand satisfaction, computational time and, it presents the best behavior with respect to the average daily multi-objective cost (ϕ_1) compared with the same indicator obtained with TB-MPC and MS-MPC approaches.

Table 2.11: Comparison of the MS-MPC, TB-MPC, CC-MPC and CE-MPC applied to the DWN case study for the aggregate DWN model.

Controller	Φ_1	Φ_2	Φ_3	Φ_4
CC-MPC	$1.4064 \cdot 10^4$	0	0	0.9056
TB-MPC	$1.4497 \cdot 10^4$	20	18.81	8.48
MS-MPC	$1.5267 \cdot 10^4$	0	0	3.24
CE-MPC	$1.2038 \cdot 10^4$	23	5.211	0.8442

As expected, the SMPC approaches have a better performance indicators with respect to CE-MPC approach, which does not take into account the stochastic nature of water demand in the formulation of FHOP.

Simulation results show that all the considered methods require less than 1 min to solve the optimization problem in each case, much shorter than the sampling time of 1 h. Hence, it is possible to choose an approach that shows the best performance in terms of demand satisfaction, which is given by the number of time instants where water demands were not satisfied and by the cumulated volume of non-satisfied water demand. In this sense, the results in this work show that CC-MPC is more appropriate when requiring a low probability of constraint violation because the use of TB-MPC and MS-MPC implies the inclusion of a higher number of scenarios, which hinders the application of these control strategies to large DWNs. However, the use of these scenario-based approaches may be very demanding in terms of computational time.

These results have been published in [32].

2.4 Case Study: Stock management in a hospital pharmacy

Stock management is a common problem that is present in almost all the companies and organizations. The solution for this problem is given by a policy that determines how and when the orders should be placed. However, there are different difficulties associated to the problem. In the first place, there are uncertainties in the demand and delays in the deliveries, which make the problem not deterministic and require a degree of conservatism to avoid stockouts. It is needless to say that the lack of certain drugs in a hospital may endanger the life of the inpatients and, in the worst case, may have catastrophic consequences in the form of human losses. In order to avoid this situation, it is preferred to increase stock levels, but this is not always possible due

to economical constraints. Actually, the pharmacy is a major source of expenses in hospitals. In [64], it is estimated that about 35% of the total budget of a public hospital comes from the pharmacy department. In a wider sense, the limitations imposed by the budget are also translated into the human resources in the pharmacy and the room available for storing drugs, which introduce additional constraints for the management. Hence, it may not be possible to place and receive orders too often due to the lack of pharmacists. Moreover, space constraints are important for example in drugs that must be stored in a fridge. Therefore, there is a need to develop advanced cost-efficient safe policies for stock management in hospitals capable of dealing with many different type of constraints.

In general, the typical method used to solve inventory control problems is simple. An usual policy is a point of reorder one (s, S), that is, whenever the stock is below the level s, an order is placed to increase the stock up to the value S. Another option is to fix a size for the orders, Q, and submit an order once the stock is at level s. Other related policies about how to solve this problem are given in [65] and [66]. The major drawback with these techniques is that they are not able to take into account all the factors involved in the decision problem. For example, [67] presents an analytical model for the coordination of inventory and transportation in supply-chain systems considering a vendor realizing a sequence of random demands. Also in [68], a supply chain network model consisting of manufacturers and retailers, where the demand is random, is developed. More strategies are presented in [69], where a competitive and cooperative selection of inventory policies in a supply chain with stochastic demand are studied. On the other hand, [70] develops a model to design a supply chain network with deterministic demand. In this sense, CC-MPC is applied to cope with the uncertainty that involves the drug demand in a hospital pharmacy.

2.4.1 Pharmacy Inventory Management

In this section, the mathematical background needed to build the optimization problem to be solved by the CC-MPC is presented.

System Definition

In general, it will be assumed that there are N_i different drugs in the pharmacy inventory. The stock level of each one follows an evolution depending on the orders and on the demand. This evolution is represented by a discrete linear model, which for the

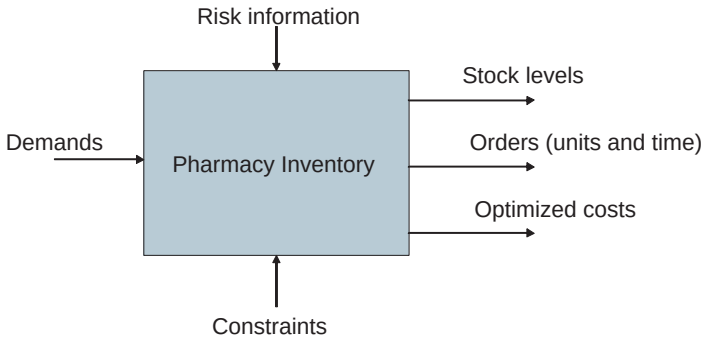

Figure 2.8: Block System

particular case of drug i is

$$s_i(t+1) = s_i(t) + \sum_{j=1}^{np_i} o_i^j(t-\tau_i^j) - d_i(t), \tag{2.32}$$

where $s_i \in \mathbb{Z}$ is the stock of drug i, $o_i^j \in \mathbb{Z}$ is the number of ordered items to the j-th of the np_i providers of the drug i, τ_i^j is its corresponding transport delay, and $d_i(t)$ represents the aggregate demand of drug i.

The number of ordered items can be modeled as $o_i^j = \delta_i^j(t-\tau_i^j)o_i^j(t-\tau_i^j)$, where $\delta_i^j(t)$ is a Boolean variable, that is, $\delta_i^j(t) = 1$ if an order of drug i to provider j is placed during time t, otherwise $\delta_i^j(t) = 0$, and $o_i^j \in \mathbb{Z}$ represents the number of ordered items of drug i to provider j, only in those cases where $\delta_i^j(t) = 1$.

Single Hospital Optimization Problem

The system can be represented according to Figure 2.8. In this figure, the inputs represent the information that the pharmacy managers have available in order to make the decisions about the order placement. The information consists of the estimated drug demands, the information about the disturbances and the constraints. The outputs are the optimal stock levels, minimum costs and data about when and how many orders should be placed.

Every time an order is placed, the following costs are associated to it:

- p_i^j, the j-th provider offers this price for drug i. It is supposed in this paper that it does not depend on the number of ordered items.
- $C_{sh,i}^j$, asking drug i to provider j has associated this shipping cost.
- $C_{op,i}$ is the cost of ordering drug i.
- $C_{os,i}$ is the cost associated with having less stock of drug i in the pharmacy than the minimum stock level allowed for drug i. This situation is particularly dangerous since there is a high risk for the hospital of running out of drug i and not satisfy the clinical needs of the patients. In this case, it would be possible to ask the drugs to other hospitals, but these kind of loans may have a high cost.
- $C_{s,i}$ is the cost of storage of drug i.
- $C_{o,i}$ is the opportunity cost of having drug i in the pharmacy storage.

Note that both stock levels and costs are direct consequence of the orders placed. Finally, the goals that the managers reach are the following: *i)* the demand has to be satisfied; *ii)* the fixed assets must be reduced; and *iii)* the number of orders placed has to be minimized. This goals are considered in the optimization problem. In particular, the performance index considered in this work involves a multicriteria weighted function where demand satisfaction, expenses and number of orders are included, i.e.,

$$\min_o J := \beta_1 J_1(o,t) + \beta_2 J_2(o,t) + \beta_3 J_3(o,t), \tag{2.33}$$

where J_1, J_2 and J_3 are the terms associated to demand satisfaction, costs and orders, respectively. Weights β_i prioritize the different terms, being the solution of the problem strongly dependable on them.

The terms in the objective function (2.33) are described next in decreasing priority:

1. J_1: Demand satisfaction. The main objective is the minimization of stockout probability. The main issue here is that the demand is not known in advance, i.e., it is stochastic. There may also be uncertainty in the transport delays. For this reason, it is usual in practice to set a safety stock to mitigate the impact of uncertainty. There are two possibilities in the way the safety stock is set: it can be either fixed or variable. The former proposes that the minimum stock level is introduced as a fixed parameter in the optimization problem. The latter treats the safety stock as an optimization variable. The mathematical condition is expressed as

$$\min_{\delta_i^j, o_i^j \ \forall i,j} \sum_{k=0}^{N} \sum_{i=1}^{N_i} C_{os,i} \lambda_{\text{stockout}}^i, \tag{2.34}$$

with

$$\lambda^i_{\text{stockout}} = \begin{cases} 1 & \text{if } s_i(t+k) < \text{S}^i_{\min}, \\ 0 & \text{if } s_i(t+k) > \text{S}^i_{\min}, \end{cases} \tag{2.35}$$

where $\lambda^i_{\text{stockout}}$ is a variable that tells whether or not the safety stock has been violated, $\text{S}^i_{\min}$ is the minimum stock level allowed for the drug i, N is the length of the time horizon in which the condition has to be satisfied and N_i is the number of different drugs.

2. J_2: Expenses. This term of the objective function (2.33) deals with the minimization of the expenses in the orders of drugs and the inventory levels, i.e.,

$$\begin{aligned} \min_{\delta^j_i, o^j_i \ \forall i,j} & \sum_{k=0}^{N} \sum_{i=1}^{N_i} \sum_{j=1}^{np_i} \delta^j_i(t+k)(p^j_i o^j_i(t+k) + C^j_{sh,i}) \\ & + \sum_{k=0}^{N} \sum_{i=1}^{N_i} C_{s,i} s_i(t+k) + \sum_{k=0}^{N} \sum_{i=1}^{N_i} C_{o,i} s_i(t+k). \end{aligned} \tag{2.36}$$

3. J_3: Orders. With the inclusion of this term in the objective function, the number of placed orders is trying to be minimized. That is useful because each order has associated certain costs. For example, in a hospital such as Reina Sofía (Cordoba, Spain) more than twelve thousand orders are placed during a year. This condition can be written as the following minimization problem:

$$\min_{\delta} \sum_{k=0}^{N} \sum_{i=1}^{N_i} \sum_{j=1}^{np_i} C_{op,i} \delta^j_i(t+k). \tag{2.37}$$

Furthermore, the problem considers the following constraints:

- **Storage constraints.** As explained before, the level of the stock of drug i has to be greater than a safety stock $\text{S}^i_{\min}$, to reduced the probability of running out of the drug. Furthermore, the space restrictions in the storage room must also be considered, which limits the maximum number of drugs that can be stored in the pharmacy. Therefore,

$$s_i \in [\text{S}^i_{\min}, \text{S}^i_{\max}]. \tag{2.38}$$

- **Order constraints.** In order to formulate these constraints, two type of variables are going to be used. The first one is a Boolean variable $\delta^j_i(t) \in [0, 1]$, where the value 1 means that an order of drug i has been placed to provider j during time t, and the value 0 means that no order has been placed. In case of placing an

order ($\delta_i^j(t) = 1$), the other variable, that represents the ordered number of items, is used. This variable should be bounded by both a minimum and a maximum values, i.e.,

$$o_i^j \in [\min_{o_i^j}, \max_{o_i^j}]. \tag{2.39}$$

There are also some considerations about the minimum number of items to order:

- There is a minimum of items to order at each time, $\min_{\text{item}_i^j}$. That is because the distributors do not work if the number of items is too small. Hence, there is a threshold for the number of items to order.
- The pharmaceutical laboratories do not provide the drugs unless a minimum quantity of money is spent. That is translated into a minimum order size, $\min_{\text{lab}_i^j}$. Taking into account these quantities,

$$\min_{o_i^j} = \max(\min_{\text{item}_i^j}, \min_{\text{lab}_i^j}).$$

- There is also another consideration to take into account related to the *non-working days* of the laboratory (e.g., Sundays, holidays). The controller will have to be synthesized in such a way this constraint is considered. That leads into the following constraint:

$$\delta_i^j(t) = 0, \quad \forall t \notin \{\text{working days}\}. \tag{2.40}$$

- **Operational constraints.** These constraints take into account the limited capacity of the pharmacy for placing orders and receiving shipments. This fact limits the number of orders placed along a time horizon of length N, i.e.,

$$\sum_{k=0}^{N} \sum_{j=1}^{np_i} \delta_i^j(t+k) \leq \Delta_i, \tag{2.41}$$

where Δ_i is the maximum number of orders of drug i that can be placed along N.

- **Economical constraints.** The money spent during the time horizon N has to be also limited, being $\max_{\$}$ the maximum amount. Therefore, the mathematical constraint is expressed as

$$\sum_{k=0}^{N} \sum_{i=1}^{N_i} \sum_{j=1}^{np_i} \delta_i^j(t+k)(p_i^j o_i^j(t+k) + C_{sh,i}^j + C_{op,i}) \leq \max_{\$}. \tag{2.42}$$

Multiple-hospitals Extension

In order to reduce the minimal stock of drugs required in a hospital pharmacy, different hospitals could collaborate between them, e.g., if they are close to each other and the consumption of certain drugs is uncorrelated between them. Consequently, the expenses derived from loans between them are getting lower or can even be neglected. This way, the hospitals can focus on the joint stockout probability instead of the individual one, which should be higher, resulting in lower safety and average stock levels. In the simplest case, each hospital would keep its original optimization problem only with different constraints. Likewise, it could also be possible to pose this problem as a distributed control one, where the hospitals are agents that have to reach a consensus on the safety levels. The optimization problem is

$$\min_{o} \sum_{h=1}^{H} J_h, \tag{2.43}$$

where J_h stands for the cost of each hospital and H is the number of collaborating hospitals. The overal objective function taking into account all considered hospitals is given by

$$J_h = \sum_{i=1}^{3} \sum_{j=1}^{H} \beta_{i,j} J_{i,j}(o,t),$$

where the demand, expenses and orders terms are like in (2.34)-(2.37). The difference here is that, in the demand term, the probability $Pr(s_i^h(t+k) < 0)$ can be greater.

The constraints are, like in the previous case, (2.38)-(2.42), and:

$$s_i^h(t+1) = s_i^h(t) + \sum_{j=1}^{np_i} o_i^{j,h}(t-\tau_i^j) - d_i^h(t), \quad \forall h \in \{1,...,H\}. \tag{2.44}$$

2.4.2 MPC Setup

The implementation of the control problem will be detailed, adding some consideration to make it easier. The objective is the minimization of the objective function, which will minimize the number of orders. Consider the system defined by

$$s(t+1) = s(t) + o(t-\tau) - d(t), \tag{2.45}$$

where $s(t) = [s_1(t), ..., s_{N_i}(t)]$, $d(t) = [d_1(t), ..., d_{N_i}(t)]$ and $o(t-\tau) = \sum_{j=1}^{np_i} \delta_i^j(t - \tau_i^j) u_i^j(t-\tau_i^j)$ represent the total number of items ordered. Note that system (2.45) is equivalent to (2.32).

The control variables taken into account in this problem are $\delta_i^j(t)$ and $o_i^j(t)$, both components of the control variable $o(t)$. Solving the optimization problem by using directly the control variable $o(t)$ (i.e., $\delta_i^j(t)$ and $o_i^j(t)$ together) is a difficult task, since they have different nature because $\delta_i^j(t)$ is a Boolean variable. The way to proceed will be the use of an exhaustive search algorithm, which will solve the problem as many times as possible scenarios depending on the value of $\{\delta_i^j(t), ..., \delta_i^j(t+N_\mathrm{p})\}$, i.e., $2^{np_i \times N_i(N_\mathrm{p}+1)}$ times. In that way, the optimization problem can be solved with respect to the variable $o_i^j(t)$.

It is straightforward to see that if $\delta_i^j(t+k) = 0$, for $k \in \{0, 1, ..., N_\mathrm{p}\}$, the quantity of ordered items is $o_i^j(t+k) = 0$. Furthermore, the variable $o_i^j(t)$ can be considered as a real one, in order to simplify the problem, since the obtained solution is an integer one because of the problem features. Besides, that fact also accelerates the problem resolution. Moreover, the vector of control variables $\{o_i^j(t), ..., o_i^j(t+N_\mathrm{p})\}$ is reduced by eliminating the components $o_i^j(t+k)$ that are equal to zero. Hence,

$$\forall \delta_i^j(t+k) = 0, \quad k \in \{0, 1, ..., N_\mathrm{p}\},$$

then

$$\underbrace{\begin{bmatrix} o_i^j(t) \\ \vdots \\ o_i^j(t+k) \\ \vdots \\ o_i^j(t+N_\mathrm{p}) \end{bmatrix}}_{\mathbf{o_i^j(t)}} \quad \rightarrow \quad \underbrace{\begin{bmatrix} o_i^j(t) \\ \vdots \\ o_i^j(t+k-1) \\ o_i^j(t+k+1) \\ \vdots \\ o_i^j(t+\tilde{N}_\mathrm{p}) \end{bmatrix}}_{\tilde{\mathbf{o}}_\mathbf{i}^\mathbf{j}\mathbf{(t)}},$$

where $\mathbf{o_i^j(t)} \in \mathbb{R}^{\mathbf{N_p+1}}$ and $\tilde{\mathbf{o}}_\mathbf{i}^\mathbf{j}\mathbf{(t)} \in \mathbb{R}^{\tilde{\mathbf{N}}_\mathbf{p}\mathbf{+1}}$ is a reduced vector of non-zero orders, where

$$\tilde{N}_\mathrm{p} = N_\mathrm{p} - \sum_{k=0}^{N_\mathrm{p}} \big(1 - \delta_i^j(t+k)\big),$$

is the number of non-zero orders.

The vector reduction from $\mathbf{o_i^j(t)}$ to $\tilde{\mathbf{o}}_\mathbf{i}^\mathbf{j}\mathbf{(t)}$ can be represented by the following change of variable:

$$\mathbf{o}_i^j(t) = M\tilde{\mathbf{o}}_\mathbf{i}^\mathbf{j}\mathbf{(t)},$$

where $M \in \mathbb{R}^{(N_\mathrm{p}+1)\times(\tilde{N}_\mathrm{p}+1)}$.

Matrix M is used to reduce the dimension of the order vector $\mathbf{o}_i^j(t)$ depending on the value of $\delta_i^j(t)$. Therefore, M is defined as

$$M(i,j) = \begin{cases} 1 & \text{if } \delta_i^j(t) = 1 \wedge i = j, \\ 0 & \text{if } \delta_i^j(t) = 0 \vee i \neq j. \end{cases} \tag{2.46}$$

As direct consequence, $\tilde{\mathbf{o}}_{\mathbf{i}}^{\mathbf{j}}(\mathbf{t})$ contains only non-null components, i.e., the orders that are non-zero.

As it was explained before, this optimization problem will be solved as many times as many possible combinations with the values of $\{\delta_i^j(t), ..., \delta_i^j(t+N_\mathrm{p})\}$. This way, this variable can be avoided in the optimization and then the same number of values of the objective function will be obtained. Of course, the optimal solution corresponds with the combination of the values of $\{\delta_i^j(t), ..., \delta_i^j(t+N_\mathrm{p})\}$ that provides the minimal value of the objective function.

Taking into account the integer nature of the variable $\delta_i^j(t)$, the resulting optimization problem is a mixed integer one (MIP). There are different techniques to solve them like branch and bound [71], genetic algorithms [72] or the cutting-plane method [73].

Remark 2 *It is necessary to pay special attention to the constraints while solving this problem. It is not possible to impose the whole matrix of constraints to the reduced vector* $\tilde{\mathbf{o}}_{\mathbf{i}}^{\mathbf{j}}(\mathbf{t})$*, so it is necessary to also apply the change matrix* M *to the matrix of constraints to impose them only to the considered control components.*

CC-MPC

The aggregate demand $d(t)$ in (2.45) includes a stochastic disturbance component given its uncertain nature. Due to the presence of these uncertainties, the constraints have a stochastic nature, i.e., they can not be written as deterministic ones. Therefore, the constraints can be expressed as

$$P(s(t+k) \geq \mathrm{S_{min}}) \geq 1 - \delta_\mathrm{s}, \quad \forall k \in \{1, .., N_\mathrm{p}\},$$

where δ_s is the probability of having less stock than $\mathrm{S_{min}}$. This expression can be developed along N_p and obtain the mean and standard deviation of the state.

Remark 3 *It is also possible to assume that the behavior of the disturbances can be adjusted as a function of a certain probability distribution. In [74], a normal distribution is used to characterize the behavior of the perturbations, with mean* μ *and standard deviation* σ*, i.e.,* $d(t) = \mathcal{N}(\mu, \sigma)$*. This assumption could be extended to other patterns or even work directly with historical data, like in this case.*

For the first time instant along N (i.e., $k = 1$), it yields

$$\begin{aligned} P(s(t+0) + o(t+0) - d(t+0) \geq \mathrm{S_{min}}) &\geq 1 - \delta_\mathrm{s}, \\ P(-d(t+0) \geq \mathrm{S_{min}} - s(t+0) - o(t+0)) &\geq 1 - \delta_\mathrm{s}, \\ P(\underbrace{d(t+0)}_{Random} \leq \underbrace{-\mathrm{S_{min}} + s(t+0) + o(t+0)}_{Deterministic}) &\geq 1 - \delta_\mathrm{s}, \end{aligned}$$

which can be rewritten as

$$\phi_0(-\mathrm{S_{min}} + s(t+0) + o(t+0)) \geq 1 - \delta_\mathrm{s},$$

where $\phi_0(\cdot)$ is the cumulative distribution function (cdf) of the random variable $d(t+0)$. The deterministic equivalent for this chance constraint is

$$\begin{aligned} -\mathrm{S_{min}} + s(t+0) + o(t+0) &\geq {\phi_0}^{-1}(1 - \delta_\mathrm{s}), \\ -o(t+0) &\leq -\mathrm{S_{min}} + s(t+0) - {\phi_0}^{-1}(1 - \delta_\mathrm{s}). \end{aligned}$$

For the next time instant along N (i.e., $k = 2$), it yields

$$\begin{aligned} &P(s(t+2) \geq \mathrm{S_{min}}) \geq 1 - \delta_\mathrm{s} \\ &P(s(t+1) + o(t+1) - d(t+1) \geq \mathrm{S_{min}}) \geq 1 - \delta_\mathrm{s} \\ &P((s(t+0) + o(t+0) - d(t+0)) + o(t+1) - d(t+1) \geq \mathrm{S_{min}}) \geq 1 - \delta_\mathrm{s} \\ &P(-d(t+0) - d(t+1)) \geq \mathrm{S_{min}} - s(t+0) - o(t+0) - o(t+1)) \geq 1 - \delta_\mathrm{s}, \\ &P(d(t+0) + d(t+1) \leq -\mathrm{S_{min}} + s(t+0) + o(t+0) + o(t+1)) \geq 1 - \delta_\mathrm{s}. \end{aligned}$$

Defining $\phi_1(\cdot)$ as the cumulative distribution function of the variable $d(t+0)+d(t+1)$ yields

$$\begin{aligned} &\phi_1(-\mathrm{S_{min}} + s(t+0) + o(t+0) + o(t+1)) \geq 1 - \delta_\mathrm{s}, \\ &-\mathrm{S_{min}} + s(t+0) + o(t+0) + o(t+1) \geq {\phi_1}^{-1}(1 - \delta_\mathrm{s}), \\ &o(t+0) + o(t+1) \geq \mathrm{S_{min}} - s(t+0) + {\phi_1}^{-1}(1 - \delta_\mathrm{s}), \\ &-o(t+0) - o(t+1) \leq -\mathrm{S_{min}} + s(t+0) - {\phi_1}^{-1}(1 - \delta_\mathrm{s}). \end{aligned}$$

Iteratively (e.g., $k = 3$) and according to the previous development, it can written as

$$-o(t+0) - o(t+1) - o(t+2) \leq -\mathrm{S_{min}} + s(t+0) - {\phi_2}^{-1}(1 - \delta_\mathrm{s}),$$

where $\phi_2(\cdot)$ denotes the cumulative distribution function of the variable $d(t+0) + d(t+1) + d(t+2)$. Generalizing for a prediction horizon N_p,

$$-\begin{bmatrix} 1 & 0 & 0 & \cdots & 0 \\ 1 & 1 & 0 & \cdots & 0 \\ 1 & 1 & 1 & \cdots & 0 \\ \vdots & & & & \vdots \\ 1 & 1 & & \cdots & 1 \end{bmatrix} \begin{bmatrix} o(t+0) \\ o(t+1) \\ o(t+2) \\ \vdots \\ o(t+N_\mathrm{p}-1) \end{bmatrix} \leq \begin{bmatrix} 1 & 1 \\ 1 & 1 \\ 1 & 1 \\ \vdots & \vdots \\ 1 & 1 \end{bmatrix} \begin{bmatrix} s(t+0) \\ -\mathrm{S_{min}} \end{bmatrix} - \begin{bmatrix} {\phi_0}^{-1}(1 - \delta_\mathrm{s}) \\ {\phi_1}^{-1}(1 - \delta_\mathrm{s}) \\ {\phi_2}^{-1}(1 - \delta_\mathrm{s}) \\ \vdots \\ {\phi_{N_\mathrm{p}-1}}^{-1}(1 - \delta_\mathrm{s}) \end{bmatrix},$$

where $\phi^{-1}_{N_\mathrm{p}-1}(1-\delta_\mathrm{s})$ is the cumulative distribution function of the random variable $d(t+0)+d(t+1)+d(t+2)+\cdots+d(t+N_\mathrm{p}-1)$.

2.4.3 Results

Due to CC-MPC offers a significant advantage regarding computational burden, robustness, and performance; moreover, taking into account that it is possible to obtain a cumulative distribution function from historical data of demand from particular drugs, CC-MPC is going to be applied to manage the orders of two drugs available in the hospitals San Juan de Dios and Universitario Reina Sofía (both located at Córdoba, Spain). These drugs are not only expensive because of their prices but also because of their maintenance costs, since they must be stored in a fridge. Due to this fact, the reduction of their stock levels is a priority.

Regarding the controller, a prediction horizon N_p=8 days has been considered. The evolution of the stock is modeled by using the discrete-time linear model in (2.45). The orders of these drugs have a minimum amount of 4 units and the maximum has been set to 1000. The prices of the drugs are respectively 227 and 298 euros per unit, respectively, and each order placed implies an additional cost of 2 euros. The deliveries of these drugs usually have a delay of 2 days with respect to the moment in which the order was placed. The initial values of the stock levels are 500 and 1520, respectively. Finally, the demand term of (2.45) is non deterministic. A probabilistic characterization of their behavior has been calculated for these drugs based on historical data.

For simplicity, neither storage cost nor storage limits have been considered at this stage of the proposed work. The only implemented constraint with respect to the stock is that the probability of stockout event has to be lower than 0.001 (i.e., it is requested a reliability level of 99.999 %).

The 360-days simulation scenario considered here is shown in Figures 2.9 and 2.10 for each drug. In blue, the evolution of the stocks using CC-MPC is shown. In red, the real evolution of the stock according to the hospital data is shown. Tables 2.4.3 and 2.4.3 show a comparison of the behavior of these two drugs applying CC-MPC with the results register by the hospitals in this period, considering the average level, standard deviation and the number of orders. In this period the hospitals placed 9 orders for the drug 1 and 14 for the second one.

These results clearly show that the CC-MPC policy provides better results than the policy that is currently implemented in the hospital pharmacies. For the first drug, more than 1000 euros on average could be used for purposes other than having stock at the pharmacy with the same clinical results. In the case of drug 2 this amount is 27118

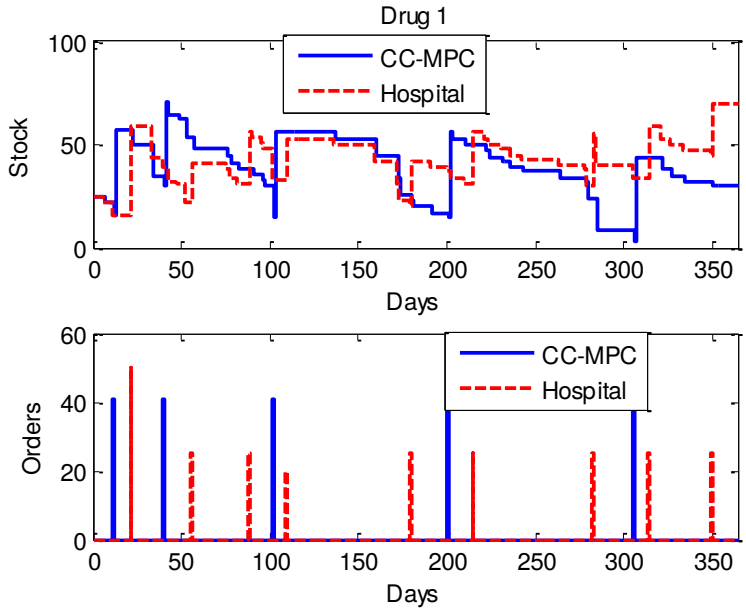

Figure 2.9: Real and simulated stock evolution and placed orders for drug 1.

euros. Another noteworthy point is that the staff at the pharmacy department is freed partially from the duties related to the placement and reception of orders. In both cases the CC-MPC placed 40% less orders than the policy followed by the hospital. Finally, note that a more aggressive tuning of the controller could be used to reduce these values at the cost of higher stockout risks.

Table 2.12: Comparison of the behavior of the drug 1 applying CC-MPC and hospital policy.

Approach	**Orders**	**Stock-out**	**Mean**	**Desviation**
CC-MPC	5	0	39	14
Hospital historical data	9	0	43	11

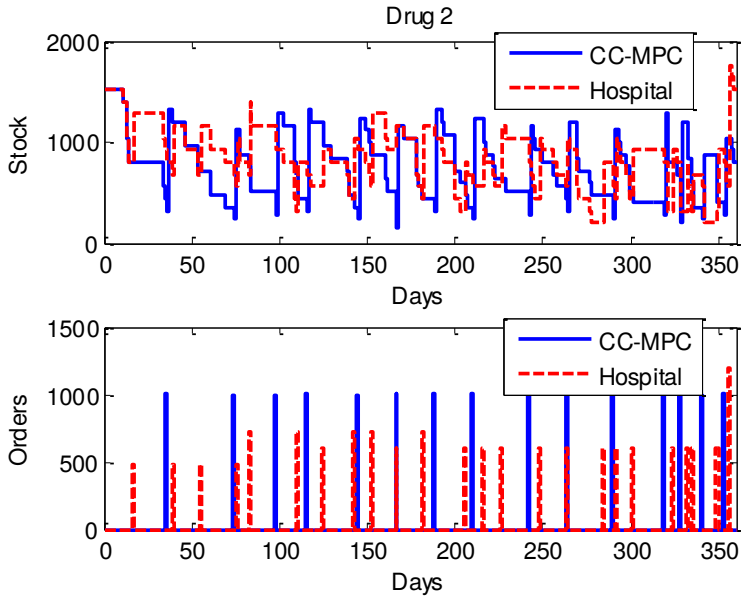

Figure 2.10: Real and simulated stock evolution and placed orders for drug 2.

Table 2.13: Comparison of the behavior of the drug 2 applying CC-MPC and hospital policy.

Approach	**Orders**	**Stock-out**	**Mean**	**Desviation**
CC-MPC	15	0	770	316
Hospital historical data	25	0	861	313

The optimization has been made taking into account the constraints (2.38)-(2.42). A problem is solved at every sampling time to compute a control sequence u that takes the system to the desired reference. For this simulation, the stock reference (security stock) has been set to 2. All optimization problems, solved for the exhaustive algorithm, were computed by using a linear programming routines (`linprog` in *Matlab*), on a machine with an Intel Core 2 Duo CPU with 3.33 GHz and 8 GB RAM. The time needed to calculate the optimal sequence of actions per drug and day was below 10 seconds. If we take into account that the orders are recomputed once a day, it is possible to

calculate optimal control actions for 8640 drugs a day with the current configuration, many more than those used in the hospitals.

These results have been published in [33].

Chapter 3

Hierarchical Stochastic MPC

A possibility to deal with the risks and uncertainties that affect to the distributed systems, e.g., energy management and water resources management (WRM) systems, is to use a hierarchical structure where an upper control layer provides instructions to the lower control layers, the latter are in charge of the regulation of smaller regions controlled by local agents. In this way, coordination is attained [27–29]. Next, two case studies are presented in this Chapter. First, a multicriteria optimal operation of a microgrid considering risk analysis, renewable resources and a centralized MPC, where identification of potential risks has been performed and two MPCs are designed: one for risk mitigation and another for the optimal control of the microgrid. The proposed algorithm considers an external loop where information about risk evaluation is updated. The risk mitigation policy may change setting points and constraints as well as execute actions. On the other hand, as a second case study, tree-based hierarchical and distributed MPC (HD-MPC) for WRM is addressed by two layer-hierarchical structure, the higher layer collects and coordinates forecast information for sending different scenarios that take into account the uncertainties to the local agents. The lower layer, comprised of local agents, solves an optimization problem in a distributed fashion. The HD-MPC method is tested on a real-world case, the North Sea Canal system.

3.1 Multicriteria Optimal Operation of a Microgrid

Renewable energies promote competition in the generation of electricity, ensuring environmental protection. They are easily accessible and inexhaustible, unlike fossil fu-

els. The investment in their development ensures a sustainable future for our planet. The objective from this Section is to undertake assessment and mitigation actions in optimal power dispatch. An external loop controls the risk factors and can change parameters on operation of the microgrid. An MPC is used at this level to reach optimal risk avoiding, as seen below.

3.1.1 A Risk-based control approach in power generation systems

Risk management is a process that includes three basic elements [75]:

1. Goal settings.
2. Risk Identification: information gathering and interpretation. Risk identification involves ensuring all key topics are considered, and lessons learnt from past risk experience are incorporated. In order to protect the microgrid and obtain an optimal dispatch of the energy, the possible faults detected in the main grid as well as the microgrid should de considered. In the first case, actions to be taken should be aimed to isolate the microgrid from the main grid as soon as possible. In the case of presenting an internal failure of the microgrid, we should define a sequence of steps to replace or repair the subsystem where the error occurred. Hazard and Operativity Analysis (HAZOP), cause/effect diagrams, brainstorming sessions, among others, can be tools to help in the identification.

   Risk can be defined with this expression:

   $$Risk = Probability * Impact$$

   Probability, is the likelihood that risk occurs and it may depend on the time. A function $P_r(t)$ is defined for each risk R_r. Impacts can be evaluated on various parameters, i.e. cost, time, efficiency, etc.

   So, we can define the total *Risk Exposure* of a risk r like the sum of the nc potential impacts that would result:

   $$RE_r(t) = P_r(t) \sum_{c=1}^{nc} II_{rc}, \tag{3.1}$$

   where $P_r(t)$ is the probability of risk R_r at instant t and II_{rc} denotes the initial impact of risk R_r affecting parameter Z_c; both of these can be time dependent.

   Note that all components of the microgrid (e.g., sources, transformers, and electric lines) are susceptible to present risks affecting parameters like cost, time delay, etc.

3. Risk Mitigation: measures to influence human behavior, treasuries system components, or both. If a mitigation plan were incorporated, an analysis about the cause of these risks should be undertaken to find out the mitigation actions. Mitigation can be performed on two different fronts: preventive and other reactive. In the case of preventive actions, efforts are made to reduce the probability of risks occurring. When reactive actions are chosen, we want to reduce the impacts of the risks. In this way, each risk can be associated to a set of actions that could mitigate it. We assume the mitigation action set to be $A = \{A_1, \cdots, A_p\}$ with p representing the number of mitigation actions. Each mitigation action is described by a set of three elements:

$$A_a = \{u_{M_a}, F_a, G_a\} \quad a = 1, ..., p. \tag{3.2}$$

where the decision variable for mitigation action A_a is denoted by u_{M_a}. $F_a = \{f_{ca} : \mathbb{R} \to \mathbb{R}\}$ with $c = 1, \ldots, nc$ is the set of functions that determine the risk impact reduction as a function of u_{M_a} at each time; thus, f_{ca} is the reduction of the initial impact affecting parameter Z_c when action A_a is applied. Actions that are chosen to mitigate risks can have an associated cost of execution; this characteristic is modelled by defining functions $G_a = \{g_{ca} : \mathbb{R} \to \mathbb{R}\}$ that describe the extra costs to be added if action A_a is also carried out as a function of the corresponding decision variable u_{M_a}. This variable is integer or real depending on the nature of the action. For example, in case of a execute/non execute decision, it will be a boolean variable. In practice, the use of a Risk Breakdown Structure to list risks and actions that can mitigate them, can improve the risk management process [76]. The equation (3.1) is modified to incorporate the risk mitigation actions and set the parameters to be optimized. It takes the following form:

$$RE_r(u_M, t) = \sum_{c=1}^{nc} RE_{rc}(u_M, t) = \tag{3.3}$$

$$= \quad P_r(t)\big(II_{rc} - \sum_{a=1}^{p} RA_{ra} f_{ca}(u_{M_a})\big) + \sum_{a=1}^{p} RA_{ra} g_{ca}(u_{M_a}), \tag{3.4}$$

where the sum of functions f means the reduction of the initial impact by taking actions; $RA_{ra} = 1$ if risk R_r is mitigated by action A_a, otherwise, $RA_{ra} = 0$. $g_{ca}(u_{M_a})$ is the extra cost of mitigation action A_a on the parameter Z_c. Hence, $RE_{rc}(u_M, t)$ means the exposure of risk R_r affecting parameter Z_c at instant t.

Optimal risk mitigation

The control goal is expressed by a multicriteria weighted index performance function where parameters to optimize are included:

$$\min_{u_M,t} J = \sum \beta_i J_i(u_M, t). \tag{3.5}$$

Terms J_i are defined as:

$$J_i(u_M, t) = \sum_{k=1}^{N} (\hat{Y}_{ic}(t+k|t) - w_c(t+k))^2, \tag{3.6}$$

where $\hat{Y}_{ic}$ is the predicted output on parameter Z_C at instant $(t+j)$ on the class of risk i. w_c is the reference to follow for parameter Z_c. Note that w_c corresponds to the reference to follow in the MPC. In this study, usually term w_c is 0, because we want to optimize the parameters. $\hat{Y}_{ic}$ is calculated as

$$\hat{Y}_{ic} = \sum_{r=1}^{m} RE_{rc}(u, t+k), \tag{3.7}$$

where m denotes the total number of risks and N the prediction horizon.
The risk analysis procedure can be described as follow:

- *Step 1:* Initialize/update the parameters of all the elements of the microgrid, i.e. load curve, simulation step, risks, impacts, probabilities and actions.
- *Step 2:* Evaluate expression 3.5 with MPC and execute actions estimated to do at time t.
- *Step 3:* Set changes in the microgrid (if proceed).
- *Step 4:* Wait for the next simulation step $k = k + 1$.
- *Step 5:* Loop back to *Step 1* if simulation period is not finished.

3.1.2 Risk management on the HyLab plant

Next, an identification about potential risks in the real microgrid is undertaken.

Photovoltaic plant

The following risks have been identified:

- R_1: Production capacity of panel.
- R_2: Difficulty in maintenance on rugged terrain.
- R_3: Long time to start supplying energy to the grid.
- R_4: Failure of mechanical parts.
- R_5: Increased need for maintenance due to dirt build up on the panel.
- R_6: Efficiency loss due to tracking failure.
- R_7: Lifetime of panel (degrading in harsh conditions).
- R_8: High maintenance costs.
- R_9: Fluctuations in supply to and hence electricity price on grid (potential overcapacity during daytime).
- R_{10}: Material durability (given high temperatures involved).
- R_{11}: On cloudy days supply to the grid could be inefficient.
- R_{12}: During low demand periods could occur an overcapacity of stored energy.

Fuel Cell

In many situations the major hazards associated with a fuel cell installation may be put into the following items:

- R_{13}: Dangerous substances.
- R_{14}: Fire and explosion.
- R_{15}: Harmful effects of exposure.
- R_{16}: Electric shock.
- R_{17}: General safety hazards, for example manual handling.

Batteries

- R_{18}: Contactor fails closed.
- R_{19}: Loss of HV continuity.
- R_{20}: Electrical short-circuit.
- R_{21}: Overcharge.
- R_{22}: Fire or elevated temperature.
- R_{23}: Low efficiency in batteries, producing not estimated SOC.

Weather conditions

The power generation by renewable sources such as solar panels or wind turbines can change due to weather conditions. Also, weather conditions can change the estimated demand for a specific period. For example, if weather conditions change appreciably, this will result in an increase/decrease in global electricity demand. This can be transferred to the following risks:

- R_{24}: Significant changes in power demand.
- R_{25}: Significant changes in solar generation capacity.

Remark 4 *The internal loop steers the microgrid satisfying the electric demand curve. An MPC, as described in Section 2.1, is also used in the internal loop, but with a different model and objective functions discussed previously in Section 2.2. Note that the frequency at the internal loop is higher that in the external loop.*

3.1.3 Results

The simulations were carried out by using a non-linear model as replacement of the real plant [54]. The initial conditions for SOC and MHL were 50% for each one. The results are presented over a simulation time of 93 days. The sampling time step was 30s for the internal loop and 1 day for the risk loop. The prediction horizon is 5 days.

Table 3.1 shows the risks that have been considered for the example and the mitigation actions that can reduce them. Initial impacts (II) are expressed on the parameters $Z = \{Z_1, Z_2, Z_3, \}$, with Z_1 being the cost (euros/day), Z_2 the estimated power demand, and Z_3 the estimated power generation by the solar panels. Table 3.2 describes

Table 3.1: Risk identification and mitigation

R_i	Impact	P_i	A_i
	Solar		
R_5	$II_{31} = 50, II_{22} = 0, II_{23} = 0$	$P_3(t)$	A_1
R_{11}	$II_{11,1} = 300, II_{11,2} = 0, II_{11,3} = 0.55 * SG$	$P_{11}(t) = N\ (0.9, 0.3), \{25 - 34\}$	A_2
	Fuel Cell		
$R_{13} - R_{17}$	$II_{13,1} = 1000, II_{13,2} = 0, II_{13,3} = 0$	$P_{13}(t)$	A_3, A_4
	Batteries		
R_{23}	$II_{23,1} = 90, II_{23,2} = 0, II_{23,3} = 0$	$P_{23}(t) = 0.6\{10 - 20\}$	A_5
	Weather		
R_{24}	$II_{24,1} = 0, II_{24,2} = 0.32 * PD, II_{24,3} = 0$	$P_{24}(t) = 1\{50, 74\}$	A_6

the actions and their reductions. Last column means if control variable is boolean (B) or real (R). Note that actions A_1 to A_5 involve boolean variables. Therefore, the CPLEX commercial package has been used for the simulations. More specifically:

Table 3.2: Mitigation actions description.

Ac	Description	f_{1i}, g_{1i} on Z_1(cost)	u_i
A_1	Periodic cleaning of mirrors	$f_{11} = 0.95 II_1 u_1, g_{11} = 250 u_1$	B
A_2	Modify the solar generation load shape	$f_{12} = 0.99 II_1 u_2, f_{32} = II_1 u_2, g_{12} = 45 u_2$	B
A_3	Properly maintenance of fuel cell	$f_{13} = 0.95 II_{13} u_3, g_{13} = 300 u_3$	B
A_4	Training for personnel	$f_{14} = 0.70 II_{14} u_4, g_{14} = 600 u_4$	B
A_5	Change upper limit of SOC in battery	$f_{15} = 150 u_5, g_{15} = u_5$	B
A_6	Change Power Demand curve as request	$f_{16} = 0, f_{26} = II_2 u_6, g_{16} = u_6 * p$	R

- Risk R_5 considers how clean panels are. The probability rises with the time and decrease if action A_1 is selected. This is done when the probability exceeds a threshold.
- Risk R_{11} represents the 50% decrease on solar generation estimation used for the prediction and control when there is a cloudy day. Probability of the solar generation between days 25 to 34 is modeled as a normal distribution with mean 0.9 and deviation 0.3. Action A_2 modifies the solar generation estimation value in the simulation.
- All the identified risks in fuel cells are grouped and the proposed action is the

skilled periodic maintenance (A_3) and training for the personnel on time at the beginning (A_4). Probability takes the same form that R_5.

- Risk R_{23} set the loss of efficiency in batteries. A change in the upper limit of battery SOC (from 90% to 70%) is proposed to mitigate it. In order to illustrate this event, probability between days 10 to 20 is set to 0.6. The unexpected changing power demand is described in risk R_{24}. To show the effects, the probability in days 50 and 74 is set to 1. Action A_6 changes the power demand with the increased value.

Figure 3.1 shows the modified power demand and solar generation curves according to risk mitigation. These data are sent to the microgrid controller. The cost function (in euros) is shown in Figure 3.2. It can be observed that a reduction of 10000 euros, by computing Z_1, is reached in 93 days if mitigation is done. Mitigation actions and the days when are running are described in Figure 3.3. Note that actions A_1 and A_3 are performed monthly and A_4 every 90 days.

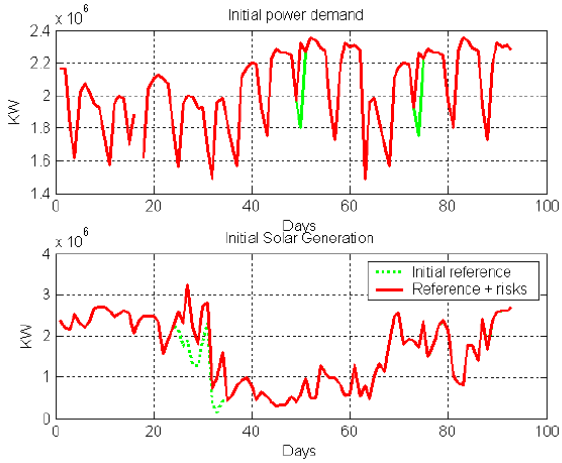

Figure 3.1: Estimations on power demand and solar generation.

Figure 3.4 shows the evolution of the variables that compose the experimental microgrid. The microgrid follows a general scheme of operation to satisfy the demand.

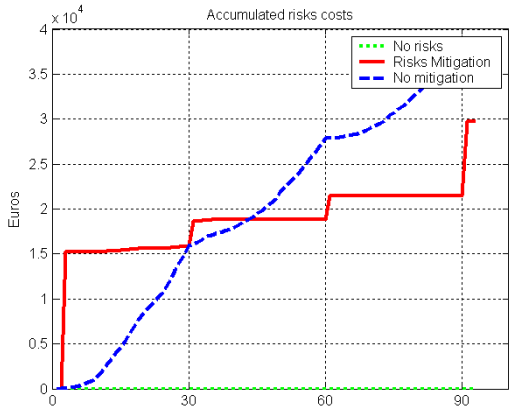

Figure 3.2: Output of the process: Cost.

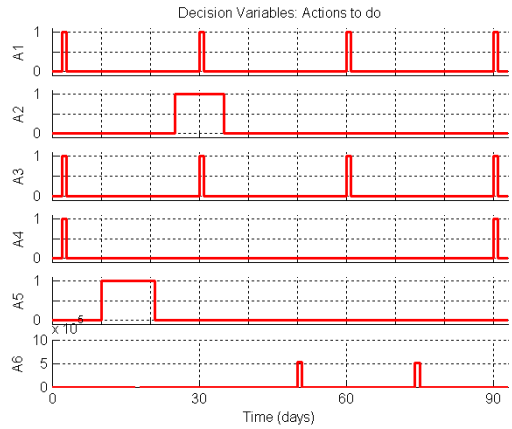

Figure 3.3: Mitigation actions and values along the study period.

The days when the power from the renewable sources is not enough to meet the electric demand, the fuel cells are turned on; SOC and MHL decrease gradually and supplies power to the load. Finally, the microgrid imports energy power from the main grid as the last resource. This can be seen along the time-period from day 30 to day 60. On the

contrary, when there exists excess of renewable energy production and the user demand has been satisfied, the electrolyzer is active, and energy is stored as metallic hydrides, batteries are charged, and power is sold to the external grid.

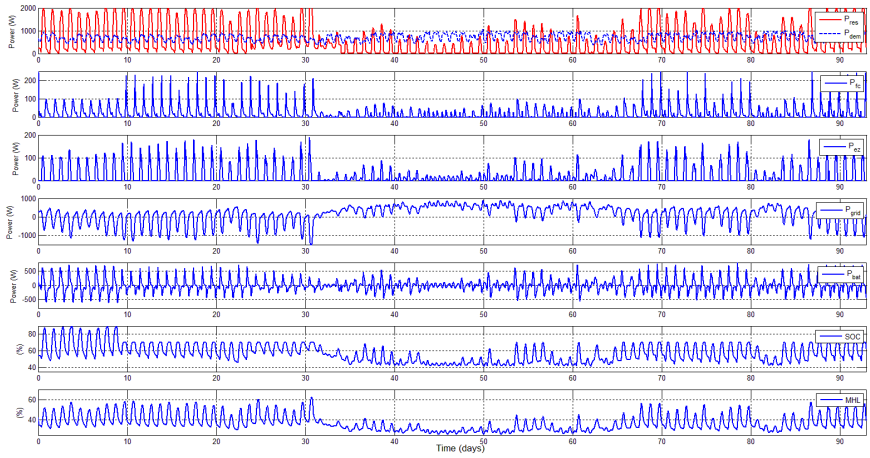

Figure 3.4: Control signals, states, and disturbances by applying multicriteria optimal power dispatch in the HyLab plant.

Figure 3.5 shows in solid line the batteries SOC by considering the risks mitigation over them. The dashed line represents the batteries SOC without a risk analysis. When the renewable power is enough, the batteries are fully charged, which could compromise their lifespan. Therefore, by implementing a risk analysis, the constraints on SOC are readjusted toward acceptable levels, in this case to a maximum level of 70%.

3.2 Tree based HD-MPC for WRM

Substantial uncertainties affect the water systems, e.g., human disturbances (channel modification, drainage, land use, etc.), climatic change and demographic changes, which cause alterations in rainfall and evaporation, changes in sea levels, melting glaciers, etc. [77]. In addition, given that the human dependence on water resources, social, economic, and technological changes are also influencing the behavior of users

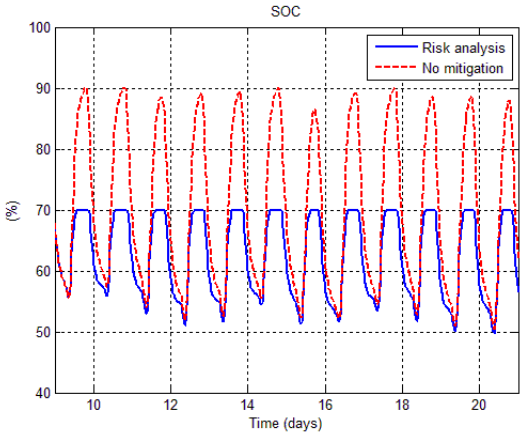

Figure 3.5: Batteries SOC by considering risk analysis and no mitigation actions.

on the demand supplies [78–80]. For these reasons, it is necessary to consider stochastic models and approaches to cope with different types of uncertainties. In this way it is possible to take into account flexible, adaptive, and robust plans, which can respond to predictable and unpredictable environmental changes [81, 82].

For the sake of representation in a control problem, meteorological and hydrological forecasts are usually expressed in the form of an ensemble forecast(EF), which is a collection of trajectories, standing for all the possible evolution along the time of the disturbances, in other words, the uncertainty is modeled by considering its dynamic behavior. Raso [83] pointed out that using EFs in MPC is both beneficial and risky. Prediction makes the control proactive and better at accommodating potential upcoming extreme events. On the other hand, jeopardized robustness may hinder the applicability of MPC. In order to enhance the robustness of MPC when considering EFs, a scenario-based approach is able to address this issue. In this sense, a tree-based approach can be introduced to transfer EFs into a computationally acceptable structure in the control problem [39]. The idea of using a tree-shaped structure is that when trajectories have the same or very similar information of forecasts, a branch of a tree can be used to represent these trajectories. Once the trajectories start to diverge, the branch begins to bifurcate and to spilt up into two or more branches. The resulting MPC controller is known as tree-based MPC (TB-MPC), and greatly improves the robustness of the controller. Regarding TB-MPC applied to WRM, some works have been presented, which deal with the uncertainties and disturbances through a set of possible scenarios

modeled as a branched tree structure.

TB-MPC has been applied in a centralized water system [20] as well as in a distributed drainage water system [84] with a single EF for all subsystems. However, since EFs are presented on different geographically disperse subsystem, their structures are different and need to be modified in the hierarchy to be sending to multi-subsystem. At this point, a scenario based Hierarchical and Distributed MPC (HD-MPC) is developed for deal with the uncertainty in WRM.

The generic MPC formulation and its application have been widely discussed in the literature [2, 3]. Below, it is briefly presented the standard framework of MPC and then explain how to apply it to a general WRM problem. For a water system that needs to be managed to meet several targets in real-time, such as flood defense and coastal management, one accepted way to model the system dynamics and its constraints is of the form [85, 86]:

$$s(x(k), u(k)) = x(k+1) = Ax(k) + B_u u(k) + B_d d(k), \tag{3.8}$$

$$g(x(k), u(k)) = \left[\begin{array}{cccc} x(k); & -x(k); & u(k); & -u(k) \end{array} \right]^{\mathrm{T}}, \tag{3.9}$$

$$b = \left[\begin{array}{cccc} x_{\max}; & -x_{\min}; & u_{\max}(k); & -u_{\min}(k) \end{array} \right]^{\mathrm{T}}. \tag{3.10}$$

The control performance can be measured by:

$$\begin{aligned} &f(x(k+1), u(k)) = \\ &[x(k+1) - r(k)]^T Q [x(k+1) - r(k)] + u^T(k) R u(k), \end{aligned} \tag{3.11}$$

where the state $x(k) = [h(k), q(k), h_{\mathrm{g}}(k)]^{\mathrm{T}}$ consists of the water level $h(k)$ of the open channel, the flow $q(k)$ via the pump and the height $h_{\mathrm{g}}(k)$ of the gate, the control variable $u(k) = [\Delta q(k), \Delta h_{\mathrm{g}}(k)]^{\mathrm{T}}$ consists of the change of the pump flow $\Delta q(k)$ and the change of the gate height $\Delta h_{\mathrm{g}}(k)$, $d(k) \in \mathbb{R}^n$ is the system disturbance, $r(k) \in \mathbb{R}^n$ is the reference vector, $Q \in \mathbb{R}^{n \times n}$, $R \in \mathbb{R}^{m \times m}$, $x_{\min} \in \mathbb{R}^n$ and $x_{\max} \in \mathbb{R}^n$ are the minimum and maximum allowed values on the state x, which are either the safety level or the maximum pump capacity or the highest and lowest gate positions, $u_{\min}(k) \in \mathbb{R}^m$ and $u_{\max}(k) \in \mathbb{R}^m$ are the minimum and maximum allowed changes of pump flows or gate positions cite. $A \in \mathbb{R}^{n \times n}$, $B_u \in \mathbb{R}^{n \times m}$ and $B_d \in \mathbb{R}^{n \times l}$ are relevant coefficients derived from the linearized De Saint-Venant equations as well as the physical parameters of the considered water system [87, 88].

Remark 5 *This study uses the formulation of A, B_u and B_d given in the Appendix B of [88].*

Remark 6 *Q is semi-definite and R is definite, and both are diagonal matrices, which guarantee the cost function (3.11) is convex. This implies that: (a) The termination of the optimization can be guaranteed [3]; (b) The problem can be solved by efficient algorithms, such as the interior-point method or the active-set method.*

Remark 7 *As known the physical parameters of the system, in this study, the control of the gate height is made by flow, as a way to conserve the linearly of the system.*

Standard MPC structure has the form:

$$\min_{u(0),\ldots,u(N_{\mathrm{p}}-1)} J(k) = \sum_{k=0}^{N_{\mathrm{p}}-1} f(x(k+1), u(k)), \tag{3.12}$$

subject to

$$x(k+1) = s(x(k), u(k), d(k)), k = 0, 1, ..., N_{\mathrm{p}} - 1, \tag{3.13}$$

$$g(x(k+1), u(k)) \leq b(k), k = 0, 1, ..., N_{\mathrm{p}} - 1, \tag{3.14}$$

where $N_{\mathrm{p}} \in \mathbb{N}^+$ is the length of the prediction horizon, $x(k) \in \mathbb{R}^n$ is the system state at time step k, $u(k) \in \mathbb{R}^m$ is the control variable at time step k, $d(k) \in \mathbb{R}^n$ is the system disturbance at time step k, $f : \mathbb{R}^{n+m} \to \mathbb{R}$ is the stage cost function (linear or non-linear), $s : \mathbb{R}^{n+m} \to \mathbb{R}^n$ is the function describing the system dynamics, $g : \mathbb{R}^{(n+m)\times l} \to \mathbb{R}^l$ is the constraint function, and $b(k) \in \mathbb{R}^l$ in the constraint vector. The idea is to use the system model to predict its behavior along a certain horizon. The cost function is optimized to calculate the best sequence of inputs that can be applied to the system, penalizing the deviations of the inputs and the state of the system with respect to the desired behavior. The sequence of inputs is also designed to satisfy the constrains of the problem.

The tree-based approach can contribute to a control problem when considering ensemble forecasts (EFs). Taking N_{r} possible scenarios into account as a tree, the formu-

lation of TB-MPC for WRM can be expressed as following:

$$\min_{\substack{u_{[1]}(0),...,u_{[1]}(N_\mathrm{p}-1)\\ \vdots \\ u_{[N_\mathrm{r}]}(0),...,u_{[N_\mathrm{r}]}(N_\mathrm{p}-1)}} \quad J(k) = \sum_{i=1}^{N_\mathrm{r}} p_{[i]} \left(\sum_{k=0}^{N_\mathrm{p}-1} f(x_{[i]}(k+1), u_{[i]}(k)) \right), \tag{3.15}$$

subject to

$$x_{[i]}(k+1) = s(x_{[i]}(k), u_{[i]}(k)),\ k = 0, 1, ..., N_\mathrm{p}-1,\ i = 1, ..., N_\mathrm{r}, \tag{3.16}$$

$$g(x_{[i]}(k+1), u_{[i]}(k)) \leq b_{[i]}(k),\ k = 0, 1, ..., N_\mathrm{p}-1,\ i = 1, ..., N_\mathrm{r}, \tag{3.17}$$

$$u_{[i_1]}(k) = u_{[i_2]}(k),\ \text{if section } i_1 \text{ overlaps section } i_2 \textit{ at step } k, \tag{3.18}$$

$$d_{[i_1]}(k)) = d_{[i_2]}(k),\ \text{if section } i_1 \text{ overlaps section } i_2 \textit{ at step } k. \tag{3.19}$$

Remark 8 *We define $p(\cdot)$ as the probability of an event. As a result, for all the scenario sections between time steps k and $k+1$, they satisfy:*

$$\sum_{i=1}^{N\mathrm{r}} p(d_{[i]}(k)) = 1, \tag{3.20}$$

and over the prediction horizon N_p, they satisfy:

$$\prod_{k=0}^{N_\mathrm{p}} p(d_{[i]}(k)) = p_{[i]}, \tag{3.21}$$

$$\sum_{i=1}^{N\mathrm{r}} p_{[i]} = 1. \tag{3.22}$$

3.2.1 Two-level hierarchy TB-MPC

A water system, especially a large-scale one, usually consists of a number of canals and reservoirs. In practical water management problems, the whole water system is often managed in a distributed way. The system is comprised of several subsystems, each of which has its own system prediction (with uncertainties) and objectives. For example, a long river may be separately managed by the countries and regions it flows through. Another example is the Dutch water system. The whole system is divided into 27 non-intersecting areas, each of which is managed by a local Water Board with

local and national management targets. Such a system is manipulated in a distributed way, which means each subsystem is municipal yet has influence on (and is influenced by) its adjacent neighbors. Consequently, the control problem cannot be solved only by a central controller.

There are two ways to exchange information between the local agents and the central unit. Either a top-down manner or a bottom-up one. In the top-down manner, the central unit gathers the complete information of the whole system and delivers it to all the subsystems. This type of information usually comes from processed satellite data. In the bottom-up manner, the subsystem with a gauge station gives its disperse information to the central unit. Then the central unit reckons other subsystems without gauge stations, for example, using the Kalman filter or the neural network algorithm. While, if the information is delivered from down to top, each subsystem has its own forecast or its forecast is calculated from forecasts of its gauged neighbors. The global scenario is obtained by combining the local EFs.

Top-down

The optimization problem can be addressed by two layers composed of a central EF in the top one, and the bottom layer compromises of local MPC problems with EF scenarios for each subsystem. Assume the system comprises N_{b} subsystems. We use the subscript $_{\{j\}}$ to denote a variable that is corresponding to subsystem j (j=1,...,N_{b}). A centralized objective function (3.15) can be distributed as follows:

$$\min J(k) = \sum_{j=1}^{N_{\mathrm{b}}} J_{\{j\}}(k) \tag{3.23}$$

$$= \sum_{j=1}^{N_{\mathrm{b}}} \sum_{i=1}^{N_{\mathrm{r},\{\mathrm{j}\}}} p_{\{j\},[i]} J_{\{j\},[i]}(k), \tag{3.24}$$

where the $J_{\{j\}}(k)$ in (3.23) implies the cost of the objective function of subsystem j. The subsystem j may also have $N_{\mathrm{r},\{\mathrm{j}\}}$ scenarios derived from the centralized EF so that $J_{\{j\}}(k)$ is the sum of all $p_{\{j\},[i]} J_{\{j\},[i]}(k)$'s, which is shown in (3.24). The optimization should also subject to the constraints corresponding to (3.16)-(3.17) within each subsystem. Note that (3.15) shows the central information of the whole system. When distributing the system, there occur coupled variables. For example, the outflow of the upstream catchment is the right inflow of the downstream catchment, which means they are coupled variables linking these two catchments. These coupled variables are important to be considered for system distribution.

Remark 9 *The prerequisite that a system can be managed in a distributed way is that the local information of each subsystem must be known. Note that, in this study, one subsystem actually stands for a certain area which has its own control targets as well as connections with its neighbors.*

It is assumed that all the local agents at the lower level obtain information from the central unit at the higher level. In other words, the prediction of all the scenarios has the same structure of the EF tree.

Figure 3.6 shows an idea of how a centralized tree can be distributed to the subsystems. We assume the system comprises two subsystems. Scenarios 1 and 2 may happen in the subsystem. Therefore, Scenario 3 does not need to be considered in subsystem 1 and the corresponding branch can be left out. So is Scenario 1 for subsystem 2. The modified EF trees only carry useful information for control. Though subsystems have different EF tree structures, they are connected with their neighbors by coupled outputs.

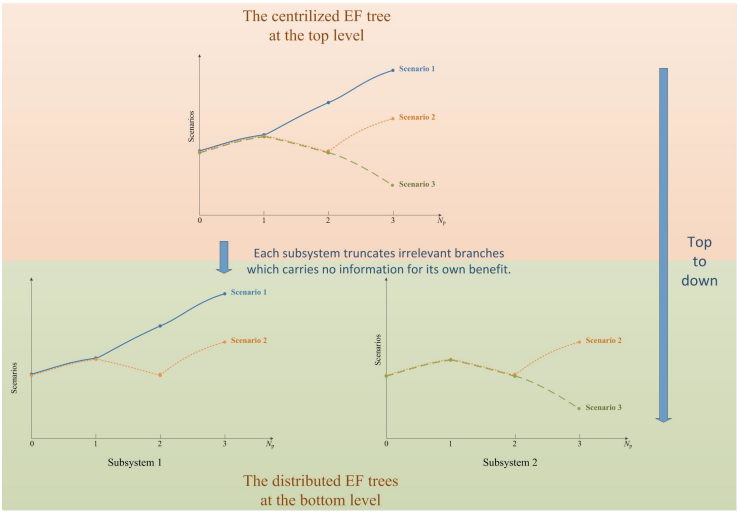

Figure 3.6: A centralized disturbances tree is distributed into the subsystems in a top-down approach.

Bottom-up

In this case, the bottom level usually solves a set of problems locally, which means any subsystem j has its objective function $J_{\{j\}}(k)$ to solve. Adjacent subsystems are linked by their coupled variables. A button-top scheme can be carried out, as shown Figure 3.7. The idea behind this approach is that all targets are merged in a single objective function at the upper level by taking into account the probability of occurrence of each scenario inside the local disturbance tree.

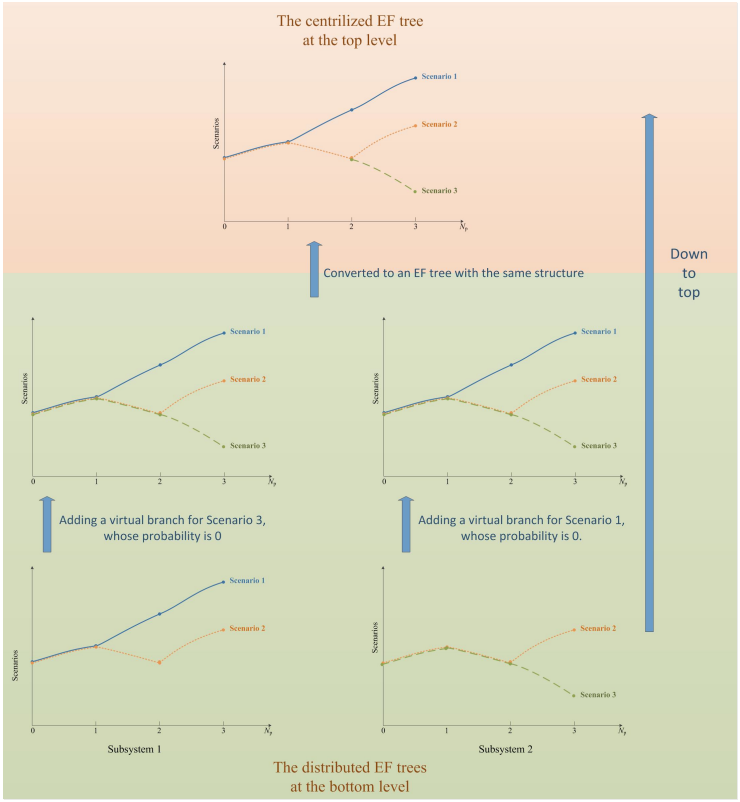

Figure 3.7: A centralized EF is built with the local EFs in a bottom-up fashion.

Remark 10 *The tree structure of any subsystem has the same (homologous) bifurcat-*

ing points and branches as the tree of the whole system. This is owing to the fact that when building the tree of the whole system based on the information of subsystems (Remark 9), all pieces of information are kept and determine where branches should bifurcate in the whole system, (the algorithm results in that when branches of a subsystem bifurcate at a certain time step k, the corresponding branches in the whole system bifurcate accordingly at time step k as well). Therefore, It is necessary to compensate some virtual branches in trees of subsystems whose probability p is made zero for the missing branches between a subsystem and the whole system.

At the bottom layer, local controllers or agents take decision, under their own EF, and share their objective, states and inputs with each others, in a reliable exchange of information in order to coordinate their actions by meaning coupled variables. A distributed fashion can be able to address these kind of problems maintaining the advantages of an MPC, see, e.g., [30]. All in all, the formulation of the tree based HD-MPC can be expressed as follows

$$\text{for } \forall k \in [0, 1, ..., N_{\mathrm{p}} - 1],\ \forall i \in [1, ..., N_{\mathrm{r},\{j\}}], \forall j \in [1, ..., N_{\mathrm{b}}]:$$

$$\min_{\text{all } u_{\{j\},[i]}(k)} \sum_{j=1}^{N_{\mathrm{b}}} \sum_{i=1}^{N_{\mathrm{r},\{j\}}} p_{\{j\},[i]} J_{\{j\},[i]}(k), \tag{3.25}$$

subject to

$$x_{\{j\},[i]}(k+1) = s(x_{\{j\}.[i]}(k), u_{\{j\},[i]}(k)), \tag{3.26}$$

$$g(x_{\{j\},[i]}(k+1), u_{\{j\},[i]}(k)) \leq b_{\{j\},[i]}(k), \tag{3.27}$$

$$u_{\{j\},[i_1]}(k) = u_{\{j\},[i_2]}(k), \text{ if } [i_1] \text{ overlaps } [i_2] \text{ in} \{j\}, \tag{3.28}$$

$$d_{\{j\},[i_1]}(k) = d_{\{j\},[i_2]}(k), \text{ if } [i_1] \text{ overlaps } [i_2] \text{ in} \{j\}, \tag{3.29}$$

$$u_{\{j_1\}}(k) = u_{\{j_2\}}(k) \text{ if they are coupled between } \{j_1\} \text{ and } \{j_2\}. \tag{3.30}$$

The above formulation only shows an idea of how all targets are merged in a single objective function at the upper level. When solving the optimization, it is possible to carry out algorithms for distributing them, such as dual decomposition, see, e.g., [89]. It implies to introduce Lagrangian multipliers many as coupling constraints the optimization problem presents. In this case, each subsystem solves its own optimization constrained by the coupled variables with a exchange information process, as following

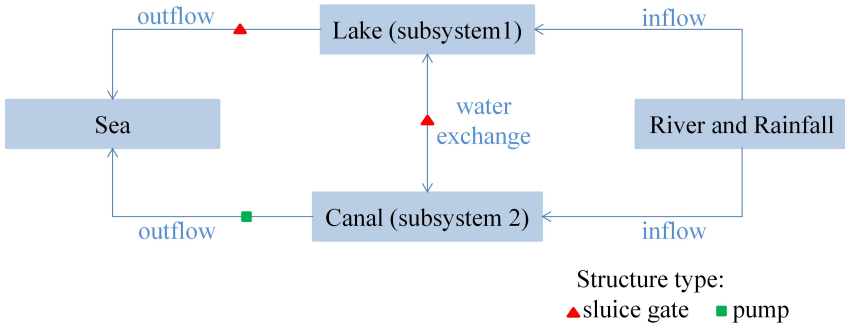

Figure 3.8: Schematic diagram of the North Dutch catchment.

$$\max_{\text{all } \lambda_{\{j_1,j_2\}}(k)} \min_{\text{all } u_{\{j\},[i]}(k)} \sum_{j=1}^{N_\text{b}} \sum_{i=1}^{N_{\text{r},\{j\}}} p_{\{j\},[i]} J_{\{j\},[i]}(k) \tag{3.31}$$
$$+\lambda_{\{j_1,j_2\}}(k)(u_{\{j_1\}}(k) - u_{\{j_2\}}(k)),$$

subject to

$$x_{\{j\},[i]}(k+1) = s(x_{\{j\}.[i]}(k), u_{\{j\},[i]}(k)), \tag{3.32}$$
$$g(x_{\{j\},[i]}(k+1), u_{\{j\},[i]}(k)) \leq b_{\{j\},[i]}(k), \tag{3.33}$$
$$u_{\{j\},[i_1]}(k) = u_{\{j\},[i_2]}(k), \text{ if } [i_1] \text{ overlaps } [i_2] \text{ in } \{j\}, \tag{3.34}$$
$$d_{\{j\},[i_1]}(k) = d_{\{j\},[i_2]}(k) \text{ if } [i_1] \text{ overlaps } [i_2] \text{ in } \{j\}. \tag{3.35}$$

Where $\lambda_{\{j_1,j_2\}}$ are the Lagrange multipliers associated with coupling constraints.

3.2.2 Simulations and results

We test the proposed controller in a North Dutch catchment, which consists of Lake IJsselmeer and Markermeer (subsystem 1) and the North Sea Canal (subsystem 2). For simplification, we use a simplified model, in which gates and pumps are regarded as a single structure if they work in a synchronized way. For example, there are two large sluice gate sets between Lake Ijsselmeer and the North Sea, which are 108 and 54 meters wide respectively. In this case, they are treated as a single 1611 meter wide gate. The North Sea is the boundary condition to be considered. Though Lake IJsselmeer

Table 3.3: Simulation parameters.

Parameters	**Value**
Storage capacity of Lake IJsselmeer and Markermeer	7.4e8 m^3
Storage capacity of North Sea Canal	3.1e7 m^3
Length of time step	1 h
Prediction horizon	24 h
Simulation time	30 days
Setpoint of the water level	-0.4 m
Quadratic penalty on the setpoint	4000
Quadratic penalty on Δq via the Houtrib Gate	1/3000
Quadratic penalty on Δq via the Schellingwoude Gate	1/200
Quadratic penalty on Δq via the IJmuiden pumps	1/260

and Markermeer may have differences in water levels, they are connected via two sluice gates by gravity flows. In this study, they are combined and regarded as one reservoir for simplification. Finally, the model can be depicted as in Figure 3.8. The Lake and the Canal are linked by a locked gate (Schellingwoude Gate), which is the coupled variable that shows the water exchanged between subsystems 1 and 2. The lake, and the canal, discharge into the sea via the Houtrib Gate and the Schellingwoude Gate. Both subsystem carry out a water exchange via IJmuiden pumps. The subsystems' outflows are denoted as q_1 and q_2, respectively. The maximum capacity for the outflow via the Houtrib Gate, the Schellingwoude Gate, and the IJmuiden pumps are constrained to 1000 m^3/s, 260 m^3/s, and 50 m^3/s, respectively. The parameters used for simulation are listed in Table 3.3.

Both subsystems, the Lake and the Canal, have inflows as disturbance $d(k)$ that come from the Rhine River and rainfall. Stochastic inflows have been obtained by sampling historical data from a Dutch live web service operated by Rijkswaterstaat[1]. Twenty scenarios with a Gaussian distribution, which mean value is the historical sequence and standard deviation is 250 m^3/s. These scenarios are used to evaluate the performance of the whole system at the top layer. Figure 3.9 shows the maximum, mean, and minimum values from the EF during the simulation horizon. Therefore, the disturbances fall between these maximum and minimum values. It is possible to note that the disturbances present an increased level due to rainfall from day 6 to day 12, where the maximum value of the EFs is around 1400 m^3/s. Moreover, remaining time

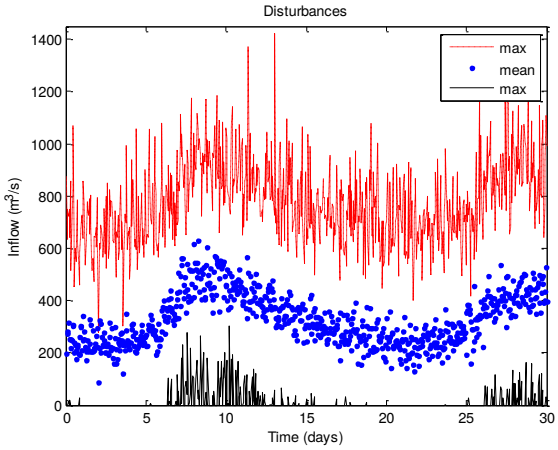

Figure 3.9: Inflow scenarios generated at the top layer.

shows a regular input for two subsystems,

The hierarchy of the system is given as follows: the top level deals with the distribution of the system, in which the system and disturbance are distributed into the two subsystems as mentioned earlier. The top layer delivers two different EF trees, which are composed of the most likely N_{s} scenarios, for subsystem 1 and subsystem 2, respectively, which may be mainly due to different precipitation in different areas or different water demand for various purposes, i.e., different hydrological conditions. Figure 3.10 shows two different disturbance trees, one for each subsystem, for the first instant of the simulation time over five hours. These disturbance trees collect the most relevant probabilistic patterns that each local controller will use to solve the optimization problem dealing with its proper uncertainty at each time instant. While, the bottom layer focuses on the local subsystem, in which local controllers are designed by taking account of multiple scenarios given by the top layer.

In order to show the advantages of the implemented control strategy, we carried out the simulation along 30 days, with a prediction horizon of 24 hours. At each time instant, a new disturbance tree is generated and delivered from the top layer to local controllers. Each tree starts with its measured value as the root of the tree, and their N_s branches result from the EF at the top level for the prediction horizon. The tree construction algorithm is carried out by GAMS [56].

[1] http://live.waterbase.nl

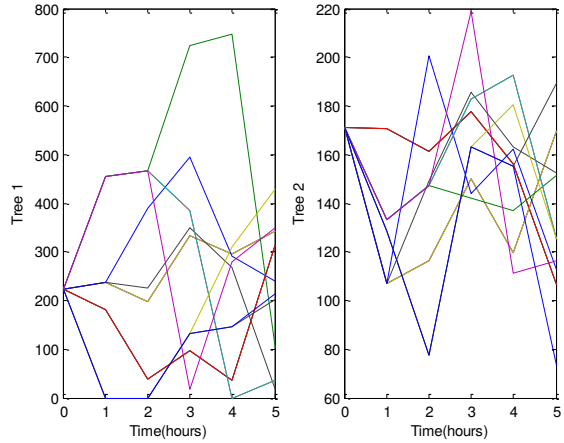

Figure 3.10: Inflows of the local subsystems.

The constraints for the local controllers are given as follows: the maximum capacities for the outflows are set as 1000 m^3/s for subsystem 1, and 260 m^3/s for subsystem 2. The water exchange is constrained between 0 and 50 m^3/s. The water level for both subsystems is bounded between -5 m and 5 m.

The control inputs result from a tree composed of N_s control actions, where only the first component of the sequence is implemented, which corresponds to the control action for the current measured disturbance in each subsystem. The pumps actuate over the outflows; these variables represent the control action carried out by these actuators. Figure 3.11 shows the behavior of the pumps for both subsystems. The pumps turn on for dealing with rainfall. The pumps reach their first peaks; these are 334 m^3/s and 255 m^3/s, respectively.

The pump via the Houtrib Gate, which corresponds to subsystem 1, gets its maximum level, 552 m^3/s, at the time instant which corresponds to the maximum inflows at day 10, approximately. It increases its capacity to give free space in the catchment and maintain the water level. After this period the outflow from pump 1 decreases gradually during 13 days. The inflows present an augmented value, while the discharge increases again to prevent an overflow. On the other hand, the pump 2, via the Schellingwoude Gate, enhances its capacity until it gets its peak value since this subsystem receives the water from the subsystem 1 as well as the rainfall input. Then the outflow, which is operated by pump 2, works between 50 and 143 m^3/s during 15 days. After this period, the inflow increases its value. Therefore the outflow from pump 2 must increase too.

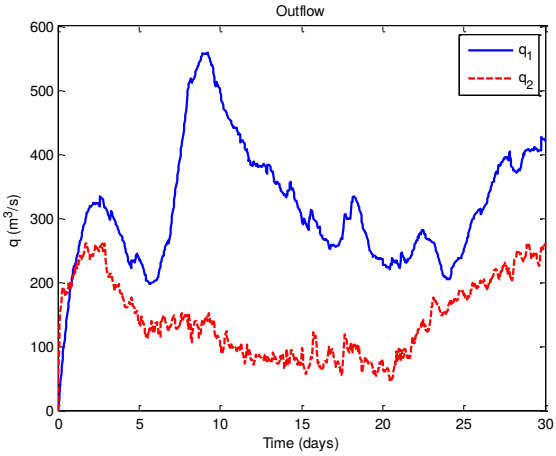

Figure 3.11: Outflows of the local subsystems.

The behavior of the water exchange via the IJmuiden pumps is shown in Figure 3.12. The water exchange is carried out from the sea to the canal. It displays a peak at three times by getting its maximum capacity until the highest rainfall input is over; out of these periods, the water exchanged is reduced remarkably due to the disturbances decrease and it is necessary to keep the water into the reference values.

The water level for both subsystems remains around the reference despite the presence of disturbances. The reference level for the Lake is shown in Figure 3.13. This reference level has a mean value of -0.3967m and a standard deviation of 0.025. Regarding subsystem 2, the water level has a mean level of -0.3984m with a standard deviation that corresponds to 0.034. The water level for the Canal system is shown in Figure 3.14. It is possible to note that both reference levels do not violate the established constraints, at any time instant.

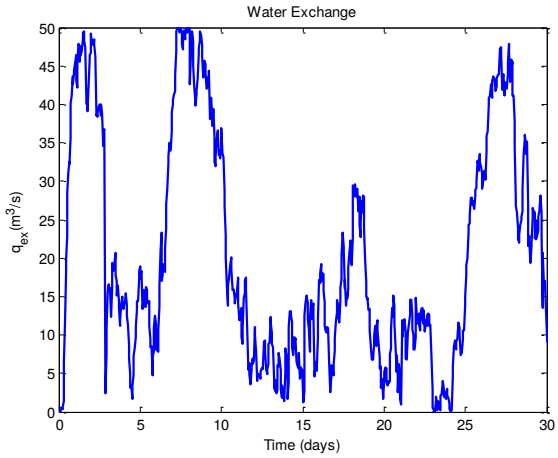

Figure 3.12: Water exchange between the local subsystems.

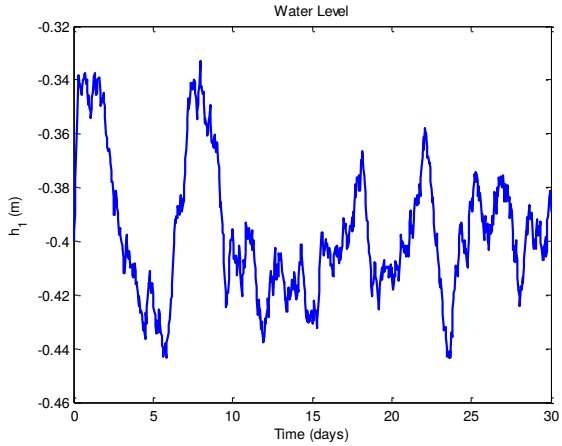

Figure 3.13: Water level of the Lake IJsselmeer and Markermeer.

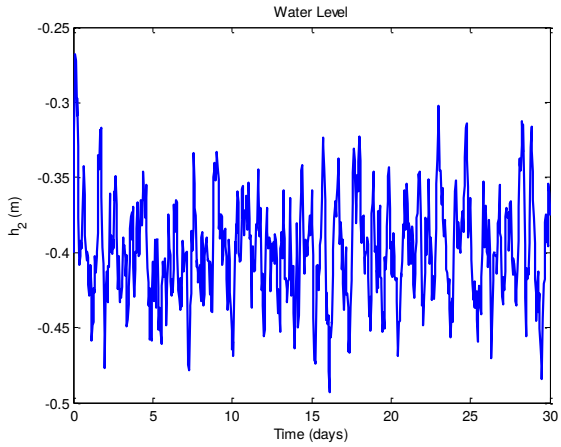

Figure 3.14: Water level of the North Sea canal.

Chapter 4

Stochastic MPC to Deal with Vulnerabilities in Distributed Schemes

There are several geographically disperse systems such as road-traffic, logistics, transportation, water, electrical networks, etc., where it is not possible to apply a centralized MPC due to computational burden, issues with centralized modeling, data collection, etc., as reported in [90]. An alternative to deal with this kind of problems is to divide the whole system into subsystems, each one governed by an MPC controller (or agent) that takes decisions and exchanges information with the other controllers under a negotiation process to obtain an optimal global solution. This control scheme is the so-called distributed MPC (DMPC). Ease of implementation, low computational effort in comparison with centralized MPC, modularity of the system, among others are the potential advantages that DMPC offers, as discussed in [30].

Many approaches for DMPC schemes have been developed in recent years, as described in [30]. A topic that deserves attention is the regular exchange of information during the negotiation process among the controllers. In this sense, DMPC schemes have been carried out by considering a coordinated negotiation process where all controllers work in a reliable way. However, a malicious controller could exploit the vulnerabilities of the network by sharing false information with other controllers, producing an undesirable behavior in the optimization process. At this point, it is possible to speak about cyber-security in the context of DMPC.

Cyber-security can be defined as the activities for protecting cyber-space from in-

fringements, and for defending its technology infrastructure, the services provided and the information, i.e., the set of methods and tools for protecting systems against threats. Cyber-security goals are confidentiality, availability, and integrity of information [91]. Some general applications have been developed in this context. Application areas for which cyber-security needs to be considered are protection systems [92], Internet home users [93], logistics [94–96], and power systems [97, 98]. Control systems are not exempt from possible cyber-attacks, as reported in [99, 100]; the consequences of a cyber attack within a control system can go from performance loss to instability. In particular, [101] presents cyber-security risk assessment for supervisory control and data acquisition (SCADA) and distributed control system networks. So far, cyber-security issues have not been considered in the DMPC literature. Hence, one of the most popular schemes is analyzed, Lagrange based DMPC. In particular, it is shown how a malicious controller in the network can take advantage of the vulnerabilities of the scheme to increase its own benefit at the cost of other controllers. These issues are addressed by considering two well known scenario-based techniques to ensure robustness within the DMPC network, as well as a secure dual decomposition based DMPC which is a heuristic defense inspired by [102]. In this sense, it is possible to robustify the control network against possible malicious controllers.

On the one hand, both types of scenario-based MPC, MS-MPC and TB-MPC, provide robustness by considering several possible scenarios in the optimization problem [32]. On the other hand, the secure dual decomposition based DMPC based on a consensus approach that dismisses the extreme control actions is presented as a way to protect the distributed system from potential threats.

In this work, these approaches are applied toward distributed systems to cope with internal threats and mitigate the effects of the attacks from malicious controllers. Based on this background, and to deal with the internal threats from the distributed network, these approaches are incorporated in the DMPC formulation as a way to secure dual decomposition DMPC. Also, in order to illustrate the proposed defense methods, the control of a local grid of households is presented as a case study [103].

4.1 Dual Decomposition based DMPC

This section presents a commonly used distributed optimization algorithm based on dual decomposition [89, 104]. Let us consider a distributed system composed of N_{b} subsystems defined by discrete-time linear time-invariant models. The dynamics of subsystem i are given by

$$x_i(k+1) = A_i x_i(k) + B_i u_i(k), \tag{4.1}$$

where $x_i \in \mathbb{R}^{n_{x,i}}$ and $u_i \in \mathbb{R}^{n_{u,i}}$ denote the states and input of the system, respectively. $A_i \in \mathbb{R}^{n_{x,i} \times n_{x,i}}$ is the state matrix and $B_i \in \mathbb{R}^{n_{x,i} \times n_{u,i}}$ represents the input matrix. The variables $n_{x,i}$ and $n_{u,i}$ represent the number of states and the number of inputs of the subsystem i, respectively. Each subsystem is subject to convex state and input constraints:

$$x_i(k) \in \mathcal{X}_i, \quad \forall k \in \mathbb{Z}_+, \tag{4.2a}$$

$$u_i(k) \in \mathcal{U}_i, \quad \forall k \in \mathbb{Z}_+, \tag{4.2b}$$

where $\mathbb{Z}_+$ denotes the set of non-negative integer numbers. Let the aggregated vectors of states and inputs be $x(k) = \left[x_1(k)^{\mathrm{T}} \cdots x_{N_\mathrm{b}}(k)^{\mathrm{T}}\right]^{\mathrm{T}}$, and $u(k) = \left[u_1(k)^{\mathrm{T}} \cdots u_{N_\mathrm{b}}(k)^{\mathrm{T}}\right]^{\mathrm{T}}$, where $x \in \mathbb{R}^{n_x}$, $n_x = \sum_{i=1}^{N_\mathrm{b}} n_{x,i}$, $u \in \mathbb{R}^{n_u}$, and $n_u = \sum_{i=1}^{N_\mathrm{b}} n_{u,i}$.

The N_b subsystems are also subject to constraints coupling the inputs:

$$Cu(k) = \sum_{i=1}^{N_\mathrm{b}} C_i u_i(k) \leq c, \tag{4.3}$$

where $C \in \mathbb{R}^{n_c \times n_u}$, $C_i \in \mathbb{R}^{n_c \times n_{u_i}}$ and $c \in \mathbb{R}^{n_c}$.

Remark 11 *This formulation is used for simplicity and it can be easily extended to other types of coupling constraints in the dynamics, e.g., coupling in the states.*

It is assumed that a convex stage cost function for each subsystem is given by

$$\ell_i(x_i(k+1), u_i(k)). \tag{4.4}$$

This cost has to be minimized by the controller i.

Each subsystem i is controlled by a local MPC controller. The main idea of (centralized and distributed) MPC is to obtain a control signal by solving, at each time step, a finite-horizon optimization problem (FHOP) that takes into account the prediction model of each subsystem. In particular, (4.1) is used to predict the evolution of the system along a given horizon N_p as a function of the sequence of inputs provided. In this way, it is possible to calculate a control sequence $u_i^*[k : k+N_\mathrm{p}-1]$ that optimizes (4.4) along the horizon. The first component of the control sequence is implemented at the current time step, and the problem is solved at the next time step following a receding horizon strategy. The optimization problem over a fixed time prediction horizon $N_\mathrm{p} \in \mathbb{Z}_+$ can be written as

$$u_i^*[k : k+N_\mathrm{p}-1] = \arg \min_{u_i[k:k+N_\mathrm{p}-1]} \sum_{j=k}^{k+N_\mathrm{p}-1} \ell_i(x_i(j+1), u_i(j)), \tag{4.5}$$

subject to (4.1)-(4.3), assuming that the predicted control actions and states of the rest of the subsystems are known.

From an overall perspective, the stage cost function is

$$\ell(x(k), u(k)) = \sum_{i=1}^{N_{\mathrm{b}}} \ell_i(x_i(k), u_i(k)). \tag{4.6}$$

In this way, the optimization problem, from a global point of view, is given by

$$\min_{u[k:k+N_{\mathrm{p}}-1]} \sum_{j=k}^{k+N_{\mathrm{p}}-1} \ell(x(j+1), u(j)), \tag{4.7}$$

subject to (4.1)-(4.3).

Due to the coupling in (4.3), controllers have to share information. It is necessary to consider the role played by coupling variables explicitly. Hence, the controllers have to coordinate their actions using a negotiation process.

The dual decomposition approach consists of decomposing the *coupled* variables in local versions with additional constraints to guarantee that they have a coordinated value. The constraints are relaxed by introducing associated Lagrange multipliers. In this sense, the optimization problem is formulated by minimizing

$$L(\eta(k), \Lambda(k)) = \sum_{j=k}^{k+N_{\mathrm{p}}-1} (\ell(x(j+1), u(j)) + \lambda(j)^{\mathrm{T}}(Cu(j) - c)), \tag{4.8}$$

where $\eta(k) = \left[x[k+1 : k+N_{\mathrm{p}}]^{\mathrm{T}}, u[k : k+N_{\mathrm{p}}-1]^{\mathrm{T}}\right]^{\mathrm{T}}$ is defined as the vector composed of the states and inputs along the horizon N_{p}, $\lambda(j) \in \mathbb{R}^{n_c}$ are the multipliers associated with the coupling constraints (4.3), and $\Lambda(k) = \lambda[k : k+N_{\mathrm{p}}-1]$ is the sequence of the Lagrange multipliers along the horizon.

Remark 12 *Each coupling constraint is associated with a Lagrange multiplier, which can be interpreted as a price. These prices are used to coordinate the subsystems to respect collectively the coupling constraints [89].*

The optimal value of the problem is defined as

$$\begin{aligned} g(\Lambda(k)) = \min_{u[k:k+N_{\mathrm{p}}-1]} \sum_{j=k}^{k+N_{\mathrm{p}}-1} & (\ell(x(j+1), u(j)) \\ & + \lambda(j)^{\mathrm{T}}(Cu(j) - c)), \end{aligned} \tag{4.9}$$

subject to (4.1) and (4.2).

The optimization problem (4.7) can be solved in a distributed manner by solving its dual problem

$$\begin{aligned} &\text{maximize } g(\Lambda(k)), \\ &\text{subject to } \Lambda(k) \succeq 0, \end{aligned} \tag{4.10}$$

by using a distributed gradient search, where $\succeq$ represents componentwise inequality.

The distributed control problem solved by dual decomposition is summarized in Algorithm 1 [89].

Algorithm 1 Dual decomposition based DMPC.

1: Each controller initializes its prices (Lagrange multipliers) $\Lambda[k] \succeq 0$.
2: **repeat**
3: Each controller solves its local optimization problem with the current value of $\Lambda(k)$, i.e.,

$$\min_{u_i[k:k+N_\mathrm{p}-1]} \sum_{j=k}^{k+N_\mathrm{p}-1} (\ell_i(x_i(j+1), u_i(j)) + \lambda(j)^T C_i u_i(j)), \tag{4.11a}$$

subject to

$$x_i(j+1) = A_i x_i(j) + B_i u_i(j), \quad \forall j \in \mathbb{Z}_+, \tag{4.11b}$$
$$x_i(j) \in \mathcal{X}_i, \quad \forall j \in \mathbb{Z}_+, \tag{4.11c}$$
$$u_i(j) \in \mathcal{U}_i, \quad \forall j \in \mathbb{Z}_+. \tag{4.11d}$$

The solution of the optimization problem is denoted as $x_i^*[k+1 : k+N_\mathrm{p}]$, $u_i^*[k : k+N_\mathrm{p}-1]$. Then these values are exchanged with other controllers.
4: Each controller i determines the violations of the coupling constraints $s(k) \triangleq \sum_{i=1}^{N} C_i u_i^*(k) - c$, $S(k) = s[k : k+N_\mathrm{p}-1] \in \mathbb{R}^{N\mathrm{p} \times n_c}$ and calculates the new prices along the horizon $\Lambda(k) := \max[0, \Lambda(k) + \gamma S(k)]$, where γ is the step size.
5: **until** $\max(S(k)) < \epsilon$, where ϵ is a prespecified threshold, **or** the maximum number of iterations reached.
6: Each subsystem implements at the current time step the first component of the control sequence $u_i^*[k : k+N_\mathrm{p}-1]$.
7: Let $k = k+1$ and return to step 1.

Dual decomposition has been used in several applications, e.g., [105] shows a distributed predictive control approach for building temperature regulation; in [106], a DMPC based on dual decomposition is applied to a network of households; in [107] and [108] is used DMPC for ships and logistics, respectively.

4.2 Attacks in a DMPC scheme

Algorithm 1 works in a reliable information exchange setting. If one of the controllers is malicious, the whole system can fail. In particular, we consider that one of the controllers is an attacker that shares false information with others. The attacker can lie about its information: states, control variables, constraints, and goals. This kind of information is typically exchanged among the controllers. However, some of them could be manipulated and produce a potential failure of the control system or at least loss of optimality/performance. Four different ways in which an attacker can take advantage by exchanging false information with other controllers of the subsystems are presented.

4.2.1 Fake reference

At this point, the whole system is composed of N_{b} subsystems, where the controller $m \in \mathbb{N} = \{1, ..., N_{\mathrm{b}}\}$ attacks the remaining controllers by using a false reference ($x_{m^*_{\mathrm{ref}}}$) to bias the negotiation. Therefore, the stage cost function optimized by controller m is given by

$$\begin{aligned} &\ell^*_m(x_m(k+1), u_m(k)) \\ &\qquad = \ell_m(x_m(k+1) - x_{m^*_{\mathrm{ref}}}, u_m(k)). \end{aligned} \tag{4.12}$$

The optimization problem for controller m can be written as

$$\begin{aligned} \min_{u_m[k:k+N_{\mathrm{p}}-1]} \quad & \sum_{j=k}^{k+N_{\mathrm{p}}-1} (\ell^*_m(x_m(j+1), u_m(j)) + \\ & \qquad \lambda(j)^T C_m u_m(j)), \end{aligned} \tag{4.13a}$$

subject to

$$x_m(j+1) = A_m x(j) + B_m u_m(j), \quad \forall j \in \mathbb{Z}_+, \tag{4.13b}$$

$$x_m(j) \in \mathcal{X}_m, \quad \forall j \in \mathbb{Z}_+, \tag{4.13c}$$

$$u_m(j) \in \mathcal{U}_m, \quad \forall j \in \mathbb{Z}_+. \tag{4.13d}$$

The use of a fake reference could steer the negotiation process towards a result that is more beneficial for the attacker. In this sense, there is no incentive for the controllers to be honest regarding their real preferences because they can be better off in this way from a local perspective.

4.2.2 Fake constraints

Another way in which the attacking controller m can take advantage from the whole system is by carrying out the optimization problem using fake constraints, i.e., the remaining subsystems optimize their objective functions by considering their original constraints while the attacker uses constraints that steer the negotiation process by reducing its own cost function. The cost function optimized by the attacker is

$$\min_{u_m[k:k+N_\mathrm{p}-1]} \sum_{j=k}^{k+N_\mathrm{p}-1} (\ell_m(x_m(j+1), u_m(j)) + \lambda(j)^T C_m u_m(j)), \tag{4.14a}$$

subject to

$$x_m(j+1) = A_m x(j) + B_m u_m(j), \quad \forall j \in \mathbb{Z}_+, \tag{4.14b}$$
$$x_m(j) \in \mathcal{X}_m^*, \quad \forall j \in \mathbb{Z}_+, \tag{4.14c}$$
$$u_m(j) \in \mathcal{U}_m^*, \quad \forall j \in \mathbb{Z}_+, \tag{4.14d}$$

where $\mathcal{X}_m^*$ and $\mathcal{U}_m^*$ are the sets of false constraints that have been modified to take advantage of the other controllers.

4.2.3 "Liar" controller

The third way to manipulate other controllers is to carry out the standard negotiation process given by Algorithm 1, but implementing a different action at the end. Once the control signal has been negotiated, the malicious controller has more information regarding the shared variables and can change the value of those under its control, that is, it implements a control signal that only optimizes its own cost function. In other words, the controller m recalculates its control signal in a selfish manner for example, with $\lambda[k] = 0$ in its objective function given by (4.22).

4.2.4 Selfish attack

The attacker seeks to optimize only its own cost function, which depends on its own states and input variables and on those of its neighbors. In other words, the agent may calculate the control actions to make the coordination process more beneficial for its own interest. To cheat the system, the attacker may share false information with others to steer the negotiation process. The other controllers will compute a sequence of control actions with the information received and hence the overall optimization will be manipulated by the attacker.

To obtain a better result, agent m can modify its cost function by including a new coefficient denoted as α. In this manner, the subsystem m optimizes

$$\min_{u_m[k:k+N_\mathrm{p}-1]} \sum_{j=k}^{k+N_\mathrm{p}-1} \left[\alpha\left(\ell_m(x_m(j+1),u_m(j))\right)+\lambda(j)^T C_m u_m(j)\right]$$

with $\alpha > 1$. This is equivalent to solving the overall optimization problem expressed as minimizing

$$\ell(x(k),u(k)) = \alpha\ell_m(x_m(k),u_m(k)) + \sum_{i\neq m}\ell_i(x_i(k),u_i(k)), \tag{4.15}$$

subject to (4.1), (4.2), and (4.3).

In this way, the solution is biased towards the interests of agent m.

4.3 Secure Scenario-based DMPC

As seen in the previous section, the negotiation process can be manipulated. It is necessary to carry out a method that relieves the potential effects of an intentional attack whenever this situation is presumed. In this sense, we propose two scenario-based approaches to robustify the control network against malicious controllers.

Given that the attacker is able to manipulate the costs and negotiates considering its own benefit, trustworthy price information based on historical data will be used to generate scenarios. All in all, the price information is accessible for all controllers.

4.3.1 Scenario Generation

The scenario generation is necessary to relieve the effects of an attacker inside the network, and might be performed in a empirical manner or by using a stochastic model [109].

In order to generate different scenario evolutions, noise was added to the controllers' states $x_i[k]$ at each time step considered in the experiments, i.e.,

$$\widetilde{x}_i(k) = x_i(k) + \mathcal{N}(\mu, \sigma), \tag{4.16}$$

where $\widetilde{x}_i[k]$ represents the measurement of each state containing noise $\mathcal{N}(\mu, \sigma)$, which is a normal distribution function with mean μ and standard deviation σ. In this way, several experiments are repeated, and the price information $\lambda_i(k)$ is collected as a scenario. It is important to note that the collected information has to be reliable, i.e., any abnormal behavior has to be discarded.

The set of price scenarios of each controller i is expressed as follows

$$\Lambda_i(k) = \{\lambda_i^1(k), \lambda_i^2(k), \cdots, \lambda_i^{N_s}(k)\}. \tag{4.17}$$

Here, N_s is the number of scenarios. A higher number of scenarios increases the computational burden of each subsystem.

4.3.2 Multi-scenario DMPC (MS-DMPC)

MS-DMPC provides robustness to the subsystems in a distributed fashion. It describes the dynamics of each subsystem by considering its evolution in all the scenarios considered. The idea behind this scheme is to compute a unique input control that ensures the satisfaction of the constraints for all the potential trajectories determined by the set of scenarios. One issue that deserves special attention is the number of scenarios (N_s) that guarantees the robustness of the whole system. A higher number of scenarios results in an over conservative control input and may compromise the computational burden.

The problem formulation of MS-DMPC for each controller $i \in \mathbb{Z}_1^{N_\mathrm{b}}$ at each time instant k is expressed as

$$\min_{u_i[k:k+N_\mathrm{p}-1]} \sum_{l=1}^{N_s} \rho_i^l \sum_{j=k}^{k+N_\mathrm{p}-1} (\ell_i(x_i^l(j+1), u_i(j)) + \lambda^l(j)^T C_i u_i(j)), \tag{4.18a}$$

subject to

$$x_i^l(j+1) = A_i^l x_i^l(j) + B_i^l u_i(j), \tag{4.18b}$$

$$x_i^l(j) \in \mathcal{X}_i, \quad \forall j \in \mathbb{Z}_+, \quad \forall l \in \mathbb{Z}_1^{N_s}, \tag{4.18c}$$

$$u_i^l(j) \in \mathcal{U}_i, \quad \forall j \in \mathbb{Z}_+, \quad \forall l \in \mathbb{Z}_1^{N_s}, \tag{4.18d}$$

where ρ^l is the probability of occurrence of each scenario l.

Remark 13 *The first scenario $\lambda_i^1(k)$ results from the actualization of the prices at each iteration by carrying out the dual decomposition DMPC, while the remaining scenarios do not update their values over the current time k.*

4.3.3 Tree-based DMPC (TB-DMPC)

TB-DMPC requires transforming the different price evolutions into a scenarios tree that, through its evolution over the prediction horizon, diverges at the *bifurcation points* when the evolution of the prices cannot be confined in one branch of a tree. The formulation of the control problem involves making tree-based scenarios where only the main price patterns are modeled.

Each scenario in the tree has its own control signal, which means that the over conservativeness of MS-DMPC can be reduced. However, more optimization variables are needed: given that the control signal cannot anticipate events beyond the next bifurcation point, control sequences for different scenarios have to be equal as long as the scenarios do not branch out, i.e., non-anticipate constraints have to be introduced. The solution of the optimization problem results in a rooted-tree of control actions. Also, only the first component of this tree, which is equal for all the scenarios, is applied at the current time.

The TB-DMPC problem formulation to be solved for each controller $i \in \mathbb{Z}_1^{N_\mathrm{b}}$ at each time instant is represented by

$$\min_{u_i^l[k:k+N_\mathrm{p}-1]} \sum_{l=1}^{N_s} \rho_i^l \sum_{j=k}^{k+N_\mathrm{p}-1} (\ell_i(x_i^l(j+1), u_i^l(j)) + \lambda^l(j)^T C_i u_i^l(j)), \tag{4.19a}$$

subject to

$$x_i^l(j+1) = A_i^l x_i^l(j) + B_i^l u_i^l(j), \tag{4.19b}$$
$$x_i^l(j) \in \mathcal{X}_i, \quad \forall j \in \mathbb{Z}_+, \quad \forall l \in \mathbb{Z}_1^{N_s}, \tag{4.19c}$$
$$u_i^l(j) \in \mathcal{U}_i, \quad \forall j \in \mathbb{Z}_+, \quad \forall l \in \mathbb{Z}_1^{N_s}, \tag{4.19d}$$

and the non-anticipate constraints given by

$$u_i^l(j) = u_i^r(j) \quad \text{if} \quad \lambda_i^l(j) = \lambda_i^r(j);\ \forall\, l \neq r. \tag{4.19e}$$

4.4 Secure dual decomposition based DMPC

The idea behind this third defense approach is that each agent optimizes its own objective function, given by (4.22), in a regular manner before the negotiation process, described by Algorithm 1, starts. During the inner iteration, i.e., the negotiation on the coupled variables (4.3), the largest and smallest optimal control signals and their respective local controllers are ignored. Hence, the consensus process is performed without taking into account of two agents, because one of them could be an attacker that pretends to steer the value of the coupled variables away from the social consensus. The optimal control action for each agent is calculated by carrying out Algorithm 1 without considering the two potential attackers. Then this process is repeated at each time instant k.

This scheme tries to avoid that a malicious agent can increase the costs of the rest of the subsystems looking for its benefit. As a consequence, the attacker is ignored by the remainder of the agents during the negotiation process.

With this modification, the algorithm carried out by each local controller $i \in \mathcal{N}$ is given by Algorithm 2.

Remark 14 *The secure dual decomposition based DMPC algorithm is motivated by resilient techniques for multi-agent consensus studied in [102], whose root can be found in fault tolerant distributed algorithms, e.g., [110]. There, a consensus problem is considered where up to f agents can be malicious/faulty and may confuse the remaining normal agents by sending arbitrary signals.*

In the simple case where the agent network forms a complete graph, the normal agents can achieve consensus under the following conditions: (i) The normal agents update their states by ignoring the f smallest and f largest values received from their neighbors. (ii) The number f of malicious agents satisfies $f \leq (\lceil n/2 \rceil - 1)/2$, where $\lceil \cdot \rceil$ is a ceiling function.

For example, in a five-agent system, to satisfy (ii), up to one agent can be malicious.

4.5 Case Study and Results

This section presents a local grid composed of five households that must satisfy the overall electric demand by producing collective power, which is a modification of that in [103]. The case study is carried out by a standard dual decomposition DMPC and the aforementioned scenario based approaches to robustify the control network.

Algorithm 2 Secure dual decomposition based DMPC.

1: Each agent initializes its prices (Lagrange multipliers) $\Lambda[k] \succeq 0$.
2: Each agent solves its local optimization problem, i.e.,

$$\min_{u_i[k:k+N_\mathrm{p}-1]} \sum_{j=k}^{k+N_\mathrm{p}-1} (\ell_i(x_i(j+1), u_i(j)) + \lambda(j)^T C_i u_i(j)), \tag{4.20a}$$

subject to

$$x_i(j+1) = A_i x_i(j) + B_i u_i(j), \quad \forall j \in \mathbb{Z}_+, \tag{4.20b}$$
$$x_i(j) \in \mathcal{X}_i, \quad \forall j \in \mathbb{Z}_+, \tag{4.20c}$$
$$u_i(j) \in \mathcal{U}_i, \quad \forall j \in \mathbb{Z}_+. \tag{4.20d}$$

The solution of the optimization problem is denoted as $x_i^*[k+1:k+N_\mathrm{p}]$, $u_i^*[k:k+N_\mathrm{p}-1]$. Then these values are exchanged with other agents.
3: Each agent identifies the coupled variable that presents the largest and smallest average value along the prediction horizon. Here, $\mathcal{O} \subset \mathcal{N}$ is defined as the subset composed by the two agents that present the extreme values of the coupled variable.
4: **repeat**
5: **if** $i \in \mathcal{O}$ **then**
6: Each agent solves its local optimization problem with the current value of $\Lambda(k)$. These detected agents have to consider all coupling constraints i.e.,

$$\min_{u_i[k:k+N_\mathrm{p}-1]} \sum_{j=k}^{k+N_\mathrm{p}-1} (\ell_i(x_i(j+1), u_i(j)) + \lambda(j)^T C_i u_i(j)), \tag{4.21a}$$

subject to

$$x_i(j+1) = A_i x_i(j) + B_i u_i(j), \quad \forall j \in \mathbb{Z}_+, \tag{4.21b}$$
$$x_i(j) \in \mathcal{X}_i, \quad \forall j \in \mathbb{Z}_+, \tag{4.21c}$$
$$u_i(j) \in \mathcal{U}_i, \quad \forall j \in \mathbb{Z}_+. \tag{4.21d}$$

The solution of the optimization problem is denoted as $x_i^*[k+1:k+N_\mathrm{p}]$, $u_i^*[k:k+N_\mathrm{p}-1]$. Then these values are exchanged with other agents.
7: Each agent i determines the violations of the coupling constraints:
8: $s(k) \triangleq \sum_{i \in \mathcal{N}} C_i u_i^*(k) - c$, $S(k) = s[k:k+N_\mathrm{p}-1] \in \mathbb{R}^{N_\mathrm{p} \times n_c}$ and calculates the new prices along the horizon $\Lambda(k) := \max[0, \Lambda(k) + \gamma S(k)]$, where γ is the step size.

9: **else**

10: The remaining agents will ignore the coupling constraints provided by these potential attackers during the consensus process, with the current value of $\Lambda(k)$, i.e.,

$$\min_{u_i[k:k+N_\mathrm{p}-1]} \sum_{j=k}^{k+N_\mathrm{p}-1} (\ell_i(x_i(j+1), u_i(j)) + \lambda(j)^T C_i u_i(j)), \tag{4.22a}$$

subject to

$$x_i(j+1) = A_i x_i(j) + B_i u_i(j), \quad \forall j \in \mathbb{Z}_+, \tag{4.22b}$$
$$x_i(j) \in \mathcal{X}_i, \quad \forall j \in \mathbb{Z}_+, \tag{4.22c}$$
$$u_i(j) \in \mathcal{U}_i, \quad \forall j \in \mathbb{Z}_+. \tag{4.22d}$$

The solution of the optimization problem $x_i^*[k+1 : k+N_\mathrm{p}]$, $u_i^*[k : k+N_\mathrm{p}-1]$ are exchanged with other agents.

11: Each agent i determines the violations of the coupling constraints:

12: $s(k) \triangleq \sum_{i \in \mathcal{N} \setminus \mathcal{O}} C_i u_i^*(k) - c$, $S[k] = s[k : k+N_\mathrm{p}-1] \in \mathbb{R}^{N_\mathrm{p} \times n_c}$ and calculates the new prices along the horizon $\Lambda(k) := \max[0, \Lambda(k) + \gamma S(k)]$.

13: **end if**

14: **until** $\max(S(k)) < \epsilon$, where ϵ is a prespecified threshold, **or** the maximum number of iterations reached.

15: Each subsystem implements at the current time step the first component of the control sequence $u_i^*[k : k+N_\mathrm{p}-1]$.

16: Let $k = k+1$ and return to step 1.

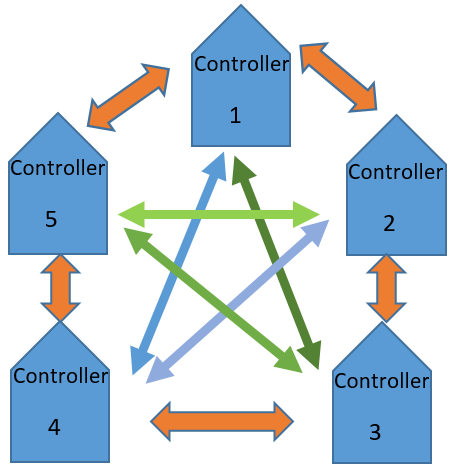

Figure 4.1: Scheme of local grid composed of five households.

4.5.1 Description

The case study consists of a network of five controllers, each one representing a prosumer that shares its imbalance information with others, as shown in Figure 4.1. The imbalance (x_i for $i \in \{1, 2, 3, 4, 5\}$) is established as the difference between its demand (d_i) and energy production (p_i). The energy production is defined as negative and the demand as positive. In this sense, the imbalance for each controller i is equal to the balance between the energy production and the energy demand. Each state is weighted by A_{ii} with a factor of 0.6 and $A_{ij} = 0.2$ represents the influence from the imbalance of the two nearest neighbors over controller i. The matrix A is defined as

$$A = \begin{pmatrix} 0.6 & 0.2 & 0 & 0 & 0.2 \\ 0.2 & 0.6 & 0.2 & 0 & 0 \\ 0 & 0.2 & 0.6 & 0.2 & 0 \\ 0 & 0 & 0.2 & 0.6 & 0.2 \\ 0.2 & 0 & 0 & 0.2 & 0.6 \end{pmatrix}. \tag{4.23}$$

At this point, the system model is described as

$$x_i(k+1) = A_{ii}x_i(k) + \sum_{j=1}^{N_\mathrm{b}} A_{ij}x_j(k) + u_i(k) + \omega_i(k) \quad \forall i \in \{1,2,3,4,5\}, j \neq i, \tag{4.24a}$$

and

$$x_i(k) = d_i(k) + p_i(k), \forall k \geq 0, \tag{4.24b}$$

where, the control input $u_i(k) = p_i(k) - p_i(k-1)$ is the increase in the energy production. The disturbance $\omega_i(k) = d_i(k) - d_i(k-1)$ represents the change in the energy demand.

Also, the systems are coupled by its imbalance, i.e.,

$$A_{ji}x_i(k+1) = A_{ij}x_j(k+1), \quad \forall i \in \{1,2,3,4,5\} \wedge j \neq i. \tag{4.25}$$

The control system uses DMPC to steer the controllers' imbalance to zero by producing energy from the generators. The optimization problem over a prediction horizon N_p is given by

$$\begin{aligned} J_i = \min_{u_i[k:k+N_\mathrm{p}-1]} & \sum_{i=k}^{k+N_\mathrm{p}} \big[x_i[k+1]^T Q x_i(k+1) \\ & + u_i(k)^T R u_i(k) + \lambda_i(k)(A_{ij}x_j(k+1) - A_{ji}x_i(k+1))\big], \\ & \forall i \in \{1,2,3,4,5\} \wedge j \neq i, \end{aligned} \tag{4.26}$$

subject to (4.24),

$$p_{min} < p_i(k) < p_{max}, \tag{4.27a}$$

$$x_i(0) = d_i(0) + p_i(0), \tag{4.27b}$$

where $p_\mathrm{min} = 0$ kW and $p_\mathrm{max} = 1$ kW. Q and R are the weights of the cost function (4.26). Also, λ_i is the Lagrangian multiplier described in Section 4.1. Finally, all values are given in cost per unit.

4.5.2 Standard Dual Decomposition DMPC

The simulations were carried out with a prediction horizon $N_\mathrm{p} = 8$ with a time step length and simulation time of 1 and 20 minutes, respectively. The demand is considered constant for controller 1 and is equal to 0.25 and the remaining controllers have a demand of 0.5. Controller 3 was chosen as the attacker.

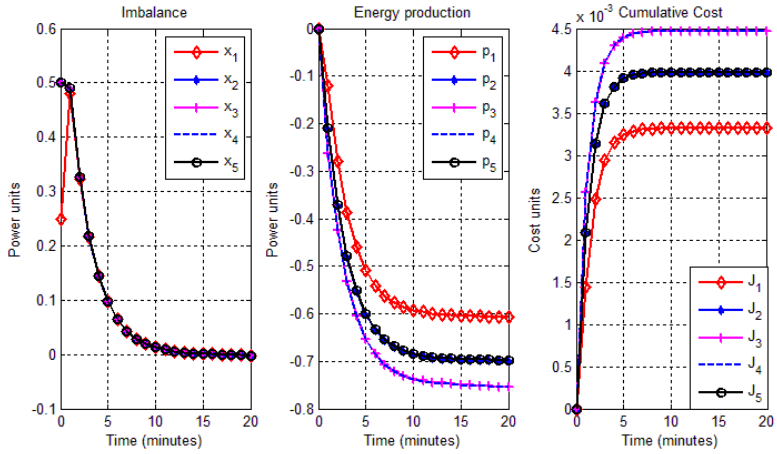

Figure 4.2: Imbalance x_i, production p_i, and cumulative cost J_i of a network composed of five households by using a standard dual decomposition.

The imbalance, the energy production, and the cumulative cost of each controller in a reliable negotiation process are shown in Figure 4.2. Here, all the controllers collaborate to satisfy the energy demand. The imbalance signals converge to zero, i.e., the demand is covered by the energy production. On the one hand, controllers 3 and 4 produce the greatest amount of energy supplied to the system. On the other, controller 1 has the lowest energy production inside the network. The final value of the cumulative cost for each controller shows the corresponding economic cost.

4.5.3 Attacks in the Control Network

Figure 4.3 shows the results by performing the "liar" controller attack. As can be seen, the imbalance converges to zero, i.e., the demand is satisfied by the energy production. In this way, controller 3 reduces its cumulative cost by forcing the others controllers to modify their behavior, i.e., their energy production and cumulative cost. Controller 3 gets economic benefits at the cost of others. In particular, controller 4 has to increase its energy production.

The "false" reference approach was performed by establishing an energy produc-

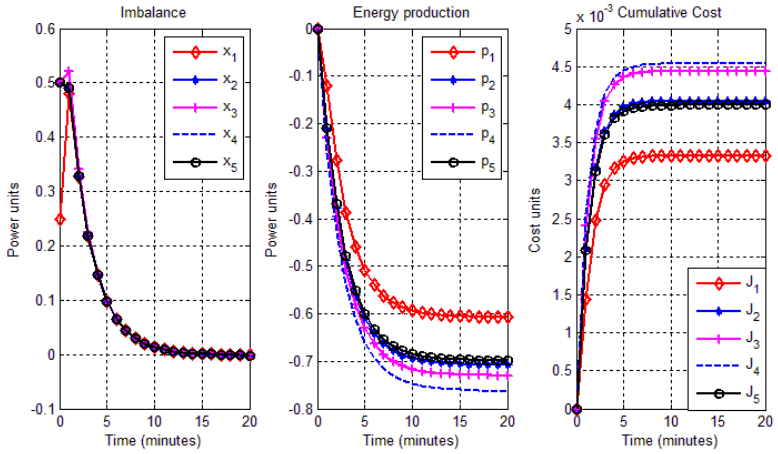

Figure 4.3: Imbalance x_i, production p_i, and cumulative cost J_i of a network composed of five households by using a "liar" controller approach.

tion reference of $x_{3_{\text{ref}}}^{*} = 0.1$ for controller 3. Figure 4.4 shows the imbalance, energy production, and the cumulative cost for the aforementioned network. It is possible to note that controller 3 reduces the amount of energy production significantly.

Figure 4.5 shows the imbalance, the energy production, and the cumulative costs of all controllers by using the third attack approach by setting "false" constraints for the energy production of the controller 3, i.e., $0 < x_3[k] < 1$. In this way, the controller reduces its imbalance bounds. It is possible to note that the attacker decreases its energy production; conversely, controllers 2 and 4 increase their energy production to steer the imbalance to zero. The final cumulative cost for all agents is increased because the attacker reduces its energy production and the imbalance has to be regulated to zero.

4.5.4 Robustifying

To ensure certain robustness, we apply scenario-based approaches, as described in Section 4.3. The price scenarios were obtained by adding a white noise $\mathcal{N}(0, 0.1)$, as described in Subsection 4.3.1. The number of scenarios used in both approaches (MS-DMPC and TB-DMPC) was $N_s = 10$.

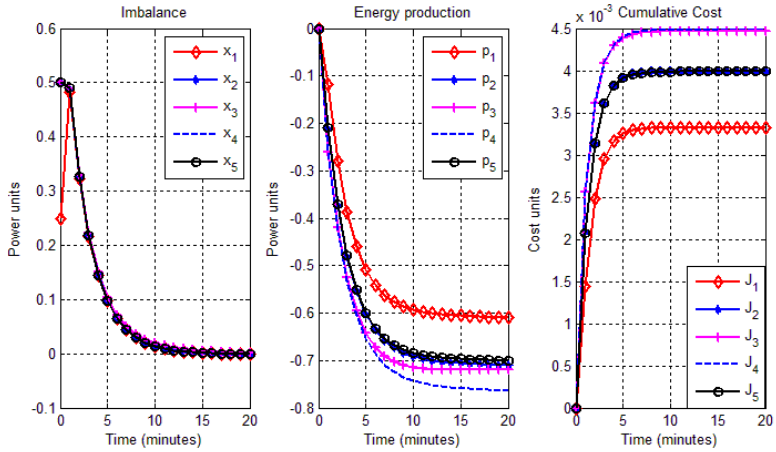

Figure 4.4: Imbalance x_i, production p_i, and cumulative cost J_i of a network composed of five households by using a "false reference" approach.

Figures 4.6 and 4.7 show the behavior of each controller after applying MS-DMPC and TB-DMPC with a false reference approach. Each one achieves the goal of avoiding that the malicious controller cheats the others. Notice that the cumulative costs from MS-DMPC are higher than TB-DMPC.

Table 4.1 shows the cumulative cost by using standard DMPC, the three described attack approaches, and the cumulative cost resulting from using MS-DMPC and TB-DMPC to the attack schemes for each controller. As can be seen, both scenario-based DMPC are able to reduce the effects that a malicious controller causes. MS-DMPC produces a single control input valid for all scenarios, resulting in an expensive cumulative cost. TB-DMPC relaxes this over conservativeness by computing as many control sequences as scenarios are considered by increasing its computational burden. Therefore, the cumulative costs are reduced with TB-DMPC compared with MS-DMPC.

It is important to remark that these scenario-based schemes give certain robustness. However, they increase the cumulative costs for the whole system, i.e., there is a loss of performance of the only system. In this sense, these schemes could be carried out when the system is under a potential attack and also has sufficient resources.

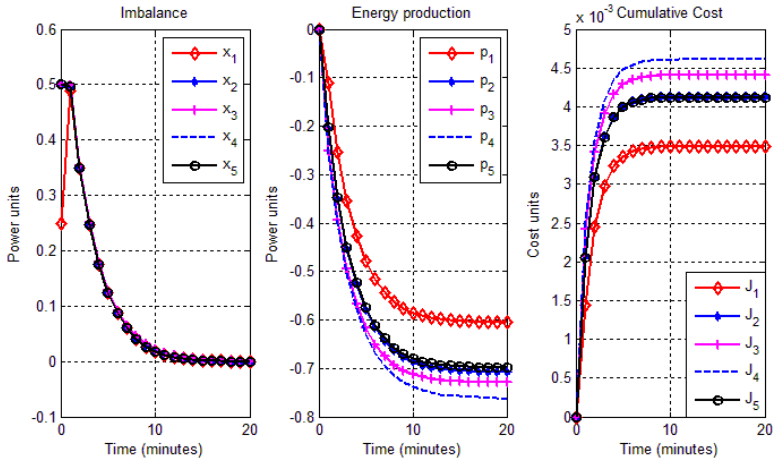

Figure 4.5: Imbalance x_i, production p_i and cumulative cost J_i of a network composed of five households by using a "false constraints" approach.

As an alternative technique to avoid these attacks, each agent performs the following actions: on the one hand, once the agents have been identified with the highest and lowest average coupled variable values along the prediction horizon, the negotiation process among the remaining agents take place ignoring the constraints that involve these two agents. On the other hand, for these two agents, they carry out the negotiation process by taking into account all the coupling constraints into the network. Table 4.2 shows the agents that present extreme values of control action at each time instant k. It is possible to note that the agent 3 is identified as a "liar" agent at each time instant.

Remark 15 *As seen, when there is an attacker inside the system, it presents an extreme value of the coupled variable. In this sense, the defense method can identify the malicious agent with any technique described in this document. However, note that if the attack is performed in such a way that the coupled variable does not present an extreme value, it cannot be detected using this method.*

Figure 4.8 shows the result obtained by applying the secure dual decomposition based DMPC approach, where it is possible to remark that all agents get a similar behavior as a standard DMPC. In this way, it achieves the goal of detecting a malicious

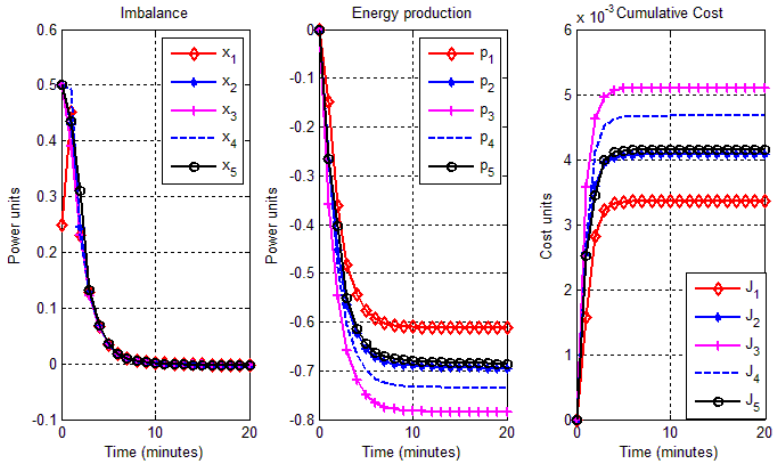

Figure 4.6: Imbalance x_i, production p_i, and cumulative cost J_i of a network composed of five households by using a "false reference" approach and MS-DMPC.

agent within the distributed controllers network, forcing all agents to negotiate in a relatively honest way, although there is a chance that an innocent agent is punished and ignored.

One disadvantage of this defense approach is that an innocent agent can be penalized for presenting an extreme value in the information exchanged. The resulting loss of performance is the price to pay in order to gain robustness against potential attackers. In any case it becomes clear in this work that DMPC schemes should introduce mechanisms that discourage or limit the consequences derived from potential attacks. Likewise, it is important to remark that the violation of some of the constraints could be derived from the attacks or even from a wrong implementation of this defense policy. Hence, its application must be carefully designed to avoid this type of issues. Moreover, it is necessary to think carefully about the role of the constraints in this context, especially since fake constraints could be used to take advantage of the DMPC scheme. In case that the fulfillment of the constraints is essential for the application considered, a supervisory layer could be included to ensure that the control actions taken do not push the system beyond its limits.

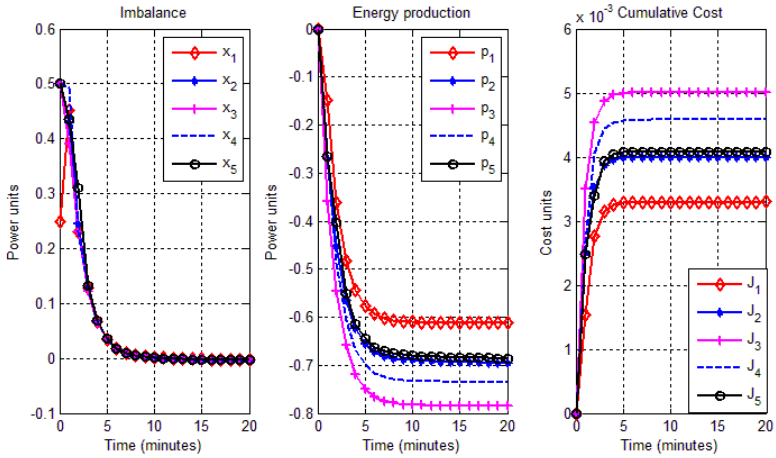

Figure 4.7: Imbalance x_i, production p_i, and cumulative cost J_i of a network composed of five households by using a "false reference" approach and TB-DMPC.

Table 4.1: Cumulative cost by using standard DMPC, attacks, and defense scenario-based methods.

Approach	**Controller 1** ($\times 10^{-3}$)	**Controller 2** ($\times 10^{-3}$)	**Controller 3** ($\times 10^{-3}$)	**Controller 4** ($\times 10^{-3}$)	**Controller 5** ($\times 10^{-3}$)
Standard DMPC	3.31	3.98	4.47	4.47	3.98
Liar controller	3.33	4.05	4.44	4.54	4.00
False reference	3.33	4.00	4.46	4.49	4.00
False constraints	3.48	4.13	4.41	4.60	4.12
MS-DMPC Liar controller	3.36	4.07	5.19	4.66	4.14
MS-DMPC False reference	3.34	4.05	5.10	4.66	4.11
MS-DMPC False constraints	3.49	4.35	5.09	4.88	4.37
TB-DMPC Liar controller	3.52	4.15	4.95	4.84	4.43
TB-DMPC False reference	3.33	3.99	5.00	4.57	4.06
TB-DMPC False constraints	3.38	4.18	4.96	4.82	4.25

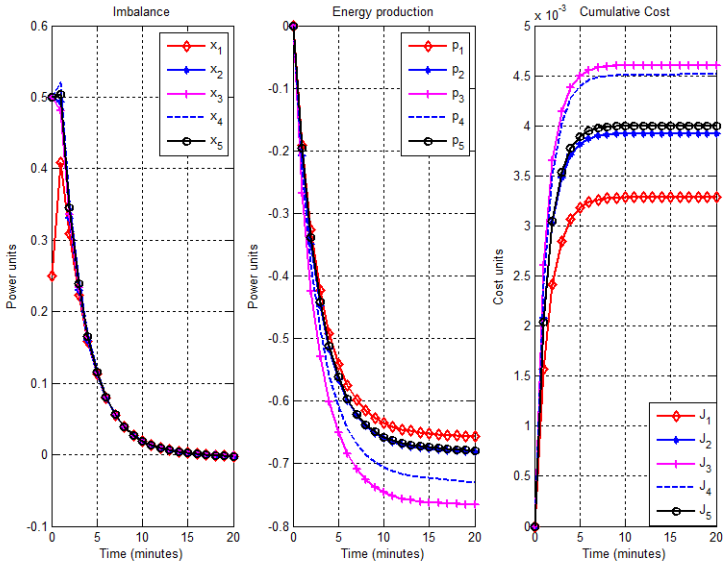

Figure 4.8: Imbalance x_i, production p_i, and cumulative cost J_i of a network composed of five households by using a "false reference" approach and secure dual decomposition based DMPC.

Table 4.2: Agents that present extreme values of control action at each time instant.

k	**Agents**	k	**Agents**	k	**Agents**	k	**Agents**
1	$3, 5$	6	$1, 3$	11	$1, 3$	16	$3, 5$
2	$1, 3$	7	$1, 3$	12	$1, 3$	17	$3, 5$
3	$1, 3$	8	$1, 3$	13	$3, 5$	18	$3, 5$
4	$1, 3$	9	$1, 3$	14	$3, 5$	19	$3, 5$
5	$1, 3$	10	$1, 3$	15	$3, 5$	20	$3, 5$

Chapter 5

Conclusions and Future Researches

Several control approaches cope with the operational management of distribution systems as a hierarchical control given by layers of planning, management, and regulation of the nonlinear system. However, those techniques, in spite of the inherent robustness of optimization-based controllers, do not guarantee the proper disturbance rejection related to the uncertainties of the whole system.

The novelty of this work consists in the design and assessment of three stochastic controllers applied to the operational management of distribution systems, in this case, energy dispatch systems and water resource management. These stochastic controllers are designed to deal with internal and external uncertainties with different configurations, i.e., centralized, hierarchical, and distributed fashion. The common advantage of all the proposed approaches relies, apart of the robustness features, on the compromise between profits, reliability, and computational burden. Moreover, this thesis offers a deep discussion about the tractability and performance of the closed loops based on the proposed approaches.

During the last years, distributed model predictive control (DMPC) has become a very active optimal control field where many algorithms and strategies have been proposed to ease the coordination in multi-agent systems where there are coupled dynamics. This work raises an important issue in the field of DMPC. In particular, DMPC schemes rely on the assumption that the information shared across the network is trustworthy. A malicious controller could send false information to the rest of the controllers to steer the negotiation process, which may result in a loss of performance or

even in the instability of the closed loop system. To illustrate and raise awareness of this problem, this work has presented the vulnerabilities of a very popular distributed model predictive control scheme. More specifically, it has shown how a malicious agent in the network could exploit the information exchange to steer the negotiation process arbitrarily. Also, stochastic based MPCs and a heuristic technique have been proposed as alternatives to give some robustness the DMPC scheme against this problem.

5.1 Conclusions

Below, the main conclusions of each chapter of this thesis are provided.

- *Centralized Stochastic Model Predictive Control*

  In Chapter 2, stochastic MPC schemes have been designed and applied to ensure robustness against external disturbances in the context of distribution systems, more specifically, a real microgrid, the drinking water network of Barcelona, and the stock management of a hospital pharmacy. In this context, it is possible to conclude that MS-MPC controller is over-conservative because it does not consider the controller capacity to adapt. It calculates a control series valid to all possible scenarios by means an open-loop formulation. However, it is possible to solve the optimization problem by using a control tree and increasing the number of optimization variables and the computational time. Regarding the control point of view, TB-MPC controller works in a closed-loop fashion to adapt the control actions to the expected evolution of the disturbances. Finally, CC-MPC controller formulates the optimization problem by taking into account the statistical features of the uncertainty without increasing the number of variables. The results obtained with the three presented versions of stochastic MPC controllers show their effectiveness in energy management and drinking water network under economic and optimal criteria. According to the results obtained and the evaluation of the case studies, it can be said that CC-MPC controller relaxes the constraints of the optimization problem by assuming a risk to offer better performance, resulting in a lower cost, less energy exchange with the network and a lower number of constraints violation for energy management and drinking water networks compared MS-MPC and TB-MPC controllers. This is also the approach with the lowest computational burden. The downside of this approach is that it requires a statistical characterization of the disturbances.

  Also, a solution for the problem of stock management in a hospital pharmacy has been proposed. A control methodology has been described to deal with the different and contradictory objectives of the problem. The proposed control strategy

is a based on MPC, which allows the fulfillment of the management objectives while imposing different operational constraints. In that way, it has been possible to guarantee, with a high probability, that the drugs will be available for the patients, knowing explicitly the allowed risk level. In addition, we have shown that several hospitals could collaborate to reduce their stock levels. Finally, some simulations have been carried out to show the performance of the proposed management approach. It has been seen how the average level of stocked drugs has been reduced, which reduces the economical costs for the hospital, and how the work burden in the pharmacy was also reduced while guaranteeing the needs of the patients.

- *Hierarchical Stochastic MPC*

  In Chapter 3, this work has shown a risk assessment methodology applied to microgrids. Although many risks have been identified, only a reduced set of them has been used in the example for illustrating the method. Two different model predictive controllers have been used. One for the external loop in order to evaluate risks and determine the optimal mitigation actions and another for the control of the plant. Results show that the benefits that can be obtained are very positive.

  By another site, it has been considered a water resource management system, which is subject to dynamical uncertainty. The system is distributed into subsystems at the bottom, but the overall performance is checked for the whole system at the top layer. The final goal was to decompose the overall problem into different regions and under different hydrological conditions. In this sense, a scenario based Hierarchical and Distributed Model Predictive Control have been used to address the disturbances and uncertainties, which commonly affect this kind of systems. For the uncertainty, the tree based approach based on scenarios has been widely applied principally in the field of centralized water systems due to its adaptability at the moment to generate the disturbances tree. A drawback that presents this approach is its higher computational burden, this problem was addressed by the hierarchical controller, which collects the whole information and sends only the most likely scenarios to be taken into account by the distributed controllers at the time to solve the local optimization problem. Results show the effectiveness of this method to ensure the water level into the desired reference despite the presence of uncertainties for a large scale system.

- *Stochastic MPC to Deal with Vulnerabilities in Distributed Schemes*

  In Chapter 4, cyber-security issues in DMPC have been considered. An analysis of the vulnerability of a popular Lagrange-based DMPC scheme has been

presented. By using a relevant case study involving a power network, we have illustrated the potential of this mechanism, and how a controller can attack the system to obtain benefits. It has been addressed the problem of providing robustness to DMPC for defending it from a malicious controller by carrying out scenario-based mechanisms. We have also proposed a heuristic mechanism to defend the attacked agents, that is, to identify false information and perform the negotiation process among agents regardless of the actions of the attacker. A highly relevant case study involving a power network illustrates the potential of this mechanism.

5.2 Future Researches

The research of stochastic MPC techniques applied to distribution systems has been a major issue in recent years. However, some important issues fall out of the scope of this thesis and can be studied in the future. Next, several research lines are pointed out for their study and analysis.

- On the one hand, centralized stochastic MPCs have been analyzed and implemented via simulation and experimental setup, describing their advantages and drawbacks. However, in this work the bounds for violating constraints were assumed in the same way for MS-MPC and TB-MPC, this assumption may be modified, and a further study for TB-MPC may be developed. Moreover, some algorithms for obtaining three disturbances deserve particular attention for improving the computational burden. Regarding CC-MPC, the formulation of deterministic constraints to replace the stochastic ones by considering other well-known probability distribution functions instead of normal distribution functions or historical data, as been discussed, may be an accurate bullet for being developed.

- On the other hand, regarding hierarchical and distributed MPC, it is important to remark the possibility to design, implement, and compare the assessment and performance of other stochastic MPC at the lower level to deal with the uncertainty that the distribution system present. Furthermore, some results have been carried out by simulation and show the benefit of these approaches described in this document; however, an aggregated value will apport an experimental setup in real case studies.

- Cyber-security issues is a very relevant and critical topic that has not been explicitly considered in the DMPC literature in a structured way. In this thesis,

one of the most popular distributed MPC schemes has been considered. However, other kinds of attacks will be discussed in different distributed algorithms. In this sense, there are many important issues in the context of distribution systems related to the reliable information exchange that can be exploited, such as uncertainty in the demand patterns will be considered as a manner to robustify the system against possible internal attackers. Moreover, the use of the quality of service (QoS) as an index of trustworthiness of each agent will be investigated. It will also address cyber security issues in DMPC from other points of view, e.g., by considering other stochastic MPC methods or by developing new approaches to identify and isolate the attackers from the whole distributed system. In this manner, it is possible to mitigate losses and the impact from malicious agents in the performance of the system.

5.3 Publications from this work

Several publications have taken place as peer-reviewed articles and conference papers. The list of scientific articles is enumerated as follows:

- Jurado, I., Maestre, J. M., Velarde, P., Ocampo-Martinez, C., Fernndez, I., Tejera, B. I., del Prado, J. R. (2016). Stock management in hospital pharmacy using chance-constrained model predictive control. *Computers in biology and medicine*, 72, 248-255.

- Grosso, J. M., Velarde, P., Ocampo-Martinez, C., Maestre, J. M., Puig, V. (2016). Stochastic model predictive control approaches applied to drinking water networks. *Optimal Control Applications and Methods*. DOI:10.1002/oca.2269.

- Velarde, P., Valverde, L., Maestre, J. M., Ocampo-Martinez, C., Bordons, C. (2017). On the comparison of stochastic model predictive control strategies applied to a hydrogen-based microgrid, *Journal of Power Sources*, 343, 161-173.

- Velarde, P., Maestre, J. M., Ishii, H., Negenborn, R. R., (2017). Vulnerabilities in Lagrange-based Distributed Model Predictive Control. Submitted to *Optimal Control Applications and Methods*.

- Maestre, J. M., Velarde, P., Jurado, I., Ocampo-Martnez, C., Fernandez, I., Tejera, B. I., del Prado, J. R. (2014, December). An application of chance-constrained model predictive control to inventory management in hospitalary pharmacy. In 53rd IEEE Conference on Decision and Control (pp. 5901-5906). IEEE.

- Velarde, P., Maestre, J. M., Jurado, I., Fernandez, I., Tejera, B. I., del Prado, J. R. (2014, September). Application of robust model predictive control to inventory management in hospitalary pharmacy. In Proceedings of the 2014 IEEE Emerging Technology and Factory Automation (ETFA) (pp. 1-6). IEEE.

- Velarde, P., Maestre, J. M., Ocampo-Martinez, C., Bordons, C. (2016, June). Application of robust model predictive control to a renewable hydrogen-based microgrid. In Proceedings of the 2016 European Control Conference (ECC), Aalborg, Denmark, 2016, pp. 1209-1214.

- Velarde, P., Maestre, J. M., Ishii, H., Negenborn, R. R., Vulnerabilities in Lagrange-based DMPC in the Context of Cyber-Security. Submitted to The 20th World Congress of the International Federation of Automatic Control (IFAC).

- Velarde, P., Maestre, J. M., Ishii, H., Negenborn, R. R., Scenario Based Defense Mechanism for Distributed Model Predictive Control. Submitted to The 20th World Congress of the International Federation of Automatic Control (IFAC).

- Zafra-Cabeza, A., Velarde, P., Maestre, J. M., Multicriteria Optimal Operation of a Microgrid considering Risk Analysis, Renewable Resources and MPC. Submitted to The 20th World Congress of the International Federation of Automatic Control (IFAC).

- Maestre, J. M., Velarde, P., Muros, F. J., An Application of the Logarithmic Mean Divisia Index Method to Distributed and Coalitional Control. Submitted to The 20th World Congress of the International Federation of Automatic Control (IFAC).

Bibliography

[1] C. Ocampo-Martinez, V. Puig, G. Cembrano, J. Quevedo, Application of predictive control strategies to the management of complex networks in the urban water cycle, Control Systems, IEEE 33 (1) (2013) 15–41.

[2] E. F. Camacho, C. Bordons, Model Predictive Control. Second Edition, Springer-Verlag, London, England, 2004.

[3] J. Maciejowski, Predictive control with constraints, Prentice Hall, Essex, England, 2002.

[4] D. Bernardini, A. Bemporad, Scenario-based model predictive control of stochastic constrained linear systems, Joint 48th IEEE Conference on Decision and Control and 28th Chinese Control Conference, Shanghai, P.R. China (2009) 6333–6338.

[5] M. Cannon, P. Couchman, B. Kouvaritakis, MPC for stochastic systems, in: R. Findeisen, F. Allgöwer, L. Biegler (Eds.), Assessment and Future Directions of Nonlinear Model Predictive Control, Vol. 358 of Lecture Notes in Control and Information Sciences, Springer Berlin Heidelberg, 2007, pp. 255–268.

[6] D. Muñoz de la Peña, A. Bemporad, T. Alamo, Stochastic programming applied to model predictive control, in: Proceedings of 44th IEEE Conference on Decision and Control and European Control Conference (CDC-ECC), Seville, 2005, pp. 1361 – 1366.

[7] D. Muñoz de la Peña, A. Bemporad, T. Alamo, Stochastic programming applied to model predictive control, in: Proceedings of the 44th IEEE Conference on Decision and Control, and European Control Conference (CDC-ECC), Seville, Spain, 2005, pp. 1361–1366.

[8] G. Calafiore, F. Dabbene, Probabilistic and randomized methods for design under uncertainty, Springer, London, England, 2006.

[9] G. Calafiore, F. Dabbene, R. Tempo, Research on probabilistic methods for control system design, Automatica 47 (7) (2011) 1279 – 1293.

[10] P. J. van Overloop, S. Weijs, S. Dijkstra, Multiple model predictive control on a drainage canal system, Control Engineering Practice 16 (5) (2008) 531–540.

[11] D. E. Olivares, J. D. Lara, C. A. Cañizares, M. Kazerani, Stochastic-predictive energy management system for isolated microgrids, IEEE Transactions on Smart Grid 6 (6) (2015) 2681–2693.

[12] T. Niknam, R. Azizipanah-Abarghooee, M. R. Narimani, An efficient scenario-based stochastic programming framework for multi-objective optimal microgrid operation, Applied Energy 99 (2012) 455 – 470.

[13] G. Calafiore, M. Campi, The scenario approach to robust control design, IEEE Transactions on Automatic Control 51 (5) (2006) 742–753.

[14] S. Lucia, T. Finkler, D. Basak, S. Engell, A new robust NMPC scheme and its application to a semi-batch reactor example., In Proc. of the International Symposium on Advanced Control of Chemical Processes, Singapore (2012) 69–74.

[15] M. Petrollese, L. Valverde, D. Cocco, G. Cau, J. Guerra, Real-time integration of optimal generation scheduling with MPC for the energy management of a renewable hydrogen-based microgrid, Applied Energy 166 (2016) 96–106.

[16] J. M. Maestre, L. Raso, P. J. Van Overloop, B. De Schutter, Distributed tree-based model predictive control on an open water system, in: Proceedings of the American Control Conference (ACC), Montréal, Canada, 2012, pp. 1985–1990.

[17] Q. Wang, Y. Guan, J. Wang, A chance-constrained two-stage stochastic program for unit commitment with uncertain wind power output, IEEE Transactions on Power Systems 27 (1) (2012) 206–215.

[18] M. Ono, U. Topcu, M. Yo, S. Adachi, Risk-limiting power grid control with an arma-based prediction model, in: Proceedings of the 52nd IEEE Annual Conference on Decision and Control (CDC), Florence, Italy, 2013, pp. 4949–4956.

[19] J. Grosso, C. Ocampo-Martinez, V. Puig, B. Joseph, Chance-constrained model predictive control for drinking water networks, Journal of Process Control 24 (5) (2014) 504–516.

[20] J. Grosso, J. Maestre, C. Ocampo-Martinez, V. Puig, On the assessment of tree-based and chance-constrained predictive control aproaches applied to drinking water networks, 19th IFAC World Congress, Cape Town, South Africa (2014) 6240–6245.

[21] A. Hooshmand, B. Asghari, R. Sharma, A novel cost-aware multi-objective energy management method for microgrids, in: Proceedings of the Innovative Smart Grid Technologies (ISGT), IEEE PES, Washington, DC, USA, 2013, pp. 1–6.

[22] Z. Yu, L. McLaughlin, L. J., M. Murphy-Hoye, A. Pratt, L. T., Modeling and stochastic control for home energy management, in: Proceedings of the IEEE Power and Energy Society General Meeting, San Diego, California, USA, 2012, pp. 1–9.

[23] P. Meibom, R. Barth, B. Hasche, H. Brand, C. Weber, M. O'Malley, Stochastic optimization model to study the operational impacts of high wind penetrations in Ireland, IEEE Transactions on Power Systems 26 (3) (2011) 1367–1379.

[24] T. Hovgaard, L. Larsen, J. Jorgensen, Robust economic MPC for a power management scenario with uncertainties, in: Proceedings of the 50th IEEE Conference on Decision and Control and European Control Conference (CDC-ECC), Orlando, Florida, 2011, pp. 1515–1520.

[25] X. Tian, J. Maestre, P. van Overloop, R. Negenborn, Distributed model predictive control for multi-objective water system management, in: Proceedings of 10th Int. Conf. hydroinformatics, Hamburg, Germany, 2012, p. 175.

[26] R. R. Negenborn, P.-J. van Overloop, T. Keviczky, B. De Schutter, Distributed model predictive control of irrigation canals., NHM 4 (2) (2009) 359–380.

[27] A. Zafra-Cabeza, J. Maestre, M. A. Ridao, E. F. Camacho, L. Sánchez, A hierarchical distributed model predictive control approach to irrigation canals: A risk mitigation perspective, Journal of Process Control 21 (5) (2011) 787–799.

[28] A. Sadowska, P. Overloop, C. Burt, B. Schutter, Hierarchical operation of water level controllers: Formal analysis and application on a large scale irrigation canal, Water Resources Management 28 (14) (2014) 4999–5019.

[29] A. Sadowska, B. De Schutter, P.-J. van Overloop, Delivery-oriented hierarchical predictive control of an irrigation canal: event-driven versus time-driven approaches, IEEE Transactions on Control Systems Technology 23 (5) (2015) 1701–1716.

[30] J. M. Maestre, R. R. Negenborn, Distributed Model Predictive Control Made Easy, Springer, 2014.

[31] P. Velarde, L. Valverde, J. M. Maestre, C. Ocampo-Martinez, C. Bordons, On the comparison of stochastic model predictive control strategies applied to a hydrogen-based microgrid, Journal of Power Sources 343 (2017) 161–173.

[32] J. M. Grosso, P. Velarde, C. Ocampo-Martinez, J. M. Maestre, V. Puig, Stochastic model predictive control approaches applied to drinking water networks, Optimal Control Applications and Methods In Press. doi:10.1002/oca.2269.

[33] I. Jurado, J. Maestre, P. Velarde, C. Ocampo-Martinez, I. Fernández, B. I. Tejera, J. del Prado, Stock management in hospital pharmacy using chance-constrained model predictive control, Computers in biology and medicine 72 (2016) 248–255.

[34] H. van de Water, J. Willems, The certainty equivalence property in stochastic control theory, IEEE Transactions on Automatic Control 26 (5) (1981) 1080 – 1087.

[35] J. M. Grosso, On model predictive control for economic and robust operation of generalised flow-based networks, Ph.D. thesis, Universitat Politecnica de Catalunya, Barcelona, Spain (2015).

[36] H. van de Water, J. Willems, The certainty equivalence property in stochastic control theory, IEEE Transactions on Automatic Control 26 (5) (2002) 1080–1087.

[37] G. Schildbach, L. Fagiano, C. Frei, M. Morari, The scenario approach for stochastic model predictive control with bounds on closed-loop constraint violations, Automatica 50 (12) (2014) 3009–3018.

[38] L. Giulioni, Stochastic model predictive control with application to distributed control systems, Ph.D. thesis, Politecnico di Milano (2015).

[39] L. Raso, N. Giesen, P. Stive, D. Schwanenberg, P. Overloop, Tree structure generation from ensemble forecasts for real time control, Hydrological Processes 27 (1) (2013) 75–82.

[40] L. Raso, D. Schwanenberg, N. van de Giesen, P. van Overloop, Short-term optimal operation of water systems using ensemble forecasts, Advances in Water Resources 71 (2014) 200 – 208.

[41] J. P. Lopes, C. Moreira, A. Madureira, Defining control strategies for microgrids islanded operation, IEEE Transactions on Power Systems 21 (2) (2006) 916–924.

[42] L. Valverde, C. Bordons, F. Rosa, Integration of fuel cell technologies in renewable-energy-based microgrids optimizing operational costs and durability, IEEE Transactions on Industrial Electronics 63 (1) (2016) 167–177.

[43] C. Kunusch, C. Ocampo-Martinez, M. Valla, Modeling, diagnosis, and control of fuel-cell-based technologies and their integration in smart grids and automotive systems, IEEE Transactions on Industrial Electronics 62 (8) (2015) 5143–5145.

[44] L. Valverde, F. Rosa, C. Bordons, Design, planning and management of a hydrogen-based microgrid, IEEE Transactions on Industrial Informatics 9 (3) (2013) 1398–1404.

[45] D. Recio, C. Ocampo-Martinez, M. Serra, Design of linear predictive controllers applied to ethanol steam reformers for hydrogen production, International Journal of Hydrogen Energy 37(15) (2012) 11141–11156.

[46] T. Dragicevic, J. Guerrero, J. Vasquez, A distributed control strategy for coordination of an autonomous LVDC microgrid based on power-line signaling, IEEE Transactions on Industrial Electronics 61 (7) (2014) 3313–3326.

[47] D. E. Olivares, A. Mehrizi-Sani, A. H. Etemadi, C. A. Cañizares, R. Iravani, M. Kazerani, A. H. Hajimiragha, O. Gomis-Bellmunt, M. Saeedifard, R. Palma-Behnke, G. Jimenez-Estevez, N. Hatziargyriou, Trends in microgrid control, IEEE Transactions on Smart Grid 5 (4) (2014) 1905–1919.

[48] L. Valverde, F. Rosa, A. del Real, A. Arce, C. Bordons, Modeling, simulation and experimental set-up of a renewable hydrogen-based domestic microgrid, International Journal of Hydrogen Energy 38 (2013) 11672–11684.

[49] C. Bordons, F. García-Torres, L. Valverde, Gestión óptima de la energía en microrredes con generación renovable, Revista Iberoamericana de Automática e Informática Industrial RIAI 12 (2) (2015) 117–132.

[50] B. S. Lee, H. Y. Park, I. Choi, M. K. Cho, H. J. Kim, S. J. Yoo, D. Henkensmeier, J. Y. Kim, S. W. Nam, S. Park, et al., Polarization characteristics of a low catalyst loading pem water electrolyzer operating at elevated temperature, Journal of Power Sources 309 (2016) 127–134.

[51] A. J. Del Real, A. Arce, C. Bordons, Development and experimental validation of a pem fuel cell dynamic model, Journal of Power Sources 173 (1) (2007) 310–324.

[52] M. Tanrioven, M. Alam, Reliability modeling and assessment of grid-connected pem fuel cell power plants, Journal of Power Sources 142 (1) (2005) 264–278.

[53] L. Valverde, F. Rosa, A. del Real, A. Arce, C. Bordons, Modeling, simulation and experimental set-up of a renewable hydrogen-based domestic microgrid, International Journal of Hydrogen Energy 38 (27) (2013) 11672–11684.

[54] M. Pereira, D. Limón, D. Muñoz de la Peña, L. Valverde, T. Alamo, Periodic economic control of a nonisolated microgrid, IEEE Transactions on Industrial Electronics 62 (8) (2015) 5247–5255.

[55] F. Garcia-Torres, C. Bordons, Optimal economical schedule of hydrogen-based microgrids with hybrid storage using model predictive control, IEEE Transactions on Industrial Electronics 62 (8) (2015) 5195–5207.

[56] A. Brooke, D. Kendrick, A. Meeraus, R. Raman, General algebraic modeling system (GAMS): A users guide, Boyd & Fraser publishing company, Danvers, Massachusetts.

[57] E. Karfopoulos, L. Tena, A. Torres, P. Salas, J. G. Jorda, A. Dimeas, N. Hatziargyriou, A multi-agent system providing demand response services from residential consumers, Electric Power Systems Research 120 (2015) 163 – 176.

[58] H. Alegre, J. Baptista, E. Cabrera, F. Cubillo, Performance Indicators for Water Supply Services, Manuals of Best Practice Series, IWA Publishing, 2006.

[59] G. E. P. Box, G. M. Jenkins, G. C. Reisnel, Time Series Analysis, Forecasting and Control, 3rd Edition, Prentice-Hall International, Inc., New Jersey, U.S.A, 1994.

[60] G. Schildbach, L. Fagiano, C. Frei, M. Morari, The scenario approach for stochastic model predictive control with bounds on closed-loop constraint violations, Automatica 50 (12) (2014) 3009–3018.

[61] H. Heitsch, W. Römisch, Scenario tree modeling for multistage stochastic programs, Mathematical Programming 118 (2) (2009) 371–406.

[62] L. Raso, D. Schwanenberg, N. van der Giesen, P.-J. van Overloop, Tree-scenario based model predictive control, in: Proceedings of EGU General Assembly Conference Abstracts, Vol. 12, 2010, p. 3178.

[63] S. Lucia, S. Subramanian, S. Engell, Non-conservative robust nonlinear model predictive control via scenario decomposition, in: Proceedings of IEEE Multi-Conference on Systems and Control (MSC), Hyderabad, India, 2013, pp. 586–591.

[64] T. Bermejo, B. Cuña, V. Napal, E. Valverde, The hospitalary pharmacy specialist handbook (in Spanish), Spanish Society of Hospitalary Pharmacy, 1999.

[65] S. Tayur, R. Ganeshan, M. Magazine, Quantitative models for supply chain management, Kluwer Academic Publisher, 1999.

[66] A. M. Brewer, K. J. Button, D. A. Hensher, Handbook of logistics and supply-chain management, Pergamon, 2001.

[67] S. Çetinkaya, C. Lee, Stock replenishment and shipment scheduling for vendor-managed inventory systems, Management Science 46 (2) (2000) 217–232.

[68] J. Dong, D. Zhang, A. Nagurney, A supply chain network equilibrium model with random demands, European Journal of Operational Research 156 (1) (2004) 194–212.

[69] G. Cachon, Stock wars: Inventory competition in a two-echelon supply chain with multiple retailers, Operations Research 49 (5) (2001) 658–674.

[70] S. Rezapour, R. Farahani, Strategic design of competing centralized supply chain networks for markets with deterministic demands, Advances in Engineering Software 41 (5) (2010) 810822.

[71] E. Lawler, D. Wood, Branch-and-bound methods: A survey, Operations Research 14 (4) (1966) 699–719.

[72] V. Summanwara, V. Jayaramana, B. Kulkarnia, H. Kusumakarb, K. Guptab, J. Rajesh, Solution of constrained optimization problems by multi-objective genetic algorithm, Computers & Chemical Engineering 26 (10) (2002) 1481–1492.

[73] W. Cook, R. Kannan, A. Schrijver, Chvátal closures for mixed integer programming problems, Mathematical Programming 47 (1) (1990) 155–174.

[74] J. Maestre Torreblanca, P. Velarde, I. Jurado, C. Ocampo-Martinez, I. Fernandez, B. Isla Tejera, J. del Prado Llergo, An application of chance-constrained model predictive control to inventory management in hospitalary pharmacy, in: 53rd IEEE Conference on Decision and Control, CDC 2014, Los Angeles, CA, USA, December 15-17, 2014, pp. 5901–5906.

[75] C. Hood, D. K. C. Jones, Accident And Design: Contemporary Debates On Risk Management, Taylor & Francis, 2003.

[76] A. Zafra-Cabeza, M. Ridao, E. Camacho, A mixed integer quadratic programming formulation of risk management for reverse osmosis plants, Desalination 268.

[77] P. C. D. Milly, J. Betancourt, M. Falkenmark, R. M. Hirsch, Z. W. Kundzewicz, D. P. Lettenmaier, R. J. Stouffer, Stationarity Is Dead: Whither Water Management?, Science 319 (5863) (2008) 573–574.

[78] M. Spiller, J. H. Vreeburg, I. Leusbrock, G. Zeeman, Flexible design in water and wastewater engineering Definitions, literature and decision guide, Journal of Environmental Management 149 (2015) 271–281.

[79] M. Haasnoot, J. H. Kwakkel, W. E. Walker, Dynamic adaptive policy pathways : A method for crafting robust decisions for a deeply uncertain world, Global Environmental Change 23 (2) (2013) 485–498.

[80] G. W. Characklis, B. R. Kirsch, J. Ramsey, K. E. M. Dillard, C. T. Kelley, Developing portfolios of water supply transfers, Water Resources Research 42 (5).

[81] E. H. Y. Beh, H. R. Maier, G. C. Dandy, Adaptive, multiobjective optimal sequencing approach for urban water supply augmentation under deep uncertainty, Water Resources Research 51 (3) (2015) 1529–1551.

[82] W. Walker, M. Haasnoot, J. Kwakkel, Adapt or Perish: A Review of Planning Approaches for Adaptation under Deep Uncertainty, Sustainability 5 (3) (2013) 955–979.

[83] L. Raso, D. Schwanenberg, N. van de Giesen, P. van Overloop, Short-term optimal operation of water systems using ensemble forecasts, Advances in Water Resources 71 (2014) 200–208.

[84] J. Maestre, L. Raso, P. V. Overloop, B. De Schutter, Distributed tree-based model predictive control on a drainage water system, Journal of Hydroinformatics 15 (2) (2013) 335–347.

[85] P. J. van Overloop, Model predictive control on open water systems, Ph.D. thesis, Delft University of Technology (2006).

[86] X. Tian, P.-J. van Overloop, R. R. Negenborn, N. van de Giesen, Operational flood control of a low-lying delta system using large time step model predictive control, Advances in Water Resources 75 (2015) 1 – 13.

[87] M. Xu, Real-time control of combined water quantity & quality in open channels, TU Delft, Delft University of Technology, 2013.

[88] M. Xu, P. J. van Overloop, N. van de Giesen, Model reduction in model predictive control of combined water quantity and quality in open channels, Environmental Modelling & Software 42 (2013) 72 – 87.

[89] B. Biegel, J. Stoustrup, P. Andersen, Distributed MPC via dual decomposition, in: Distributed Model Predictive Control Made Easy, Springer, 2014, pp. 179–192.

[90] R. R. Negenborn, J. M. Maestre, Distributed model predictive control: An overview and roadmap of future research opportunities, IEEE Control Systems 34 (4) (2014) 87–97.

[91] R. Radvanovsky, J. Brodsky, Handbook of SCADA/control systems security, CRC Press, 2016.

[92] S. Sheng, W. Chan, K. Li, D. Xianzhong, Z. Xiangjun, Context information-based cyber security defense of protection system, IEEE Transactions on Power Delivery 22 (3) (2007) 1477–1481.

[93] E. Kritzinger, S. Von Solms, Cyber security for home users: A new way of protection through awareness enforcement, Computers & Security 29 (8) (2010) 840 – 847.

[94] L. Li, R. R. Negenborn, B. De Schutter, Intermodal freight transport planning a receding horizon control approach, Transportation Research Part C: Emerging Technologies 60 (2015) 77 – 95.

[95] J. L. Nabais, R. R. Negenborn, R. B. Carmona, M. Ayala, Achieving transport modal split targets at intermodal freight hubs using a model predictive approach, Transportation Research Part C: Emerging Technologies 60 (2015) 278 – 297.

[96] B. van Riessen, R. R. Negenborn, G. Lodewijks, R. Dekker, Impact and relevance of transit disturbances on planning in intermodal container networks using disturbance cost analysis, Maritime Economics & Logistics 17 (2015) 440–463.

[97] Y. Chakhchoukh, H. Ishii, Coordinated cyber-attacks on the measurement function in hybrid state estimation, IEEE Transactions on Power Systems 30 (5) (2015) 2487–2497.

[98] C. Barreto, J. Giraldo, A. A. Cardenas, E. Mojica-Nava, N. Quijano, Control systems for the power grid and their resiliency to attacks, IEEE Security & Privacy 12 (6) (2014) 15–23.

[99] A. Teixeira, K. C. Sou, H. Sandberg, K. H. Johansson, Secure control systems: A quantitative risk management approach, IEEE Control Systems 35 (1) (2015) 24–45.

[100] Q. Zhu, T. Basar, Game-theoretic methods for robustness, security, and resilience of cyberphysical control systems: games-in-games principle for optimal cross-layer resilient control systems, IEEE Control Systems 35 (1) (2015) 46–65.

[101] R. Dhal, S. Roy, Vulnerability of continuous-time network synchronization processes: A minimum energy perspective, in: Proceedings of the 52nd IEEE Conference on Decision and Control, Florence, Italy, 2013, pp. 823–828.

[102] S. Dibaji, H. Ishii, Consensus of second-order multi-agent systems in the presence of locally bounded faults, Systems & Control Letters 79 (2015) 23 – 29.

[103] G. Larsen, N. van Foreest, J. Scherpen, A price mechanism for supply demand matching in local grid of households with micro-CHP, in: Proceedings of the EPJ Web of Conferences, Vol. 33, EDP Sciences, 2012, p. 01011.

[104] P. Giselsson, A. Rantzer, Generalized accelerated gradient methods for distributed MPC based on dual decomposition, in: Distributed Model Predictive Control Made Easy, Springer, 2014, Ch. 11, pp. 309–325.

[105] L. Yushen, L. Shuai, L. Xie, K. Johansson, A scenario-based distributed stochastic MPC for building temperature regulation, in: Proceedings of the 2014 IEEE International Conference on Automation Science and Engineering, New Taipei, Taiwan, 2014, pp. 1091–1096.

[106] G. Larsen, N. Van Foreest, J. Scherpen, Distributed MPC applied to a network of households with micro-CHP and heat storage, IEEE Transactions on Smart Grids, 5 (4) (2014) 2106–2114.

[107] H. Zheng, R. R. Negenborn, G. Lodewijks, Closed-loop scheduling and control of waterborne AGVs for energy-efficient inter terminal transport, Transportation Research Part E: Logistics and Transportation Reviewdoi:http://dx.doi.org/10.1016/j.tre.2016.07.010.

[108] L. Li, R. R. Negenborn, B. De Schutter, Distributed model predictive control for cooperative synchromodal freight transport, Transportation Research Part E: Logistics and Transportation Reviewdoi:http://dx.doi.org/10.1016/j.tre.2016.08.006.

[109] G. Schildbach, M. Morari, Scenario mpc for linear time-varying systems with individual chance constraints, in: American Control Conference, IEEE, 2015, pp. 415–421.

[110] N. A. Lynch, Distributed algorithms, Morgan Kaufmann, 1996.